Uncertainty and sensitivity analysis of a Materials Test Reactor

MI Modukanele
20714106

Dissertation submitted in partial fulfillment of the requirements for the degree *Master of Engineering* in Nuclear Engineering at the Potchefstroom Campus of the North-West University

Supervisor: Dr. V Naicker
Co-supervisor: Prof. PG Rousseau

November 2013

Declaration

I hereby declare that all the material used in this dissertation is my own original unaided work except where specific references are made by name or in the form of a numbered reference. The work herein has not been submitted for a degree to another university.

Signed: _____

Mogomotsi Ignatius Modukanele

Acknowledgement

The author would like to acknowledge the following people:

- Firstly I would like to thank my heavenly Father for without His guidance and strength this dissertation would not have been possible.
- Dr Vishnu Naicker and Prof. Pieter Rousseau, my supervisors, for their great wisdom, guidance and motivation throughout this project.
- My family and friends for their love and support and for always believing in me and never giving up on me.
- Necsa and NRF for their financial support.
- Lastly I would like to send special thanks to my partner Khutsafalo Moeng. Thank you for all your love and support.

Abstract

This study was based on the uncertainty and sensitivity analysis of a generic 10 MW Materials Test Reactor (MTR). In this study an uncertainty and sensitivity analysis methodology called code scaling applicability and uncertainty (CSAU) was implemented. Although this methodology follows 14 steps, only the following were carried out: scenario specification, nuclear power plant (NPP) selection, phenomena identification and ranking table (PIRT), selection of frozen code, provision of code documentation, determination of code applicability, determination of code and experiment accuracy, NPP sensitivity analysis calculations, combination of biases and uncertainties, and total uncertainty to calculate specific scenario in a specific NPP.

The thermal hydraulic code Flownex®[1] was used to model only the reactor core to investigate the effects of the input parameters on the selected output parameters of the hot channel in the core. These output parameters were mass flow rate, temperature of the coolant, outlet pressure, centreline temperature of the fuel and surface temperature of the cladding. The PIRT process was used in conjunction with the sensitivity analysis results in order to select the relevant input parameters that significantly influenced the selected output parameters. The input parameters that have the largest effect on the selected output parameters were found to be the coolant flow channel width between the plates in the hot channel, the width of the fuel plates itself in the hot channel, the heat generation in the fuel plate of the hot channel, the global mass flow rate, the global coolant inlet temperature, the coolant flow channel width between the plates in the cold channel, and the width of the fuel plates in the cold channel.

The uncertainty of input parameters was then propagated in Flownex using the Monte Carlo based uncertainty analysis function. From these results, the corresponding probability density function (PDF) of each selected output parameter was constructed. These functions were found to follow a normal distribution.

[1] Flownex® is a registered trademark.

Keywords: Uncertainty and sensitivity analysis, Flownex, Materials Test Reactor, Monte Carlo, thermal hydraulics, Phenomena Identification and Ranking Table, Probability Density Function, code scaling applicability and uncertainty.

Index

List of Figures

List of Tables

List of symbols

Symbol	Description	Unit
A_{fuel}	Area of a fuel plate	m^2
A_{flow}	Flow area	m^2
A_{heat}	Heat transfer area	m^2
A_s or $A_{cladding}$	Cladding surface area	m^2
C_p	Specific heat capacity	kJ/kg*K
D_h	Hydraulic diameter	m
f	Friction factor	
g	Gravitational acceleration	m/s^2
h	Height of a pipe (same as the length)	m
$h_{coolant}$ or h_f	Convection heat transfer co-efficient of the coolant	W/m^2*K
h_{oe}	Exit enthalpy	kJ/kg*K
h_{oi}	Inlet enthalpy	kJ/kg*K
h_o	Total enthalpy	kJ/kg*K
Hz	Height of the fuel plate	m
I	Step number	
I	Increment size	
$\sum K$	Sum of form losses	
$k_{coolant}$ or k	Thermal co-efficient of the coolant	W/m*K
$k_{cladding}$	Thermal conductivity of cladding	W/m*K
k_{fuel}	Thermal conductivity of a fuel plate	W/m*K
L	Length of a pipe	m
Lx	Coolant channel width or gap	m
$\dot{m}$	Mass flow rate	kg/s
Δm	Mass flow rate difference	kg/s
$\dot{m}_e$	Exit mass flow rate	kg/s
$\dot{m}_i$	Inlet mass flow rate	kg/s
$\dot{m}_{inlet}$	Inlet mass flow rate	kg/s
$\dot{m}_{outlet}$	Outlet mass flow rate	kg/s

μ	Viscosity	kg/m*s
Nu	Nusselt number	
N	Total number of data points	
ΔP	Pressure difference	kPa
P_{oe}	Outlet total pressure	kPa
P_{oi}	Inlet total pressure	kPa
Δp_{oL}	Pressure loss	kPa
ΔP_{losses}	Pressure drop due to major and minor losses	kPa
p	Total pressure in the control volume	kPa
$\Delta P_{o,losses}$	Total pressure loss within a control volume	kPa
Pr	Prandtl number	
$\dot{Q}$	Heat generation rate	kW
q''	Heat flux	kW/ m^2
R^2	Regression coefficient	
Re	Reynolds number	
ρ	Density	kg/m^3
SSResid	Error sum of squares	
SSTo	Overall variation or deviation	
σ	Standard deviation	
ΔT	Temperature difference	^oC
$T_{average,coolant}$	Average temperature of the coolant	^oC
$T_{centreline}$	Centreline temperature of the fuel	^oC
$T_{cladding}$	Cladding temperature	^oC
Tco	Cladding surface temperature	^oC
$T_{coolant,inlet}$	Inlet temperature of the coolant	^oC
$T_{coolant,outlet}$	Outlet temperature of the coolant	^oC
Tci	Intermediate surface temperature between the fuel and cladding	^oC
$T_{intermediate}$	Intermediate temperature	^oC
Tmax	Maximum temperature of the fuel	^oC
T_O	Total temperature of the coolant	^oC
v	Velocity	m/s
$\dot{W}$	Work done in the control volume	kW

Wy	Width of the fuel plate	m
X	Random variable	
Y	Dependent variable	
$y_{calc,i}$	Calculated data point	
$y_{obs,i}$	Observed data point	
Δz	Difference in elevation	m
z_i	Elevation in the inlet	m
z_e	Elevation in the exit	m
z_{inlet}	Elevation in the inlet	m
$\forall$	Volume of the control volume	m^3
z_{outlet}	Elevation in the outlet	m

Abbreviations

BEPU	Best Estimate Plus Uncertainty
CFA	Control Fuel Assemblies
CLT	Central Limit Theorem
CSAU	Code Scaling Applicability and Uncertainty
ESKOM	Electricity Supply Commission (South African electricity public utility)
IAEA	International Atomic Energy Agency
IET	Integral Effect Test
IMTHUA	Integrated Methodology on Thermal Hydraulics Assessment
LBLOCA	Large Break Loss Of Coolant Accident
LOCA	Loss Of Coolant Accident
LOFA	Loss Of Flow Accident
LWR	Light Water Reactor
MTR	Materials Test Reactor
NECSA	South African Nuclear Energy Corporation
NPP	Nuclear Power Plant
PDF	Probability Density Function
PIRT	Phenomena Identification and Ranking Table
PWR	Pressurized Water Reactor
SET	Separate Effect Test
USAEC	United States Atomic Energy Commission
USNRC	United States Nuclear Regulatory Commission
WNA	World Nuclear Association
SFA	Standard Fuel Assembly

CHAPTER 1 - INTRODUCTION

1.1 Background and motivation

Figure 1.1 shows the total world energy supply and generation by fuel type. In Figure 1.1 it can be seen that nuclear energy contributes about 14.8% towards the total global electricity generation. This clearly shows that nuclear energy plays a vital role in power generation today. Apart from power generation, it also finds application in the production of medical isotopes for cancer patients and silicon production (IAEA, 2003).

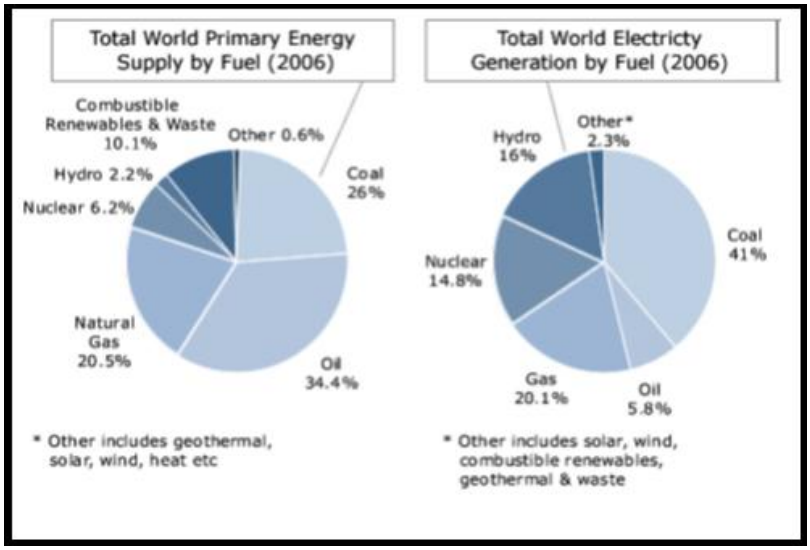

Figure 1.1 - Total world energy supply and generation by fuel respectively in 2000.

(Source: WNA, 2007).

In South Africa, the national utility Eskom supplies more than 92% of the country's electricity. Eskom has a total capacity of about 40.5 GWe. There are two nuclear reactors (which are pressurized water reactors) in South Africa that generate electricity and they are situated at Cape Town. They supply about 1.8 GWe, which is about 5% of the total capacity. In addition to this, there is a Materials Test Reactor (MTR) called SAFARI-1 which is situated at Pelindaba near Pretoria. This MTR is a 20 MW pool type light water reactor. It is a research reactor that is primarily used for the production of radioisotopes for medical use.

In the nuclear industry, safety is a major concern or consideration and there are regulatory limits that must not be exceeded. Certain acceptance criteria apply for licencing of light water reactors. Once the reactor is licensed and being operated, the licensee must always adhere to the regulatory limits presented in the acceptance criteria during normal operation and transient incidents. Some of the acceptance criteria for light water reactors are found in the 10CFR 50.46 document (USNRC, 2005). These acceptance criteria are based on the following parameters: maximum cladding temperature, maximum oxidation of cladding, maximum hydrogen generation, provision for long term cooling and retaining the core geometry in a coolable condition at all times.

One of the ways in which adherence to the safety criteria is illustrated is by performing calculations and showing that the calculated parameters remain within the imposed bounds. Historically, these calculations were based on so-called "conservative" approaches. The current international effort is to perform best estimate calculations using codes to determine the likelihood or probability of exceeding the regulatory limits during normal operation and transient accidents. In these calculations, realistic models and physical phenomena are simulated using a software code. As a result, the code that is used must be able to simulate the realistic models and/or transient accidents, for example, a loss of coolant accident (LOCA) for a certain reactor system, e.g. pressurised water reactor (PWR), materials test reactor (MTR) etc.

Safety analyses require that several steps are performed, and these include performing the uncertainty and sensitivity analysis on the simulated model. In uncertainty and sensitivity analysis the input parameters that have the largest effect on the plant's response are selected and their effects are investigated. This is of importance in understanding which parameters will contribute the most towards the uncertainty of the plant during normal operation and transient accidents. For this study, the International Atomic Energy Agency's MTR 10 MW benchmark reactor is used. The information obtained from the benchmark data was used for simulation purposes. Slabbert (2011) developed an MTR core model for simulation using the Flownex®[2] thermal hydraulic code. Since only the reactor core was modelled, the balance of the primary loop and the secondary loop of the system were not modelled. The main objective of the current study is to perform the uncertainty and sensitivity analysis on the model developed by Slabbert (2011). The uncertainty and sensitivity

[2] Flownex® is a registered trademark.

analysis is performed for steady state or normal operation only, and not for any transient scenarios as this is beyond the scope of this study.

Nuclear reactor analysis consists of both thermal hydraulics and neutronic calculations. In this study, only the thermal hydraulic aspects were investigated and this study dealt with the heat transport between the fuel and coolant. In addition to this, the thermal hydraulic calculations also addressed the fluid or coolant flow distribution in the core.

The applicable theory of thermal hydraulics and related topics are presented in Chapter 2, and a description of how Flownex is used to perform the thermal hydraulic calculation is presented in Chapter 3.

1.2 Thermal hydraulic codes

In this study a MTR Flownex model developed by Slabbert (2011) was used as already addressed. Numerous codes have been developed that are able to do thermal hydraulic calculations and perform safety analysis of nuclear reactors, apart from Flownex (Fourie, 2011). These include RELAP5, TRAC-P, RELAP5-3D, TRAC-B, TRACE, CONTAIN, MARS, ATHLET, ATLAS, BWRDYN, BOREAS and SE2-ANL.

1.3 Sources of uncertainty

Various sources of uncertainty exist that can have a significant effect on the plant's response or output parameters. These uncertainties can cause the output parameters of interest to deviate from their optimum (designed or desired) conditions and/or safety margins during normal operations or accidents. As a result, it is of importance to investigate these uncertainties in terms of their impact on the output parameters of interest. The following are the major sources of uncertainty as proposed by Reventos and Perez (2012):

- Code uncertainty e.g. code algorithms and correlations. For example, a code may have approximations to calculate phenomena like heat transfer coefficients, thermal conductivity

of the fuel etc. Thus the code's accuracy to calculate correlations needs to be evaluated or investigated in this regard.

- Plant uncertainty. This is the uncertainty due to the error on measuring instruments used to take readings of parameters like mass flow rate (using a flow meter) i.e. instrumentation error. As a result, it is important to investigate the uncertainty that can be caused by the instrumentation used for the process control of the plant.
- Simulation or model uncertainty. This addresses the uncertainty of how well the elements are represented in a code i.e. are the heat structures and control components represented well in a certain code and do their representation in a code reflect their true nature or behaviour.
- Uncertainty in input parameters. This is to investigate whether any deviation of input parameters from their optimum values can pose a serious issue on the output parameters of interest. This uncertainty in the input parameters can be due to the manufacturing or fabrication of components used in the reactor core i.e. how well a fuel plate is manufactured with respect to design specifications. Thus the manufacturing tolerances are taken into account for component input parameters since this can cause uncertainties in the output parameters of interest. In addition to component parameters, the input parameters of the system (operating parameters e.g. global mass flow rate of the coolant in the reactor core) and fluid properties of the coolant are investigated.

In this study, the uncertainty due to only the input parameters mentioned and some aspects of the fluid properties were investigated and the effect thereof determined with respect to the output parameters presented in Section 1.5. Other aspects like nodalization, discretization etc. are not investigated as these are beyond the scope of this study.

1.4 Problem statement

In performing safety analysis of any reactor or plant system, specifically in terms of transients or severe accidents, the uncertainty bands of the output parameters of interest should be calculated. The uncertainty bands depict the bounding conditions on the behaviour of the output parameters of interest with respect to the temporal progression of the accident. In order to produce meaningful

uncertainty bands, it is required to identify and select input parameters that are capable of causing significant changes on the output parameters of interest, i.e. identify and select the uncertain input parameters. In addition to this, the uncertainty boundaries or limits of the input parameters are needed. These parameters in terms of their limits are propagated to calculate the uncertainty bands of output parameters of interest. The quest of determining the uncertainty boundaries of both the uncertain input parameters and the output parameters of interest is one of the reasons for this study.

Another important motivating factor for performing this study was to implement the code scaling applicability and uncertainty (CSAU) methodology of sensitivity and uncertainty analysis as part of the development strategy in nuclear engineering studies at the School of Mechanical and Nuclear Engineering at the North-West University.

Although the CSAU methodology involves 14 steps, only steps 1-6, 9, and 12-14 were performed for purposes of this study. Thus steps 7, 8, 10 and 11 were not done and the reasons for not performing them are presented in Chapter 4.

A good starting point would be to use the IAEA MTR 10 MW which is a benchmark reactor. The uncertainty and sensitivity analysis was set up for this reactor.

1.5 Objectives of the study

The objectives of this study are outlined as follows:

- Perform a sensitivity study on all input parameters and produce ranking tables so as to select the relevant input parameters which most significantly influence the following selected output parameters:
    1. Maximum or centreline temperature of the fuel in the hot channel.
    2. Maximum cladding surface temperature in the hot channel.
    3. Temperature of the coolant in the hot channel.
    4. Mass flow rate of the coolant in the hot channel.
    5. Pressure drop in the hot channel.

- Perform uncertainty analysis of the highly ranked uncertain input parameters on the above-mentioned selected output parameters.
- Produce the PDFs of the selected output parameters, and analyse the PDFs with respect to the best estimate plus uncertainty results.

1.6 Outline of the dissertation

Chapter 2 - General theory and literature survey

This Chapter presents the general theory and literature survey relevant to the uncertainty and sensitivity analysis study. The methodologies used in performing uncertainty and sensitivity analysis are also presented.

Chapter 3 - Specific theory and continuation of literature survey

The theory that was used to undertake this study is presented in this chapter. This includes how the uncertainty and sensitivity analysis is performed in Flownex.

Chapter 4 - Methodology

This chapter presents the step-wise methodology that was followed to undertake this study.

Chapter 5 - Results, discussion and verification

This chapter presents the results produced from performing this study as well as the discussion thereof. The verification of the MTR Flownex model is also presented in this chapter. The verification was performed to ensure that the model works correctly.

Chapter 6 - Conclusion, problems experienced and recommendations

The conclusion drawn from the results produced is presented in this Chapter. The problems experienced in the study and recommendations for the future work are also addressed.

CHAPTER 2 - GENERAL THEORY AND LITERATURE SURVEY

2.1 Introduction

The main objective of this Chapter is to present a general overview of the relevant theory and a supporting literature review. An overview of uncertainty and sensitivity analysis is presented in Section 2.2. The methodologies that are widely used in uncertainty and sensitivity analysis are addressed in Section 2.3, and the CSAU methodology is described in Section 2.3.1. The conservation laws, fluid properties of the coolant, and the method of the best of fit are presented in Section 2.4-2.7.

2.2 Overview of uncertainty and sensitivity analysis

A sensitivity analysis is a study whereby input parameters are varied independently from each other within their prescribed range while investigating their effect on the output parameters of interest. The main objective of performing this analysis is to identify and select input parameters that have the largest effect on the output parameters of interest. These input parameters are known as uncertain input parameters (Wilson & Boyack, 1998). In sensitivity analysis the PIRT process (phenomena identification and ranking table) is used to identify and select uncertain input parameters. This process is discussed further in Section 2.3.1.1. These identified uncertain input parameters are used to perform the uncertainty analysis.

The uncertainty analysis is a study during which the combined uncertainty or effect of the uncertain input parameters is investigated. Thus, contrary to sensitivity analysis, it is used to investigate the combined or total effect of input parameters, specifically of the uncertain input parameters.

Various techniques exist to investigate this combined effect. The most commonly used is the Monte Carlo method which is then implemented through use in a code.

In this method, the uncertain input parameters are varied randomly and simultaneously within their prescribed range of variation, and their combined effect on the output parameters of interest is investigated. A detailed description of the Monte Carlo method is presented in Chapter 3.

2.3 Methodologies used in uncertainty and sensitivity analysis

Numerous methodologies exist that can be used to perform the uncertainty and sensitivity analysis of nuclear power plants or nuclear reactor systems for safety studies. The following are amongst the best estimate plus uncertainty (BEPU) methodologies that are widely used in uncertainty and sensitivity analysis:

- Integrated methodology on thermal hydraulics assessment (IMTHUA).
- Code scaling applicability and uncertainty (CSAU) methodology.
- Uncertainty methodology based on accuracy extrapolation.
- Automated statistical treatment of uncertainty methodology.

In this study, only the CSAU methodology is addressed since it is related to the uncertainty and sensitivity analysis methodology that is used in the Flownex code. The CSAU methodology is presented in Section 2.3.1.

2.3.1 Code scaling applicability and uncertainty (CSAU) methodology

The CSAU methodology is one of the methodologies that are used in the uncertainty and sensitivity analysis of various plant designs for safety analysis (Young *et al.,* 1998; Srivastava *et al.,* 2008; De Crécy *et al.,* 2008; Wilson, 2013; Martin & O'Dell, 2005). This methodology has been widely used for the licensing of light water reactors and especially the pressurized water reactors (PWRs). The CSAU methodology was originally developed by the USNRC (United States Nuclear Regulatory Commission) technical team.

One of the main objectives of the development of the CSAU was to account for the various uncertainties that can influence the reliability of the best estimate code calculations (De Crécy *et*

al., 2008). This includes the uncertainty due to the code or model, data used for the simulation or development of the model, etc.

In addition to this, realistic methods and physical models are used while considering the uncertainties mentioned (Young *et al.*, 1998). The CSAU methodology is independent of the code and plant design used. As a result it can be used for various safety analysis scenarios. This methodology is sub-divided into three elements namely: requirements and code capabilities, assessment and ranging of parameters, and sensitivity and uncertainty analysis. Each element is in turn sub-divided into steps, of which there are 14 in total. Figure 2.1 depicts the steps followed in the CSAU methodology. These steps are addressed briefly in Sections 2.3.1.1-2.3.1.3.

In this study only steps 1-6, 9 and 12-14 were performed. Thus steps 7, 8, 10 and 11 were not performed and the reasons for not performing them are presented in Chapter 4.

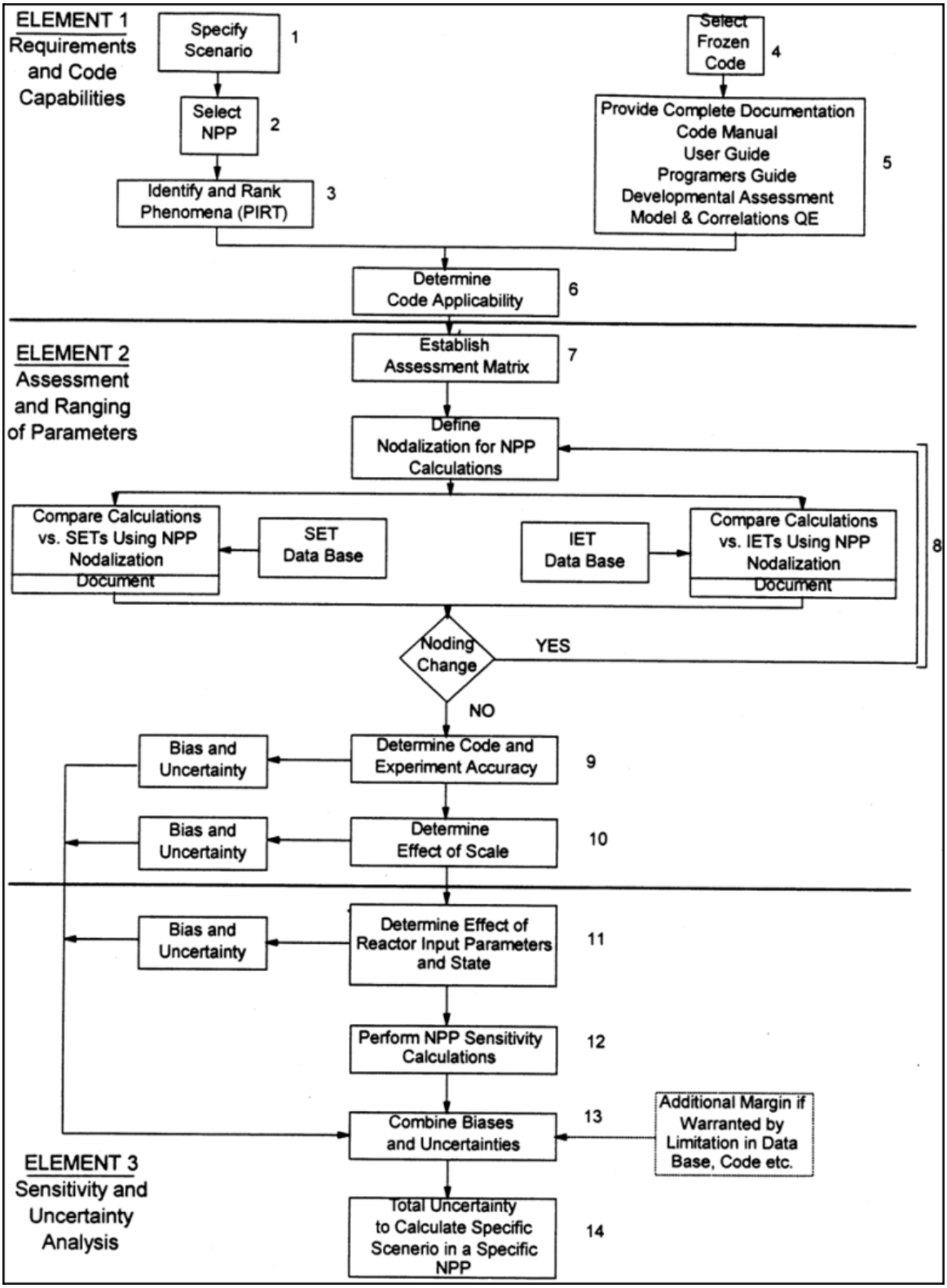

Figure 2.1 - Steps of the CSAU methodology.

(Source: Adapted from Young *et al.*, 1998).

2.3.1.1 Element 1: Requirements and code capabilities

- **Step 1: Specify scenario**

In this step of the CSAU methodology the scenario being studied and the output parameters of interest are addressed. An example of the scenario that can be analysed is the large break loss of coolant accident (LBLOCA). In addition to this, the output parameters that are investigated in the scenario are addressed. From previous studies, the output parameters that were investigated are the ones found in the acceptance criteria of light water reactors (LWRs). These output parameters include the peak cladding temperature, cladding oxidation etc.

- **Step 2: Select nuclear power plant (NPP)**

In this step, the system or nuclear power plant (NPP) that is used to study or undertake the scenario specified in step 1 is selected. An example of the NPP that can be used is a pressurized water reactor, boiling water reactor core etc. Thus the specified scenario will be based on the selected NPP e.g. the analysis of a LBLOCA in a pressurized water reactor system.

- **Step 3: Identify and Rank Phenomena (PIRT)**

The PIRT (phenomena identification and ranking table) process was initially established with the purpose of aiding the best estimate plus uncertainty (BEPU) methodologies in the licensing process (Wilson & Boyack, 1998). The main function of the PIRT process focuses on the performance of the plant. In the CSAU methodology, one of the purposes of the PIRT process is to identify the components, processes and phenomena that contribute towards uncertainties in the output parameters. The selection of these contributors in the uncertainty analysis ensures a good and effective safety analysis.

The PIRT process is independent of the code and plant system used. As a result, the PIRT process can be applied to various scenarios. The steps that are followed in the PIRT process (step 3(i) and step 3(ii)) are presented in the following paragraphs.

- **Step 3(i): Identification of influential input parameters (phenomena, components etc.).**

Previous studies showed that the development of the PIRT process is done effectively when using teams of experts with sound knowledge of the scenario under study (Larson *et al.*, 2007; Wilson & Boyack, 1998; De Crécy *et al.*, 2008; Martin & O'Dell, 2005). This team of experts then identifies all possible phenomena, processes and components that have the most significant effect on the plant response. The next step after this identification process is ranking, which is presented in step 3(ii) below. In a case where there is no team of experts available to develop the PIRT, a sensitivity or parametric study can be performed (Wilson & Boyack, 1998), in which parameters are varied one at a time while keeping other parameters constant. As a result, the individual effect of each parameter on the plant's response (output parameters) is investigated. In addition to this, the information from experiments, code simulation of the experiments and/or previous sensitivity studies of various scenarios can be used to identify influential parameters (Wilson & Boyack, 1998). The information obtained from this step is used to rank the parameters individually with respect to the influence that each parameter has on driving the plant's response.

- **Step 3(ii): Ranking of identified input parameters**

The results obtained from identifying influential input parameters are used in this step to rank the input parameters. This step is the core of the PIRT development. The input parameters are ranked between low, medium and high with respect to the influence they have on the output parameters and/or plant response (Wilson & Boyack, 1998). When ranked low, it means that a parameter has no effect on the output parameters, medium implies a moderate effect and high means that a parameter has a large effect on the output parameters. The input parameters that have no effect on the output parameters are eliminated while the ones having a moderate or large effect on the output parameters are then used for the safety analysis (De Crécy *et al.*, 2008). These selected input parameters are then propagated in the code calculation for uncertainty analysis (which forms part of the safety analysis) of the scenario. The uncertainty propagation method that is widely used in the best estimate calculations is presented in Section 2.3.1.3.

- **Step 4: Select frozen code**

In this step, a frozen version of a computational code that will be used to undertake the scenario being studied, is selected.

- **Step 5: Provide documentation of the code, developmental assessment model and correlations**

In this step the documentation of the code selected in step 4 must be provided. One of the documents required is the code manual. The code development assessment is also performed with respect to its modelling capabilities. Part of this development assessment is the verification of the code.

- **Step 6: Determine code applicability**

The code's applicability to the scenario specified in step 1 is assessed or evaluated. This is done by comparing the capabilities of the code (done in step 5) to the modelling requirements presented in steps 1-3. As a result, the analysis code is evaluated as to whether it is able to simulate and/or model the scenario, NPP and the dominant phenomena presented in step 1, 2 and 3 respectively. The shortcomings or limitations of the code with respect to its applicability to the scenario are also addressed.

2.3.1.2 Element 2: Assessment and ranging of parameters.

- **Step 7: Establish assessment matrix**

In this step, a further assessment of the code in terms of the capability to model the dominant phenomena selected in step 3 is performed. It must therefore be demonstrated that the code selected in step 4 is applicable to the scenario specified.

This is done by establishing an assessment matrix in which the phenomena or processes modelled by the code are evaluated against a set of experiments, benchmarks etc. Examples of the assessment matrices are presented in Table 2-1 and Table 2-2.

Table 2-1 - Blowdown evaluation for WCOBRA/TRAC code.

Facilities simulated		Processes assessed						
	Test feature	Number of tests	Crit flow	Break resis	Fuel temp	Heat tran	TMIN	ECC bypass
ORNL	Upflow blow-down cooling, 17 × 17	3				X	X	
G-1	Downflow blowdown cooling, 15 × 15	6				X	X	
G-2	Downflow blowdown cooling, 17 × 17	6				X	X	
Marviken	Critical flow	16	X					
CREARE	1/15, 1/5 scale ECC bypass	10						X
UPTF	Full scale ECC bypass	6		X				X
Various	In pile nuclear tests				X			
LOFT	Nuclear core, scaled PWR	4	X	X	X	X	X	X

G-1 and G-2 are proprietary tests performed by Westinghouse.

(Source: Young *et al.*, 1998).

Table 2-2 - Reflood evaluation for WCOBRA/TRAC.

Facilities simulated		Processes evaluated						
	Test feature	Number of tests	Heat tran	TMIN	COND	N_2 INJ	Fuel clad	ENTR
G-2	Downflow low pressure film boiling, forced reflood	7	X	X				X
FLECHT LFR	Forced reflood, cosine power shape, core entrainment, 15 × 15	3	X	X				X
FLECHT skewed	Forced reflood, skewed power shape, core entrainment, 15 × 15	5	X	X				X
FLECHT seaset	Forced reflood, cosine power shape, core entrainment, 17 × 17	5	X	X				X
FEBA	Forced reflood, flat cosine, effect of grids	4	X	X				X
NRU	Forced reflood, skewed power shape nuclear rods, cladding rupture	2	X	X			X	
Various	Cladding rupture, fuel relocation	4					X	
SCTF	Forced and gravity reflood, radial power, core and up plen entrainment	5	X	X				X
Achilles	Gravity reflood with nitrogen inj.	1	X			X		X
UPTF 8	Full scale steam water mixing				X			
UPTF 10	Full scale up plen, DC entrainment	7						X
UPTF 25	Full scale downcomer entrainment	1						X
CCTF	Gravity reflood, loop flows, core and upper plenum entrainment	5	X	X	X			X
LOFT	Nuclear core, scaled PWR	4	X			X		

(Source: Young *et al.*, 1998).

- **Step 8: Comparison between the experiment and code results**

The nodalization of the NPP selected in step 2 is defined. This nodalization will be used by the code for the calculations. An example of defining the nodalization is for instance specifying the number of increments or discretizations to be used in an element like a pipe, reactor vessel etc. The nodalization should be adequate to depict the behaviour or properties of the fluid at different points of the component. In this step, a code is evaluated with respect to the ability it has to accurately model and/or predict the dominant phenomena or uncertainty contributors identified in step 3 (De Crécy *et al.,* 2008). This is done by comparing the code's results of the dominant phenomena (identified in step 3) with the ones obtained from the integral effect tests (IETs) and separate effect tests (SETs).

In this way it can be assessed whether a code is capable of reflecting the true behaviour of the main contributors identified in step 3. If the nodalization results of the code's calculation deviate largely from the IETs and SETs, it is re-defined or changed until the deviation between the code and the test results is relatively low. When this is achieved, the accuracy of the code with respect to the experiment is determined as will be explained in step 9.

In a case where there are no experimental or test facility results to use for comparison, assumptions based on expert opinion and engineering judgement are made regarding the uncertainty contributors identified.

The biases are also quantified and included in this step so as to take into account a code's deficiency to simulate and predict the true behaviour of the uncertainty contributors (e.g. processes, phenomena etc.).

- **Step 9: Determine code and experiment accuracy**

In this step, the accuracy of the code with respect to the experiment (IETs and SETs) is addressed. This is referred to as the validation of the code. An example of determining the accuracy of the code with respect to the experiment is depicted in Figure 2.2. From Figure 2.2 it can be seen that the ratio of measured (experimental) results and predicted (code) results is calculated. Thus from these results, it can be determined whether a selected code accurately predicts the main

contributors to the scenario or not. This step of the CSAU methodology is done for quality assurance of the code's results.

From Figure 2.2, parameters like the σ (standard deviation) and mean can be determined for both the experiment and code data. These results are used to determine the accuracy of the experiment and code data or results.

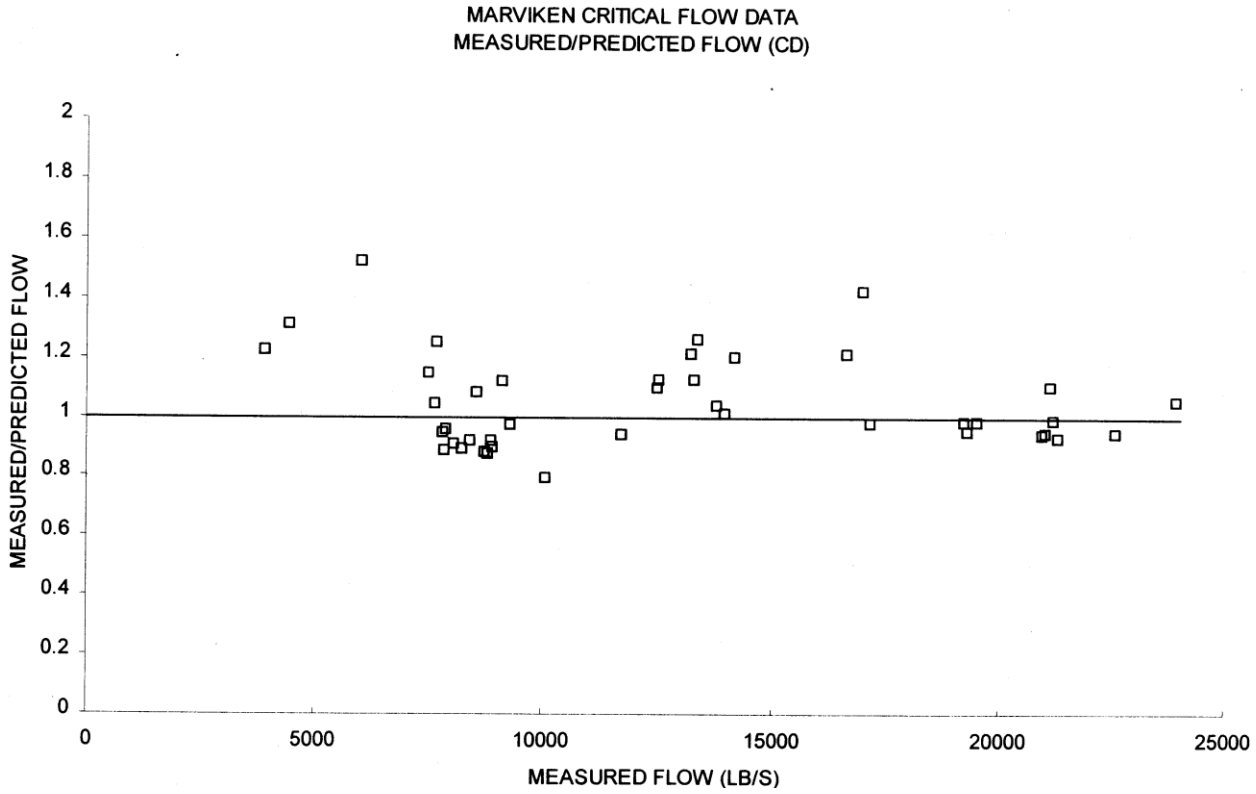

Figure 2.2 - An example of showing the code's accuracy with respect to the results of the experiment.
(Source: Young *et al.*, 1998).

- **Step 10: Determine effect of scale**

It is of importance to determine whether a code is capable in simulating not only small scale (test facility) simulations but can also perform larger scale simulations. This is important in terms of verifying if a code can produce the same results of uncertainty contributors of the scenario for both small and large scale plants. This is the intent of step 10 in the CSAU methodology.

2.3.1.3 Element 3: Performing uncertainty and sensitivity analysis of the NPP

- **Step 11: Determine the effect of reactor input parameters and state**

This step addresses the effect of the state of the reactor on the uncertain input parameters or dominant phenomena that are dependent on it. This effect is investigated at the beginning of the transient. In addition to this, the uncertainty on the transient simulation is also quantified. An example can be the investigation of the transient of running the reactor at full or at 50% power. The effect thereof on the input parameters can be highly dependent on power (reactor state).

The implications of this effect are also addressed. The uncertainties and biases of the effect of reactor state on these parameters are thus included when combining the uncertainties in step 13.

- **Step 12: Perform NPP sensitivity analysis**

In this step, the sensitivity analysis of the dominant phenomena or main contributors to the scenario is performed. The sensitivity analysis is performed so as to investigate the individual effect of each contributor on the output parameters of interest. As a result, the effect of individual contributors is evaluated independently from each other with respect to the output parameters of interest.

- **Step 13: Combine biases and uncertainties**

In this step, the biases and uncertainties determined or established in the above steps of the main contributors are combined so as to investigate their total or combined effect on the output parameters of interest. These biases and uncertainties are normally specified in an input deck before calculating their total effect on the output parameters of interest. This step of the CSAU methodology is referred to as the uncertainty propagation step.

A propagation method that is commonly used in the BEPU approach is a Monte Carlo based uncertainty analysis method (Young *et al.*, 1998). In the Monte Carlo method, contributors or input parameters are varied randomly and simultaneously within their respective variation ranges (uncertainty limits established from the above steps) and their combined effect is investigated with

respect to the output parameters of interest. A detailed description of a Monte Carlo method is presented in Chapter 3.

One of the main objectives of this step of the CSAU is to produce probability density functions (PDFs) of the output parameters of interest.

- **Step 14: Total uncertainty to calculate a specific scenario in a specific NPP**

In this step, the results (PDFs) produced in step 13 are used to determine the uncertainty bounds or limits. These limits are the ones that are used in the interpretation of the results with respect to the scenario i.e. the implication of the results with respect to the scenario specified in step 1 is analysed. For transient accidents, this analysis is normally based on the regulatory limits presented in the acceptance criteria of the NPP.

2.4 Overview on the theory of thermal hydraulics

This study is based on a thermal hydraulic analysis. Thus, it is of importance to have a good appreciation of the governing equations or conservation laws that are used to solve the thermal hydraulic parameters of interest. These parameters are as follows: mass flow rate, pressure drop, centreline temperature of the fuel and cladding surface temperature.

The conservation equations that are used to solve these parameters are presented in Sections 2.4.1-2.4.3.

2.4.1 Law of mass conservation

This mass conservation law basically gives a measure of a rate of change of mass over time with respect to the inlet and outlet mass flow rates through a control volume. Equation 2.1 (Rousseau & Van Eldik, 2011) provide the mass conservation law.

$$\forall \frac{\partial \rho}{\partial t} + \dot{m}_e - \dot{m}_i = 0 \qquad 2.1$$

In Equations 2.1, the first term is the rate of change of mass over time and the second and third terms are the outlet and inlet mass flow rate within a control volume (Munson *et al.*, 2005; MTI, 2011; Rousseau & Van Eldik, 2011). In Equation 2.1, ∀ is the volume of the control volume. In Flownex, Equation 2.1 is used to calculate the mass balance of the coolant in each control volume.

2.4.2 Law of momentum conservation

The momentum conservation equation is derived for both incompressible and compressible flow. In this study, the fluid (coolant) that is used is incompressible. Equation 2.2 represents the conservation of momentum for incompressible flow.

$$\rho L \frac{\partial v}{\partial t} + (P_{oe} - P_{oi}) + \rho g(z_{outlet} - z_{inlet}) + \Delta P_{o,losses} = 0 \qquad 2.2$$

In Equation 2.2, the first term on the left is the rate of change of momentum over time, while the second term is the difference in total pressure in the inlet and outlet within a control volume (Munson *et al.*, 2005; MTI, 2011; Rousseau & Van Eldik, 2011). The third term is the change in momentum due to elevation, and the last term is the total pressure loss within a control volume.

2.4.3 Law of energy conservation

This conservation law describes the rate of change of energy within a control volume. Equation 2.3 (Rousseau & Van Eldik, 2011) represent the conservation of energy.

$$\dot{Q} + \dot{W} = \forall \frac{\partial}{\partial t}(\rho h_o - p) + \dot{m}_e h_{oe} - \dot{m}_i h_{oi} + \dot{m}_e g z_e - \dot{m}_i g z_i \qquad 2.3$$

The first terms in Equation 2.3 denotes the energy generated and work done in the control volume. The terms on the right presents the rate change of energy and convection of energy out of a control volume (MTI, 2011; Rousseau & Van Eldik, 2011; Koretsky, 2004). Equation 2.3 is used in Flownex to calculate the total energy lost, generated and work done in the control volume.

2.5 Fluid properties of a coolant used in the MTR core

The coolant that is used in the Materials Test Reactor (MTR) is light water (H_2O) and it has the following fluid properties: density, viscosity, conductivity, specific heat capacity, thermal conductivity and bulk modulus. The coolant used is in a liquid phase, thus no two phase flow is experienced. Bulk modulus gives a measure of the compressibility of a fluid or coolant. In this study the bulk modulus is not of importance because the calculation cases do not involve fast pressure transients. As a result, the density, thermal conductivity, viscosity, conductivity and specific heat capacity of a coolant were investigated. The effect of these fluid properties on the selected output parameters was investigated by performing a parametric or sensitivity study. The detailed description of how a parametric or sensitivity study is performed in Flownex is presented in Chapter 3. The relationship between the selected output parameters of interest and the fluid properties is addressed in this section. This is of importance in predicting the expected results from Flownex. Sections 2.5.1 – 2.5.4 presents the relationship between the fluid properties and selected output parameters.

2.5.1 Cladding surface and centreline fuel temperature

The centreline temperature of the fuel and cladding surface temperature are related. This is because the heat generation in the fuel is transferred to the cladding by conduction and finally to the coolant by the convection heat transfer mechanism. Thus, in this section, the relationship between the cladding surface temperature and the fluid properties of a coolant will be addressed since the heat is removed from the cladding by the coolant. Equation 2.4 shows the relationship between the cladding surface temperature and the convection heat transfer coefficient of a coolant (Incropera *et al.*, 2006).

$$\dot{Q} = h_{coolant} A_{heat} (T_{cladding} - T_{average,coolant}) \qquad 2.4$$

OR

$$T_{cladding} = \frac{\dot{Q}}{h_{coolant} A_{heat}} + T_{average,coolant}$$

In Equation 2.4, $\dot{Q}$ is the heat generation rate in the fuel, $h_{coolant}$ is the heat transfer co-efficient of the coolant, A_{heat} is the heat transfer area of a coolant (flow coolant heat transfer area) where heat is removed by a coolant, $T_{cladding}$ is the cladding surface temperature, and $T_{average,coolant}$ is the temperature of the coolant.

The convection heat transfer coefficient of a coolant is a function of the fluid properties of a coolant. This relationship is presented by Equations 2.5 – 2.8 as follows:

$$Nu = \frac{h_{coolant} D_h}{k_{coolant}} \quad 2.5$$

OR

$$h_{coolant} = \frac{Nu * k_{coolant}}{D_h}$$

In Equation 2.5, Nu is a Nusselt number which is given by Equation 2.6, $k_{coolant}$ is the thermal conductivity (fluid property) of a coolant and D_h is a hydraulic diameter of a coolant channel.
Equation 2.6 is known as Dittus-Boelter equation for turbulent flow, and it is applicable to the following limits (Munson et al., 2005):

- Re≥10 000, and
- 0.6≤Pr≤160.

In this study the limits of both the Reynolds and Prandtl number are as follows:

- 8 505≤Re≤667 488, and
- 3.00≤Pr≤5.22.

From these limits it can be seen that the lower limit for the Reynolds number for this study is below the limits of the Dittus-Boelter equation. Equation 2.6 was used to calculate the heat transfer coefficient irrespective of the difference in the lower limits since the Dittus-Boelter is used in Flownex to calculate the heat transfer coefficient.

$$Nu = 0.023 Re^{0.8} Pr^{0.4} \quad 2.6$$

In Equation 2.6, Re is the Reynolds number and is given by Equation 2.7, and Pr is the Prandtl number which is given by given Equation 2.8.

$$\mathrm{Re} = \frac{\rho v D_h}{\mu} \tag{2.7}$$

In Equation 2.7, ρ is the density (fluid property), v is the velocity, and μ is the viscosity (fluid property) of the coolant.

$$\mathrm{Pr} = \frac{c_p \mu}{k_{coolant}} \tag{2.8}$$

In Equation 2.8, c_p is the heat capacity (fluid property) of the coolant. By substituting Equations 2.6 - 2.8 into 2.5, the following equation is obtained:

$$h_{coolant} = \frac{0.023 * \rho^{0.8} * v^{0.8} * {c_p}^{0.4} * {k_{coolant}}^{0.6}}{{D_h}^{0.2} * \mu^{0.4}} \tag{2.9}$$

Substituting Equation 2.9 into 2.4, the relationship between the cladding surface temperature and the fluid properties of a coolant is obtained as shown by Equation 2.10.

$$T_{cladding} = \frac{Q}{A_{heat}} * \left(\frac{{D_h}^{0.2} * \mu^{0.4}}{0.023 * \rho^{0.8} * v^{0.8} * {k_{coolant}}^{0.6} * {c_p}^{0.4}} \right) + T_{average,coolant} \tag{2.10}$$

2.5.2 Temperature of the coolant

Equation 2.10 can be re-written as shown in Equation 2.11 in order to show clearly the relationship between $T_{average,coolant}$ and fluid properties.

$$T_{average,coolant} = T_{cladding} - \frac{Q}{A_{heat}} * \left(\frac{{D_h}^{0.2} * \mu^{0.4}}{0.023 * \rho^{0.8} * v^{0.8} * {k_{coolant}}^{0.6} * {c_p}^{0.4}} \right) \tag{2.11}$$

2.5.3 Mass flow rate of the coolant

The mass flow rate of the coolant in the coolant flow channel is dependent upon the geometry of the coolant flow channel e.g. flow area. However, the fluid properties of the coolant have an insignificant effect on the mass flow rate of the coolant in the coolant flow channel. This is because when the pressure (momentum) and temperature (energy) of the system are kept constant the mass flow rate according to the conservation equations is the only parameter that will change in this case. The geometry of the flow area is the primary parameter that can cause the mass flow rate to change assuming the pumping power or rate is constant. The relationship between the mass flow rate of the coolant and the flow area assuming the pumping power is constant is shown in Equation 3.8.

2.5.4 Pressure drop

The pressure drop is highly influenced by the density and velocity of the coolant or fluid and the friction factor (Munson *et al.,* 2005). The relationship between the density of the coolant and the pressure drop in the hot channel is derived from the conservation of momentum equation. Equation 2.12 comes from Equation 2.2 where the transient as well as the pressure drop due to elevation terms are neglected. This momentum equation is for one dimensional incompressible steady flow (MTI, 2011, Munson *et al.,* 2005).

$$P_{o,e} - P_{o,i} = -\frac{fh\rho|v|v}{2lx} \qquad 2.12$$

In Equation 2.12 $P_{o,i}$ and $P_{o,e}$ denotes the total inlet and outlet pressures respectively of the coolant in the hot channel, f is the frictional factor which is inter alia a function of the Reynolds number, h is the height or length of the coolant flow channel and l_x is the coolant flow channel gap between the fuel plates in the hot channel.

2.6 R^2 method: Testing a distribution for a good fit

In this method a theoretical function is postulated, and the data is compared with this function. Thus, the data is tested as to whether it follows the distribution that is assumed. This method is amongst the commonly used statistical methods that are used to test a distribution for a good fit. A parameter that determines an appropriate fit in this method is represented by R^2. This parameter determines the difference between the observed and calculated data, by way of calculating the deviation between the two data sets. An appropriate fit procedure is described in detail in Section 2.6.1.

2.6.1 Calculation of the coefficient of determination (R^2)

Equation 2.13 is used to calculate the co-efficient of determination (Devore & Farnum, 2004). If R^2 is close to and or equals 1.0, this implies that the assumed distribution is a good fit. Thus, the data follows a proposed/assumed distribution.

$$R^2 = 1 - \frac{\text{SSResid}}{\text{SSTo}} \tag{2.13}$$

In Equation 2.13, $SSResid$ gives a measure of the sum of the errors squared between the calculated and observed data. Equation 2.14 is used to calculate $SSResid$.

$$\text{SSResid} = \sum(y_{obs,i} - y_{calc,i})^2 \tag{2.14}$$

In Equation 2.14, $y_{obs,i}$ denotes the observed data points (this can be from an experiment) and $y_{calc,i}$ represents the data points calculated from a model/equation which can be dependent on either one or two independent variables. $SSTo$ gives a measure of the overall variation in the observed data and it is given by Equation 2.15.

$$\text{SSTo} = \sum(y_{obs,i})^2 - \frac{(\sum y_{obs,i})^2}{n} \tag{2.15}$$

In Equation 2.15, n denotes the total number of observations or data points. The numerical values obtained from calculating both $SSResid$ and $SSTo$ are used to calculate the value of R^2. The value of R^2 is used to conclude whether the assumed/proposed distribution is a true representation of variable y.

2.7 The Materials Test Reactor (MTR)

In this study, IAEA's MTR 10 MW generic reactor was used. This is a research reactor (used as a benchmark) and it was modelled using the Flownex thermal hydraulic code. Only the reactor core was modelled as mentioned in Chapter 1. A brief description and design specifications of IAEA's MTR 10 MW reactor are presented in Section 2.7.1.

2.7.1 Description and design specifications of the IAEA MTR-10 MW reactor

Figure 2.3 depicts the plan view layout of the IAEA MTR 10 MW reactor core. This is a pool type reactor, and it uses light water as both a coolant and moderator (IAEA, 1980; IAEA, 1992). The reactor core is submerged in water. The light water also functions as a reflector. In addition to light water as a reflector, graphite blocks are also used as a reflector to reflect neutrons back to the core. This plays a major role in ensuring that the neutrons do not leak out of the reactor core. From Figure 2.3, it can be seen that the graphite reflector blocks are placed on two opposite sides (IAEA, 1980; Hamidouche *et al.,* 2009; Hainoun *et al.,* 2010).

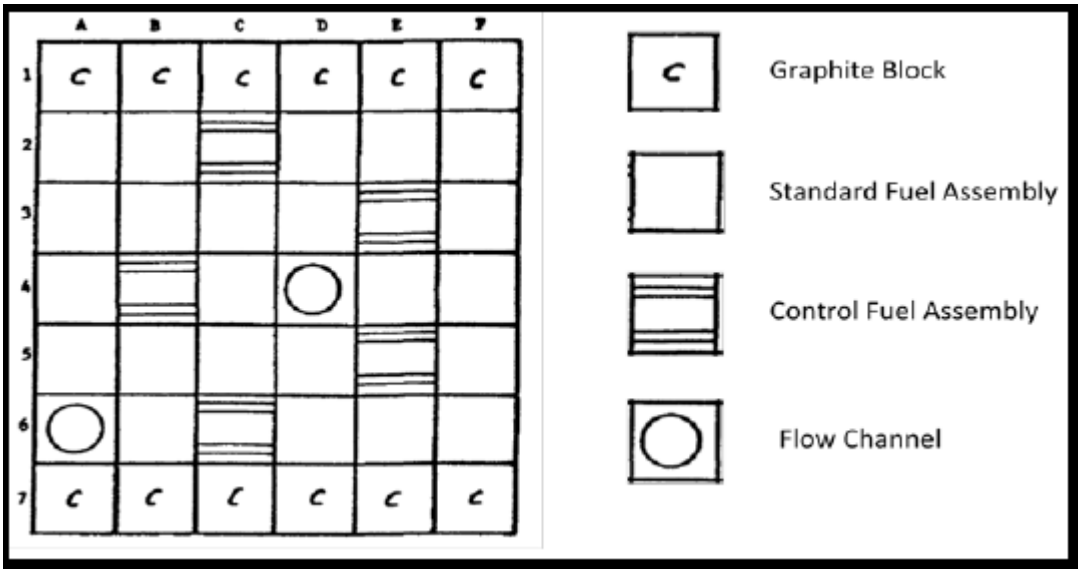

Figure 2.3 - Layout of IAEA's MTR 10 MW core.

(Source: IAEA, 1992).

In the MTR core, plate type fuel elements are used and aluminium as cladding. The reactor core is a 5 x 6 array consisting of the following:

- 23 Standard Fuel Assemblies (SFA). Each SFA contains about 23 fuel plates.
- 5 Control Fuel Assemblies (CFAs). Each CFA contains 17 fuel plates.
- 2 Flow channels. The remaining spaces are for the absorber plates used in each CFA. These absorber plates are made of chromium.

Figure 2.4 shows the SFA and the CFA with the absorber plates of the IAEA MTR 10 MW reactor. During the time when the reactor is operating, primary coolant pumps are used to pump the water into the core to remove the heat generated during the fission reaction. These pumps use forced circulation for heat removal or heat transport from the core to the secondary side of the MTR system. When more coolant is required in the core (during a transient accident), the water in the pool is used. This mode of cooling used is called natural circulation. As a result, no pump is required to perform this kind of core cooling process. Table 2-3 presents the design specifications and operating conditions of IAEA MTR 10 MW benchmark reactor.

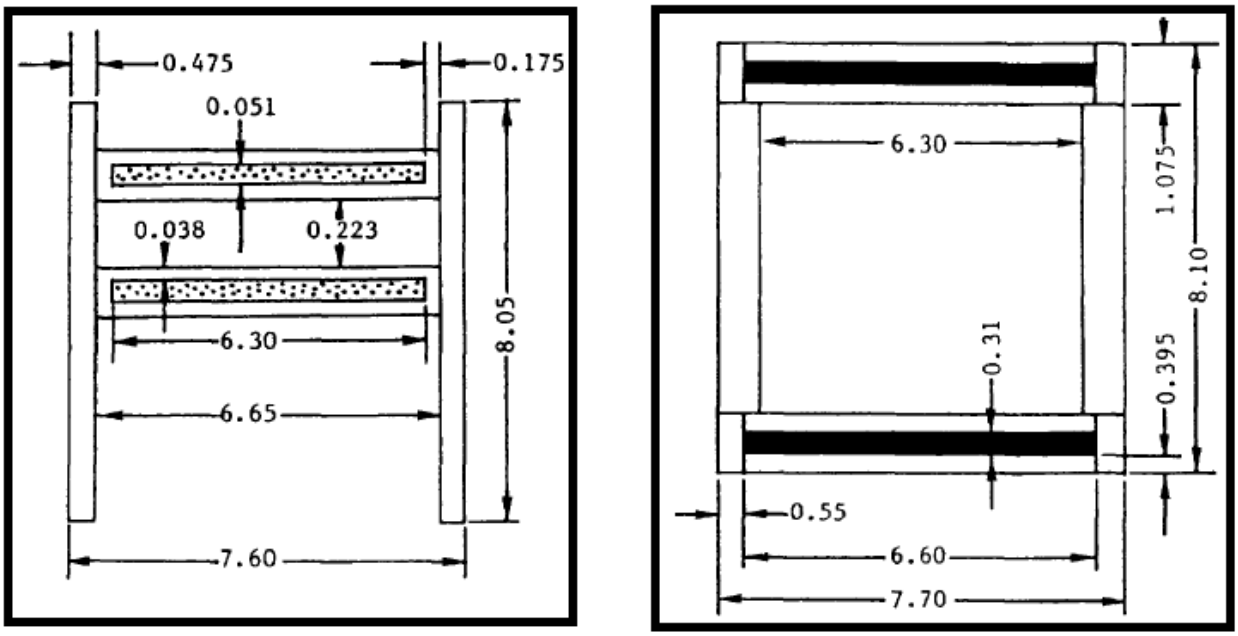

Figure 2.4 - The dimensions of the Standard Fuel Elements (left), and Control Fuel Elements (Right).

(Source: Adapted from IAEA, 1992).

Table 2-3 - Design specifications and operating conditions of IAEA's MTR-10 MW.

Description	Value	Units
Thickness of plate	1.27	mm
Dimensions of the fuel	63 x 0.51 x 600	mm
Number of SFA	23	
Number of CFA	17 fuel plates + 4 Aluminium plates	
Fuel plate shape	straight	
Coolant and moderator	Light water (H_2O)	
Reflector	Light water and Graphite	
Geometry of the core	5 x 6 grid, 1 irradiation channel in the centre and 1 at the edge of the core	
Volumetric flow rate of a coolant	1000	m^3/h
Operating pressure	1.7	bar
Inlet temperature of a coolant	38	^oC
The thickness of a coolant channel	2.19	mm
Thermal conductivity of a fuel meat	50	W/mK
Thickness of cladding	0.38 in the inner plate, and 0.495 at the outer plate	mm
Cladding material	Aluminium	

Description	Value	Units
Thermal conductivity of Aluminium cladding	180	W/mK
Density of Aluminium cladding	2.7	g/cm^3
Pitch of a lattice	81 x 77	mm
Heat capacity of Aluminium cladding	2.069 + 0.0012T (T is temperature in Kelvin)	J/cm^3K
Heat capacity of fuel meat	1.929 + 0.0007T	J/cm^3K
Density of the fuel	0.68	g/cm^3
Density of Uranium	4.45	g/cm^3
Peaking factors	1.5 for Axial, and 1.4 for Radial	
Uranium contained in a single standard fuel element	390	g
Uranium contained in a single control fuel element	288	g
Duration of a cycle	30.6	days
Enrichment of the fuel (U-235)	19.75	%

(Source: IAEA, 1980; IAEA, 1992).

CHAPTER 3 - SPECIFIC THEORY AND CONTINUATION OF LITERATURE SURVEY

3.1 Introduction

The theory that is relevant to this study with regard to the uncertainty and sensitivity analysis using the Flownex code is presented. In addition to this, a description of the Flownex code and the MTR model are provided.

3.2 The Flownex code

In nuclear reactor analysis, specifically in the field of thermal-hydraulics, there are two most important parameters namely heat generation and coolant or fluid flow distribution in the core. These parameters are of importance in performing a thermal hydraulic analysis of the reactor core. In this research study, the computational tool or code used to perform the analysis is Flownex. This code is amongst the thermal hydraulic codes that may be used to reflect the true nature or behaviour of the plant or reactor core since it accounts for all three fundamental conservation equations as well as the fluid properties and component characteristics. Flownex basically calculates or simulates how the heat is transferred from the fuel elements, where heat is generated, to the coolant. The main purpose of the coolant is to transport the heat generated in the core to the secondary side. In addition to this Flownex also calculates how the coolant is distributed in the fuel assemblies within the core. This code can solve both steady state and dynamic (transients) calculations using the above-mentioned equations. In this research study, an MTR Flownex model that has been developed by Slabbert (2011) was used. A brief description of the MTR model developed is presented in Section 3.2.1. In this section only an overview of the model is given and further information or details regarding how the model was developed or simulated can be found in Slabbert's study (Slabbert, 2011).

3.2.1 Description of the MTR Flownex model

The IAEA MTR core configuration shown in Figure 2.3 is not symmetrical, and this makes it difficult to model. Hainoun *et.al* 2010 restructured the IAEA MTR core configuration in such a way that it is symmetrical and can be split into quarters for modelling simplification and core analysis. The IAEA MTR restructured core configuration is shown in Figure 3.1. From the symmetry seen in Figure 3.1, Slabbert (2011) decided to model only a quarter of the core. The IAEA MTR 10 MW benchmark reactor specifications were used to simulate the MTR in Flownex. These specifications are presented in Table 2-3. Only the core was modelled, as a result the balance of the primary loop and the secondary loop were not modelled (Slabbert, 2011). The boundary conditions were used to take into account the pumping effect of the primary coolant pump(s). In Figure 3.1, there are 21 SFAs, 4 CFAs and 1 central flow channel containing both water and aluminium, and also bypass channels. As specified in Table 2-3, each SFA and CFA contains 23 and 17 fuel plates respectively. The core layout presented in Figure 3.1 is symmetrical, and can be divided into four symmetrical parts (Slabbert, 2011). Figure 3.2 depicts the MTR Flownex network model simulated. The coolant enters the core at the top and gets distributed in the fuel assemblies in the core. In Figure 3.2 , the boundary conditions are specified at the inlet of the core for the inlet pressure and temperature. The specified values are 38 ºC and 1.7 bar for the inlet temperature and pressure of the coolant. This is to ensure that the coolant enters the core at these desired conditions as specified in Table 2-3. A pool is also modelled so as to make the model more realistic. A mass flow rate boundary condition is specified at the exit or outlet of the core to ensure that the mass flow rate of the coolant is conserved. This is important in ensuring that a constant mass flow rate is maintained. In a case where the mass flow rate of a coolant drops below 85% of its nominal value, the pool water is used for cooling by opening a valve that is connected to the core (Slabbert, 2011). Natural circulation of water is used in this case, thus no pump is needed to deliver the water to the core during the cooling process. The same cooling phenomenon is used during transient accidents e.g. Loss Of Coolant Accident (LOCA) or Loss Of Flow Accident (LOFA).

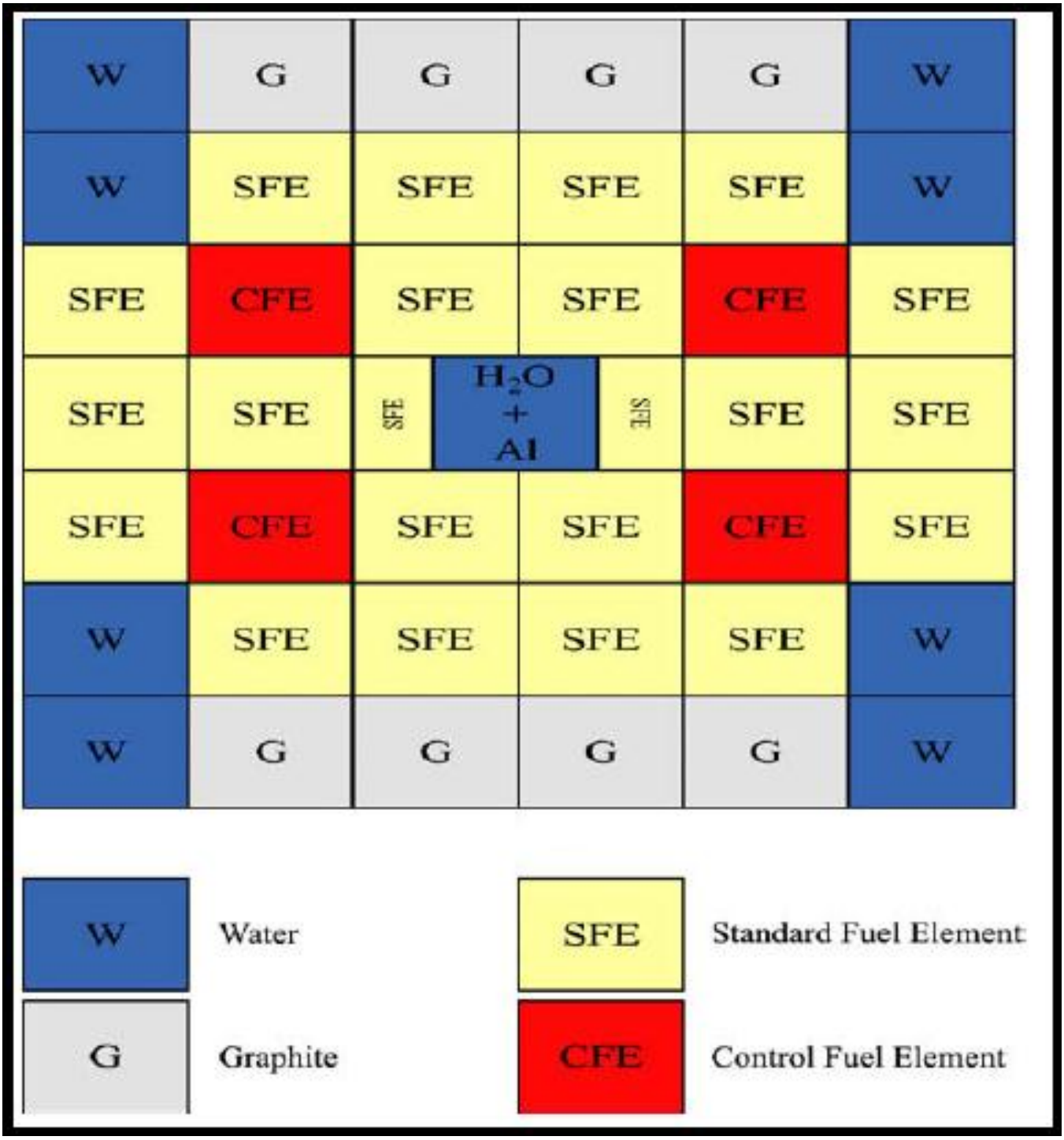

Figure 3.1 - Core layout of an MTR model.

(Source: Hainoun *et al*., 2010).

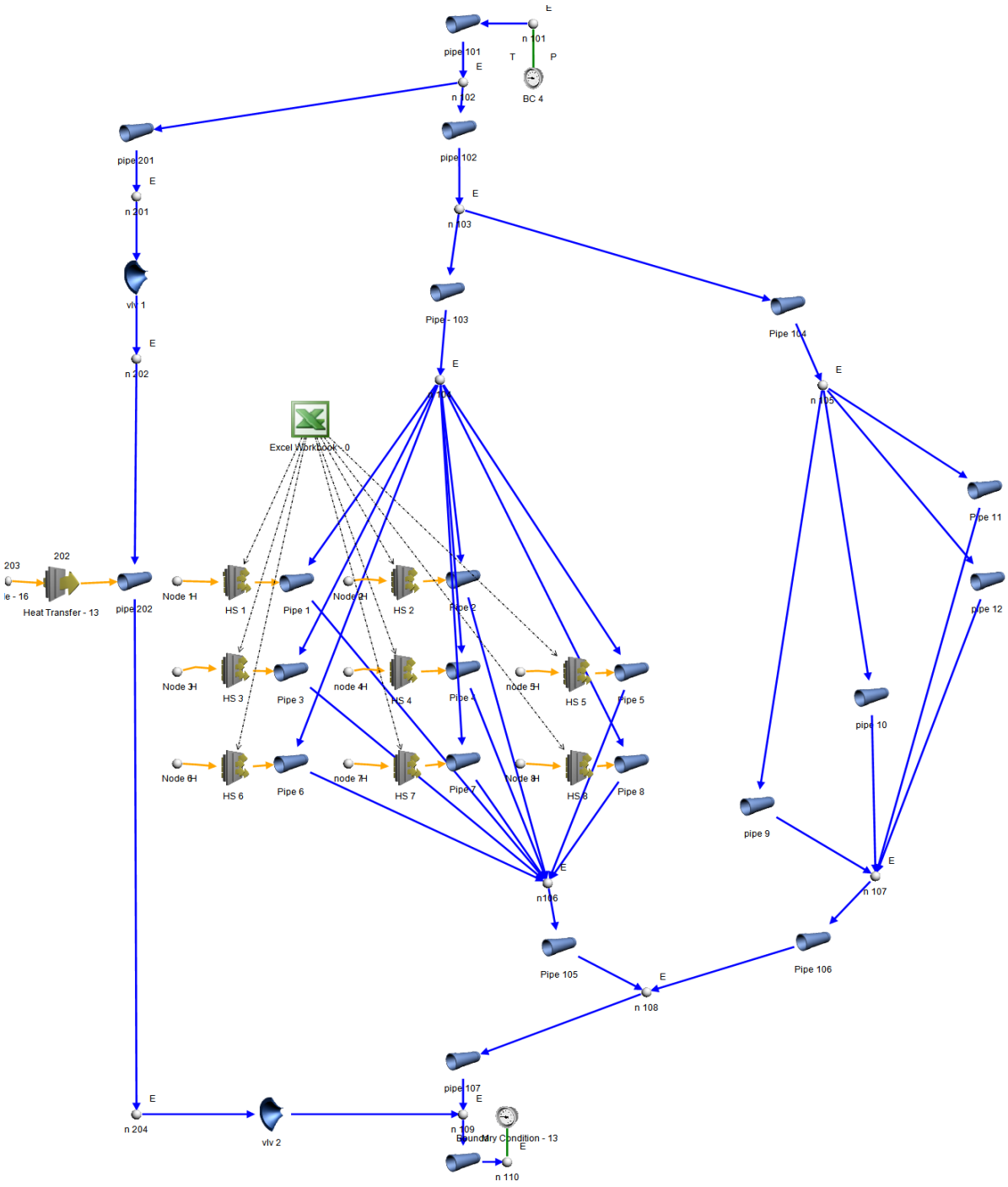

Figure 3.2 - Flownex model of an MTR 10 MW core.

3.3 Parameters with uncertainty

The input parameters that can cause uncertainties in the output parameters of an MTR model reactor core are:

- Fluid properties of a coolant e.g. density, specific heat capacity, thermal conductivity etc.
- Component parameters e.g. dimensions of the coolant flow channel, heat sources etc.
- System parameters e.g. global mass flow rate and inlet temperature of a coolant in the reactor core, global power.
- Other parameters e.g. numerical solvers, heat transfer coefficient model, discretisation etc. These parameters were considered but not investigated as they were outside the scope of this research study.

The input parameters that are likely to cause uncertainties in each output parameter of interest are presented in Sections 3.3.1-3.3.4. In these sections, the impact of the input parameters on the output parameters is addressed according to a parametric or individual effect. As a result, the effect of input parameters is addressed independently from each other.

3.3.1 Centreline temperature of the fuel and cladding surface temperature in the hot channel

The input parameters that are likely to cause a large effect on the centreline temperature of the fuel and cladding surface temperature are:

- Global mass flow rate and temperature of a coolant.
- Local power in the hot channel.
- Specific heat capacity of the coolant.
- Thermal conductivity of the coolant.
- Viscosity of the coolant.
- Thermal conductivity of the fuel and cladding.
- Dimensions of the coolant flow channel.

Sections 3.3.1.1-5 present a description of how these input parameters can impact the above-mentioned output parameters.

3.3.1.1 Global mass flow rate and temperature of a coolant

A coolant in the core is used to remove the heat from the cladding surface by means of convection heat transfer as already explained in Chapter 2. This is the heat generated in the fuel elements during the fission reaction. The relationship between the heat generated in the fuel, inlet mass flow rate (global) and the temperature difference of the coolant in the hot channel is given by Equation 3.1.

$$\dot{Q} = \dot{m}c_p(T_{coolant,outlet} - T_{coolant,inlet}) \quad 3.1$$

OR

$$T_{coolant,outlet} = T_{coolant,inlet} + \frac{\dot{Q}}{\dot{m}c_p}$$

The relationship between the heat generated in the fuel, average temperature of the coolant and the cladding surface temperature is given by Equation 3.2. In Equation 3.2 the average temperature ($T_{average,coolant}$) of the coolant is given by Equation 3.3. Substitute Equation 3.3 into 3.2 and from this Equation 3.4 is obtained.

$$\dot{Q} = h_{coolant}A_{heat}(T_{cladding} - T_{average,coolant}) \quad 3.2$$

OR

$$T_{cladding} = \frac{\dot{Q}}{h_{coolant}A_{heat}} + T_{average,coolant}$$

$$T_{average,coolant} = \frac{(T_{coolant,outlet}+T_{coolant,inlet})}{2} \quad 3.3$$

$$\frac{\dot{Q}}{h_{coolant}A_{heat}} = T_{cladding} - \frac{(T_{coolant,outlet}+T_{coolant,inlet})}{2} \quad 3.4$$

OR

$$T_{coolant,outlet} = 2 * (T_{cladding} - \frac{T_{coolant,inlet}}{2} - \frac{\dot{Q}}{h_{coolant}A_{heat}})$$

By substituting Equation 3.4 into 3.1, the relationship between the heat generated in the fuel, cladding surface temperature, and the inlet temperature of the coolant is obtained. Equation 3.5 shows this relationship.

$$T_{cladding} = \dot{Q}\left(\frac{1}{h_{coolant}A_{heat}} + \frac{1}{2\dot{m}c_p}\right) + T_{coolant,inlet} \quad 3.5$$

In Equation 3.5 it can be seen that the cladding surface temperature is directly proportional to the heat generated in the fuel and the inlet temperature (global) of the coolant. The cladding surface temperature is inversely proportional to the inlet mass flow rate of the coolant as seen in Equation 3.5.

3.3.1.2 Local power in the hot channel

Figure 3.3 depicts the heat transfer chain from the centre of the fuel (T_{max}) to the intermediate surface between the fuel and cladding (T_{ci}) and to the cladding surface (T_{co}), and finally to the coolant where the heat is finally removed. In Figure 3.3, $q'' = \frac{\dot{Q}}{A}$, and A is the area of either the fuel or cladding depending on the area of interest. The relationship between the heat generated in the fuel and the centreline temperature of the fuel is given by Equation 3.6 (Incropera *et al.*, 2006; Todreas & Kazimi, 1990, Hochreiter, 2004). This equation represents heat conduction from the centre of the fuel to the intermediate surface between the fuel and cladding.

$$\dot{Q} = k_{fuel}A_{fuel}(T_{centreline} - T_{intermediate}) \quad 3.6$$

OR

$$T_{centreline} = \frac{\dot{Q}}{k_{fuel}A_{fuel}} + T_{intermediate}$$

From Equation 3.6 $T_{centreline}$ is the centreline temperature of the fuel, k_{fuel} is the thermal conductivity of the fuel, and A_{fuel} is the surface area of the fuel where heat is transferred via conduction. $T_{intermediate}$ is the intermediate surface temperature between the fuel and the cladding as seen from Figure 3.3. In Equation 3.6 it can be seen that when the heat generation rate in the fuel increases, the centreline temperature of the fuel will also increase.

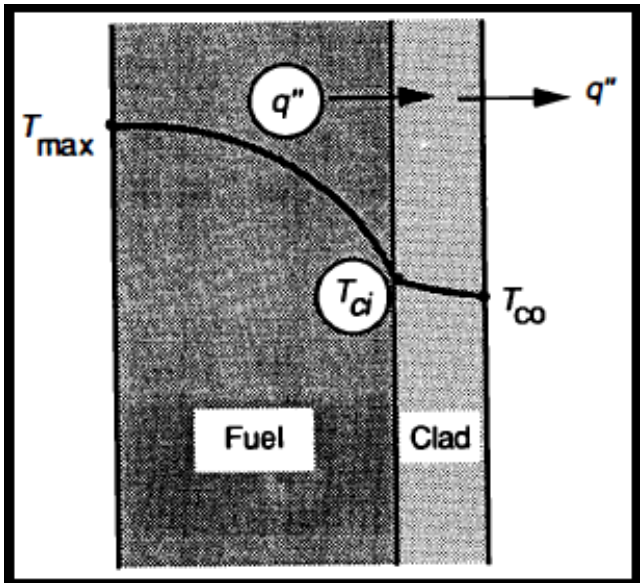

Figure 3.3 - Heat transfer chain from the centre of the fuel to the cladding surface.

(Source: Todreas & Kazimi, 1990).

3.3.1.3 Thermal conductivity of the fuel and cladding

From Equation 3.6, it can be seen that the centreline temperature of the fuel is inversely proportional to the thermal conductivity of the fuel. This implies that an increase in the thermal conductivity of the fuel will cause a decrease in the centreline temperature of the fuel. The inverse also applies. The thermal conductivity is defined as the ability of a material to conduct heat effectively from one point to another (Incropera *et al.*, 2006, Todreas & Kazimi, 1990). Equation 3.7 shows the relationship between the cladding surface temperature and the cladding's thermal conductivity. From this equation it can be seen that cladding surface temperature is inversely proportional to the cladding's thermal conductivity. The same effect as in the centreline temperature of the fuel also applies to the cladding surface temperature since it has the same relation to thermal conductivity.

$$\dot{Q} = k_{cladding} A_{cladding} (T_{intermediate} - T_{cladding}) \quad 3.7$$

OR

$$T_{cladding} = -\frac{\dot{Q}}{k_{cladding} A_{cladding}} + T_{intermediate}$$

3.3.1.4 Fluid properties of a coolant

The relationship between the cladding surface temperature and the fluid properties of the coolant (specific heat capacity, viscosity and thermal conductivity) is given by Equation 2.10. From Equation 2.10, it can be seen that the cladding surface temperature is directly proportional to viscosity to the power of 0.4. As a result, a decrease in the viscosity will result in a decrease in the cladding surface temperature.

The cladding surface temperature is inversely proportional to thermal conductivity to the power 0.6 and specific heat capacity to the power 0.4 as given by Equation 2.10. Thus, an increase in these fluid properties will affect the value of the Prandtl number as seen in Equation 2.8. This will in turn affect the value of the convection coefficient, which affects the rate of the heat transfer and temperature gradient.

3.3.1.5 Dimensions of the coolant flow channel in the hot channel

Equation 3.8 shows the relationship between the area of the coolant flow channel and the velocity of the coolant.

$$\dot{m} = \rho v A_{flow} \quad 3.8$$

OR

$$v = \frac{\dot{m}}{\rho A_{flow}}$$

In Equation 3.8 it can be seen that the velocity of the coolant is inversely proportional to the coolant flow area. Thus a decrease in the area of the coolant flow channel and keeping the mass flow rate constant will cause an increase in the velocity. This will cause an increase in the Reynolds number as seen in Equation 2.7, which will in turn cause an increase in the convection

coefficient. This increase in the convection coefficient will affect the rate of the heat transfer and temperature gradient.

3.3.2 Mass flow rate of the coolant in the hot channel

The input parameters that are likely to cause a large effect on the mass flow rate of the coolant in the hot channel are:

- Global mass flow rate of the coolant.
- Dimensions of the coolant flow channel.

The description of the effect of these parameters on the mass flow rate is addressed in Sections 3.3.2.1-2.

3.3.2.1 Global mass flow rate of the coolant.

The global mass flow rate (inlet mass flow rate in the core) of the coolant has a direct influence or effect on the mass flow rate of the coolant in the hot channel. This is because the inlet mass flow rate of the coolant in the core is distributed directly in the fuel assemblies. As a result, if the global mass flow rate decreases, the mass flow rates in different coolant channels will decrease by approximately the same factor.

3.3.2.2 Dimensions of the coolant flow channel

The relationship between the mass flow rate of the coolant and the coolant flow channel is given by Equation 3.8.

In Equation 3.8 it can be seen that the mass flow rate of the coolant is directly proportional to the coolant flow channel area. As a result, when the flow area decreases it will cause a decrease in the mass flow rate of the coolant if the velocity remains constant, as expected, because less coolant is allowed to flow through the channel.

3.3.3 Temperature of the coolant in the hot channel

The input parameters that can have a large impact on the temperature of the coolant are:

- Global temperature of the coolant.
- Dimensions of the coolant flow channel.
- Global mass flow rate of the coolant.
- Local power in the hot channel.

Sections 3.3.3.1-3 present a description of how these input parameters can have an impact on the above-mentioned output parameters.

3.3.3.1 Global temperature of the coolant

The global temperature (inlet temperature in the core) of the coolant has a direct influence or effect on the temperature of the coolant in the hot channel. This is because the inlet temperature of the coolant in the core is same as that in the inlet of the fuel assemblies or coolant channels. As a result, if the global temperature decreases, the inlet temperatures in different coolant channels will decrease by approximately the same factor. This will in turn cause a decrease in the temperature of the coolant in the hot channel, as expected. Thus there is reason to expect this parameter to have a direct or primary effect on the results.

3.3.3.2 Dimensions of the coolant flow channel and global mass flow rate of the coolant

Equation 3.1 can also be written as Equation 3.9. This equation shows a relationship between the mass flow rate of the coolant and the coolant temperature.

$$T_{coolant,outlet} = \frac{\dot{Q}}{\dot{m}c_p} + T_{coolant,inlet} \qquad 3.9$$

In Equation 3.9 it is evident that the temperature of the coolant is inversely proportional to the mass flow rate of the coolant. When the mass flow rate of the coolant decreases, the coolant that is in the channel will heat up gradually since the same heat should be removed from the cladding surface by less flow.

3.3.3.3 Local power in the hot channel

An increase in heat generation in the fuel will cause an increase in the temperature of the coolant. This is because the heat that is generated in the fuel is removed by the coolant on the cladding surface. This relationship is given by Equation 3.9.

3.3.4 Pressure drop in the hot channel

The pressure drop in the hot channel is highly influenced by the following input parameters (Rousseau & Van Eldik, 2011):

- Friction factor of the coolant channel, mass flow rate and density of the coolant.

Section 3.3.4.1 presents how these parameters impact on the pressure drop.

3.3.4.1 Friction factor, mass flow rate and density of the coolant

Equation 3.10 gives the relationship between pressure drop and the above-mentioned input parameters.

$$\Delta p_{oL} = \left(\frac{fL}{D_h} + \sum K\right) * \left(\frac{|\dot{m}|\dot{m}}{2\rho A_{flow}^{\ 2}}\right) \qquad 3.10$$

In Equation 3.10 Δp_{oL} denotes the pressure drop, f is the frictional factor, L is the length of the coolant channel, D_H is the hydraulic diameter, $\sum K$ is the sum of loss factors due to valves, elbows etc. on the coolant channel. The pressure drop is directly proportional to the mass flow rate squared, directly proportional to the friction factor, and inversely proportional to the density as seen in Equation 3.10.

3.4 Uncertainty and sensitivity analysis

In this study, the input uncertainties are investigated with respect to the effect they have on the selected output parameters. The uncertainties can be due to the following:

- Manufacturing tolerances of materials used in the reactor core e.g. fuel elements, pipes etc.

- Errors in measuring instruments e.g. flow meter, thermocouple, barometer etc. used in a power plant to take measurements of parameters (mass flow rate).

The above-mentioned uncertainties can have a large effect on the output parameters during plant operation. As a result, it important to take into account these uncertainties in the input parameters. Numerous methods exist that can be used to evaluate the effect of uncertainties with respect to the output parameters. The parametric or sensitivity study and Monte Carlo methods are widely used to quantify uncertainties in best estimate calculations. A brief description of the parametric or sensitivity study and Monte Carlo methods are presented in Section 3.4.1 and 3.4.2 respectively.

3.4.1 Parametric or sensitivity study

The identification of uncertain input parameters is primarily done by applying expert judgement or engineering knowledge as described in Chapter 2. In Flownex, a built-in parametric function is used to perform a parametric study. The specified range of variation represents the lower and upper values/boundaries. The number of runs to be performed can also be specified. In addition to this, the increment size is constant for each run. In Flownex, Equation 3.11 is used to calculate the increment size from the specified number of runs and boundaries or limits (MTI, 2011). Figure 3.4 depicts an algorithm that is used in Flownex to perform a parametric or sensitivity study.

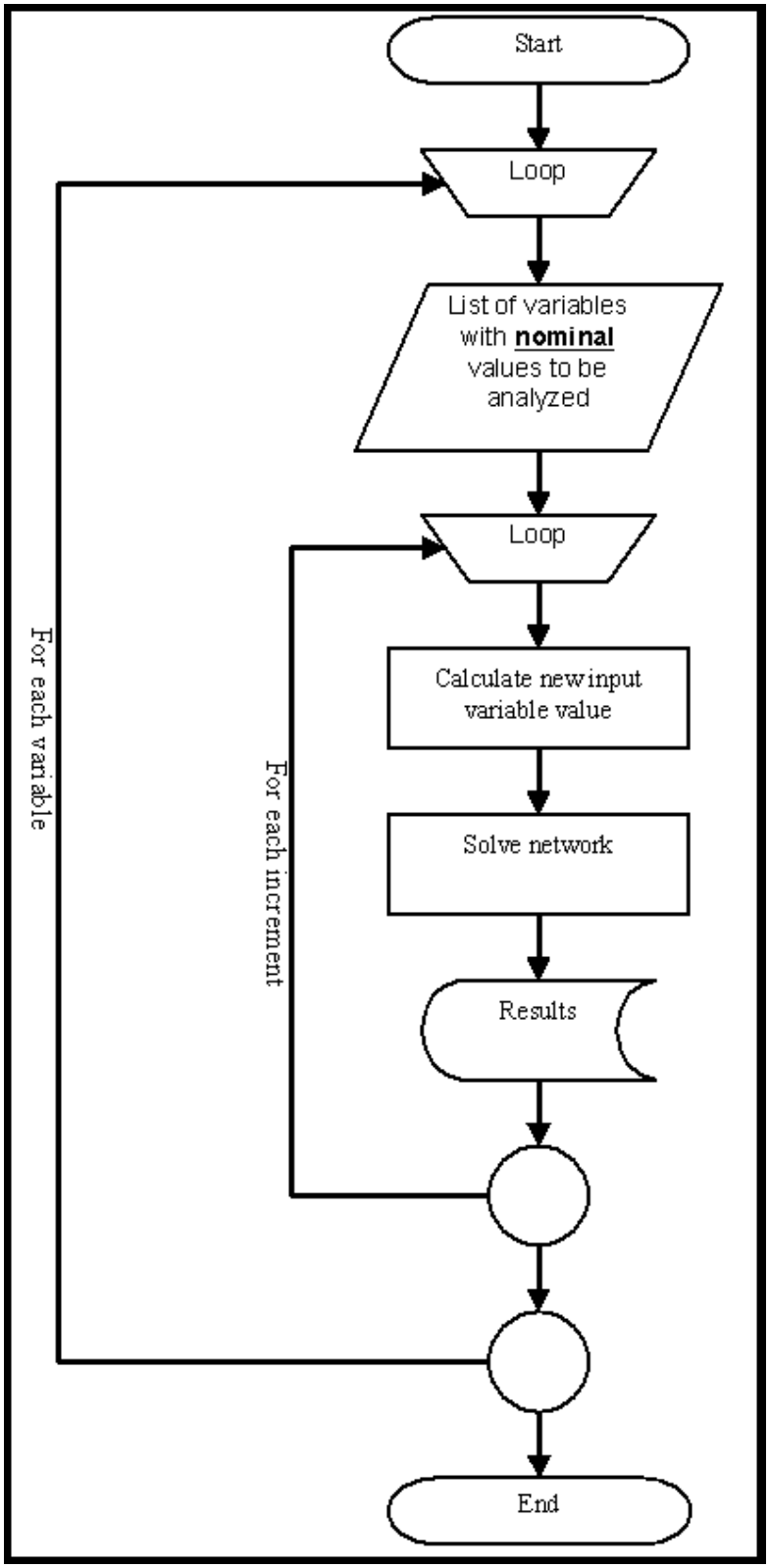

Figure 3.4 - An algorithm used in Flownex to perform a parametric study.

(Source: MTI, 2011).

In Figure 3.4, it can be seen that parameters are varied one at a time.

$$\mathrm{I} = \frac{\text{Upper limit value} - \text{Lower limit value}}{\text{number of runs}} \qquad 3.11$$

In Equation 3.11, I denotes the increment size. A new value for each run of an input parameter must be calculated as seen from Figure 3.4. This value in Flownex is calculated using Equation 3.12 (MTI, 2011). In Equation 3.12, i denotes a step number.

$$\text{New value} = \text{lower limit value} + \mathrm{i} * \mathrm{I} \qquad 3.12$$

After generating parametric results in Flownex, the input parameters are then ranked according to the effect they have on the output parameters. This is done to select uncertain input parameters that will be used in the propagation step of the Monte Carlo method presented in Section 3.4.2. The ranking criterion used in this research study is presented in Chapter 4.

In conclusion, a parametric or sensitivity study is used to identify uncertain input parameters that influence output parameters.

3.4.2 The Monte Carlo method

The Monte Carlo method is stochastic i.e. it is based on probability theory and it uses a random sampling technique to propagate uncertainties of input parameters. In this method a combined or total uncertainty effect of the input parameters on the output parameters is investigated. This method is different from a parametric or sensitivity study because in this method input parameters are not varied independently from each other but the variation is done simultaneously. The variation of input parameters is random rather than successive as compared to a parametric study. Monte Carlo is one of the methods that are widely used to perform uncertainty propagation in best estimate calculations. This method is straightforward to apply yet very powerful, but it has its disadvantages. Previous studies have shown that this method is expensive to implement since large numbers of simulation runs should be performed in order to get good results. Thus, it is of importance to run the simulations on a computer that has a high performance. The most important

outcome of using this method is to produce the probability density functions (PDFs) of the output parameters from the combined or total uncertainties of input parameters. In Flownex, the uncertainty propagation of input parameters is performed using a Monte Carlo uncertainty analysis based function. This function is a built-in feature in Flownex. Figure 3.5 depicts the algorithm that is used in Flownex for Monte Carlo uncertainty analysis calculations.

The following should be specified in a Monte Carlo function before performing the calculations:

- The boundary range i.e. upper and lower limits.
- A probability distribution that an input parameter follows e.g. normal, uniform distribution etc.
- Number of runs.

A Monte Carlo function in Flownex works with the following probability distributions: uniform, double triangular, normal and triangular distributions. As a result, Flownex is limited to these distributions. In this study, the uncertain input parameters investigated follows a normal distribution. The Monte Carlo function in Flownex could therefore be used to perform the uncertainty analysis calculations in this study. In Figure 3.5 it can be seen that for each run, a new random value is generated for each input parameter. As a result, different random values for each parameter are generated within their specified range until the specified runs end.

The random values are calculated or generated by using the boundary range and the probability distribution specified (MTI, 2011). This is done by evaluating the chance or likelihood of obtaining certain values within the specified range on the probability distribution and is how random values of input parameters are generated for each run. The random and simultaneous variation of input parameters generate the results of the output parameters. From these results, the PDFs of output parameters can be produced.

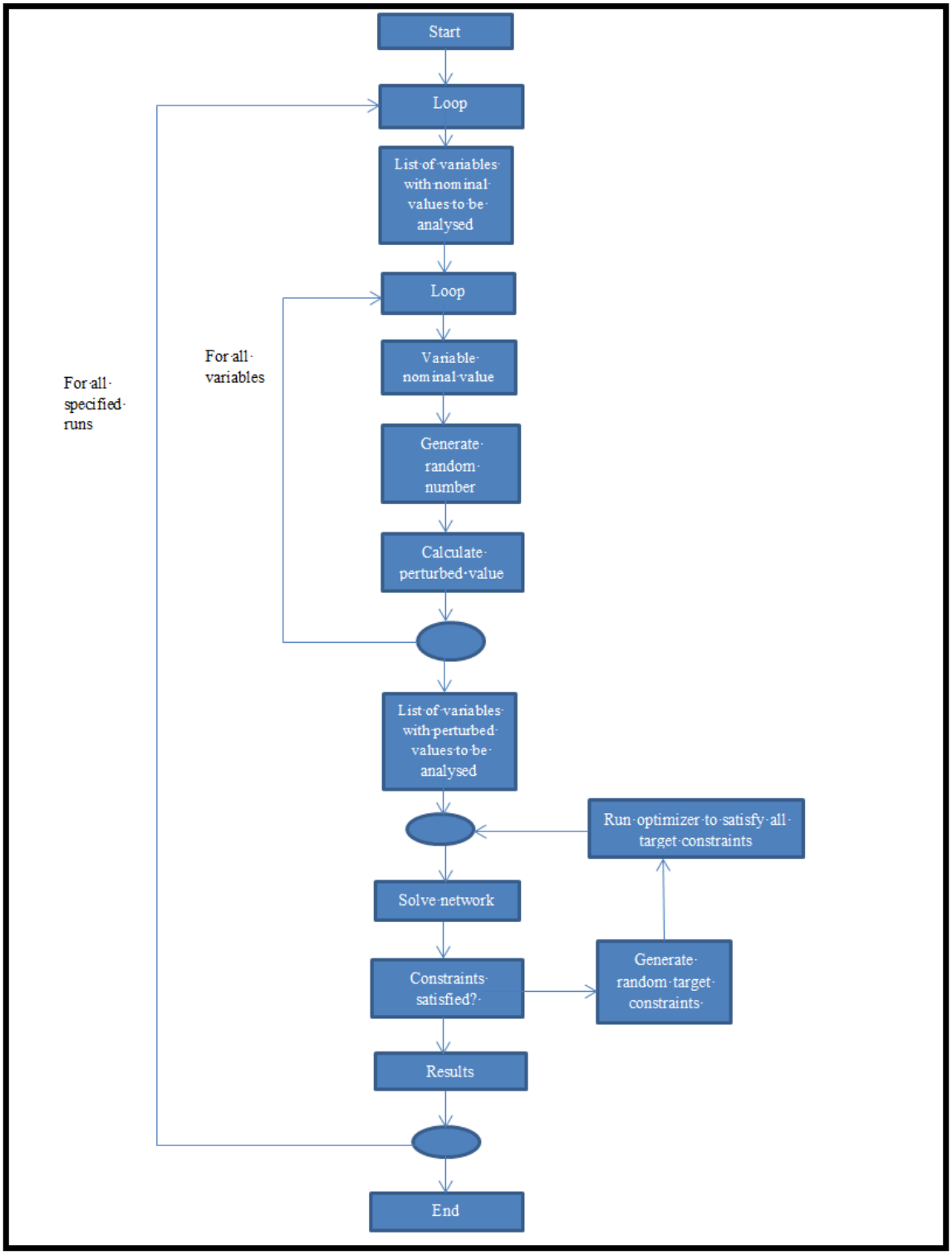

Figure 3.5 - An algorithm used in Flownex to perform Monte Carlo uncertainty calculations.

(Source: MTI, 2011).

3.5 Normal distribution

In the field of statistics, the normal distribution is an essential distribution that is widely used, or which has been used previously to describe various phenomena. For example, one of the phenomena includes describing the population of humans, animals, etc. in a certain environment.

A random variable x with parameters σ (standard deviation) and μ (mean) is said to follow a normal distribution if it exhibits the following properties (Devore & Farnum, 2004; Walpole *et al.*, 2011; Montgomery & Runger, 2002): $\sigma > 0$, and -infinity< mu >infinity and if its behaviour is described by the following function:

$$f(x) = \frac{1}{\sqrt{2\pi}\sigma} e^{-\frac{1}{2}\left(\frac{x-\mu}{\sigma}\right)^2}, \text{ -infinity< x >infinity} \qquad 3.13$$

Figure 3.6 depicts a normal density curve of random variable x, with its parameters. Cases where random variables are assumed to follow a normal distribution must be proven. In this case, a theorem called the central limit theorem (CLT) can be applied to indicate when these variables can be approximated by the normal distribution. In this research study, some uncertain input parameters were taken to follow a normal distribution. It was therefore necessary to show that these variables or parameters can be approximated by a normal distribution. The central limit theorem was applied in addition to the r^2 method presented in Chapter 2. This theorem is addressed in Section 3.6.

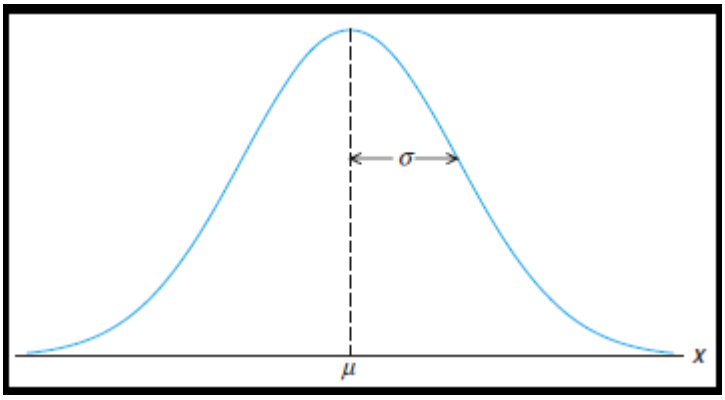

Figure 3.6 - The normal distribution curve of variable x, with its parameters.

(Source: Walpole *et al.*, 2011).

3.6 Central limit theorem

As already stated in Section 3.5, there are instances where a normal distribution can be assumed to approximate a random variable. The solution to this problem is to apply the central limit theorem. This theorem basically states that if a random variable x of sample size n is large enough, the average value of x will have a normal distribution (Devore & Farnum, 2004; Walpole *et al.*, 2011; Montgomery & Runger, 2002). This method is primarily or highly dependent on the sample size n of a random variable x. As the sample size n increases, random variable x becomes a normal distribution (Devore & Farnum, 2004; Walpole *et al.*, 2011; Montgomery & Runger, 2002). This effect (central limit theorem) is depicted in Figure 3.7. Previous studies showed that a sample size of $n \geq 30$ is large enough to invoke this method (Montgomery & Runger, 2002). If a small sample size of $n < 30$ exhibits a symmetrical normal distribution, then the central limit theorem is not needed. In conclusion, if a random variable x is assumed or deviates slightly from a normal distribution, it is important to take a large sample size n to ensure that it can be approximated by a normal distribution.

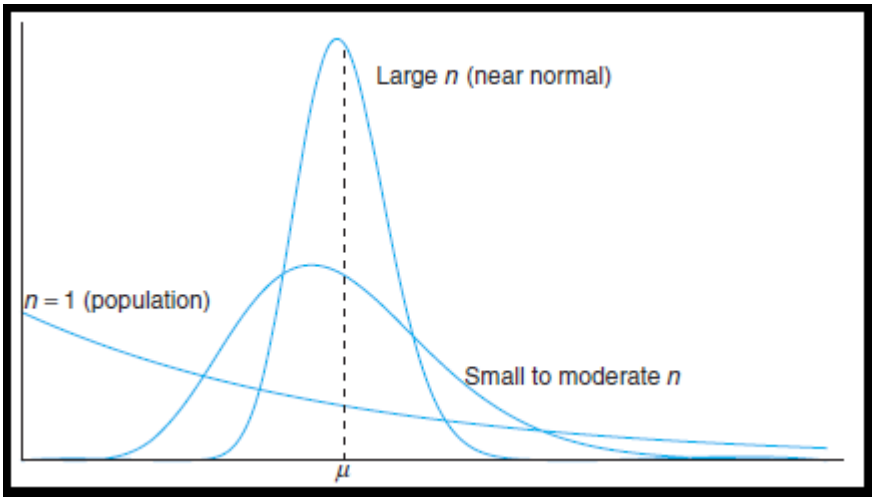

Figure 3.7 - Depiction of the central limit theorem.

(Source: Walpole *et al*., 2011).

CHAPTER 4 - METHODOLOGY

4.1 Introduction

The objective of this chapter is to present the steps of the code scaling applicability and uncertainty (CSAU) methodology and procedures that were performed to undertake the uncertainty and sensitivity analysis of this study. A description of how the uncertainty and sensitivity analysis is performed in Flownex is addressed. The sensitivity and Monte Carlo analysis were performed for steady state (normal operation), thus no transient analysis was performed as it is not in the scope of this study.

As already mentioned in Chapter 1, only steps 1-6, 9 and 12-14 were considered and/or performed. The IAEA MTR 10 MW reactor is not a physical reactor. This is a reactor developed as a benchmark so that other MTR reactors which operated or operates at high enrichment can be converted to low enrichment fuel using the details of this benchmark. Steps 7 (establish assessment matrix) and 8 (comparison between experiment and code results) were not performed because the data from experiments is not available. Since a quarter of a full scale core was modelled, step 10 (determine effect of scale) was also not investigated. This is because a quarter of a core still represents the full core, thus this cannot be considered as a small scale of the reactor core. Step 11 (determine the effect of reactor input parameters and state) was not performed because in this study only the steady state calculations were done and not the transient calculations. The step-wise procedures of the CSAU methodology that were implemented in this study are presented in Section 4.2.

4.2 Steps of the CSAU methodology and procedures

4.2.1 Step 1 and 2: Specify scenario and select NPP

The system is the IAEA MTR 10 MW benchmark reactor, and the scenario is the uncertainty and sensitivity analysis of the steady state (normal operation).

4.2.2 Step 3 and 12: PIRT and perform sensitivity analysis or calculations

As already described in Chapter 2, the identification of the main contributors to the output parameters of interest is primarily done using teams of expert to develop the phenomena identification and ranking table (PIRT). In this study, a team of experts was not available to develop the PIRT so as to identify and select the phenomena or parameters that have the largest effect on the output parameters of interest. The solution to this was to perform a sensitivity study on all input parameters (about 80 input parameters) in the Flownex MTR model in order to select input parameters that have the largest effect on the output parameters of interest i.e. selection of the uncertain input parameters in terms of the output parameters of interest. Section 4.2.2.1 presents the procedure followed in this study to perform the sensitivity analysis.

4.2.2.1 Sensitivity study

As already mentioned in chapter 3, the following input parameters were investigated for uncertainty on output parameters of interest:

- Fluid properties of the coolant.
- Component and system parameters.

The procedure that was followed to investigate the effect of the fluid properties of the coolant, component and system parameters is presented below. The main objective of the PIRT process is to identify and select uncertain input parameters. These parameters are the ones that are used in the uncertainty propagation step in Monte Carlo analysis presented in Section 4.2.9. In this research study all input parameters were investigated in order to minimize the probability of accidentally omitting input parameters that can have an impact on the selected output parameters, thereby increasing the chances of identifying and selecting relevant uncertain input parameters. In Flownex, a parametric function is used to perform a sensitivity study. As explained in Chapter 3, this function is a built-in function in the Flownex code. In order to perform a parametric study in Flownex, the following should be specified:

- The boundary limits i.e. the lower and upper variation range.
- The distribution that an input parameter follows i.e. a distribution that characterizes the parameter.

The variation range that was used for the input parameter variation was -10% and +10% of their base values for the lower and upper limits respectively. These limits are calculated as presented in Equation 4.1 and 4.2.

$$\text{Lower limit} = \text{Base value} - \text{Base value} * 10\% \quad (4.1)$$

OR

$$\text{Lower limit} = 0.9 * \text{Base value}$$

The values obtained from Equation 4.1 and 4.2 are specified as the lower and upper limits of input parameters respectively in Flownex.

$$\text{Upper limit} = \text{Base value} + \text{Base value} * 10\% \quad (4.2)$$

The ±10% variation range was decided upon by the Nuclear Engineering research group based on expert and/or engineering judgement regarding the behaviour of the MTR model developed. This was so because it was believed that most engineering data, including correlations, have on average this band of uncertainty.

Provided that the same percentage variation was applied to all the parameters, this would result in a consistent comparison. ±5% or ±15% could have also been considered.

As a basis, all input parameters were assumed to follow a normal distribution. This was assumed based on the previous studies that were done in uncertainty and sensitivity analysis (De Crécy *et al*., 2008; Srivastava *et al.*, 2008; Mesado *et al.*, 2012). The sensitivity result generated by a parametric function in Flownex was then used to determine the effect or impact of input parameters on selected output parameters. This effect of the input parameters on the selected output parameters was calculated or quantified using Equation 4.3.

$$\%\text{Change} = \frac{\text{New value due to input parameter variation} - \text{Base value}}{\text{Base value}} * 100\% \quad (4.3)$$

In Equation 4.3, %Change quantifies the effect on selected output parameters due to the input parameter variation (-10% or +10% variation). The new value due to input parameter variation presents an output parameter value obtained after varying an input parameter. Since only input parameters that have the largest effect are selected, this minimizes the number of input parameters that will be propagated for uncertainty analysis in Monte Carlo. This in turn will minimize the computational time for Monte Carlo calculations since not all input parameters have to be propagated. As a guide, a ranking criterion that was used to select uncertain input parameters is as follows:

- The input parameters that cause a %Change of $\geq 0.5\%$ on selected output parameters were regarded as the ones that have a largest effect on the selected output parameters. This ranking criterion proved to be reasonable since the input parameters that were expected to have the largest effect on selected output parameters were part of the uncertain input parameters.

In conclusion, the purpose of performing a sensitivity or parametric study is to identify and select the uncertain input parameters. The PIRT process was basically followed to select the uncertain input parameters. The investigation of all input parameters added an advantage since the effect of all input parameters was calculated and/or determined with respect to the selected output parameters, which increased the chances of identifying and selecting relevant uncertain input parameters. As a result, this ensures a good uncertainty analysis since only uncertain input parameters have to be propagated. These parameters are the ones that are used in the uncertainty propagation step in the Monte Carlo method.

- **Sensitivity study of the fluid properties of the coolant**

The sensitivity analysis of the fluid properties was not performed using a parametric function. This is because in Flownex these properties cannot be varied automatically using a parametric function as is done for the input parameters of the component and system parameters. The fluid properties were varied manually to investigate their effect on the selected output parameters. This is one of the limitations of Flownex. The results that were obtained initially from investigating the fluid properties with respect to the selected output parameters did not give the correct or expected results. This was because the secondary effect of other parameters on the selected output

parameters played a role. The secondary effect observed was the result of other neighbouring channels, thus the primary effect of the fluid properties in the output parameters of the hot channel was not observed. In order to ensure that a direct effect was investigated with respect to the selected output parameters, a MTR Flownex model of the hot channel (pipe 6) only was used as is portrayed in Figure 4.1. This in turn minimized the significance of the secondary effects on the output parameters. Since the selected output parameters under investigation are those of the hot channel, it was reasonable to choose the hot channel assembly for this analysis. The sensitivity results of fluid properties of the coolant are presented in Chapter 5.

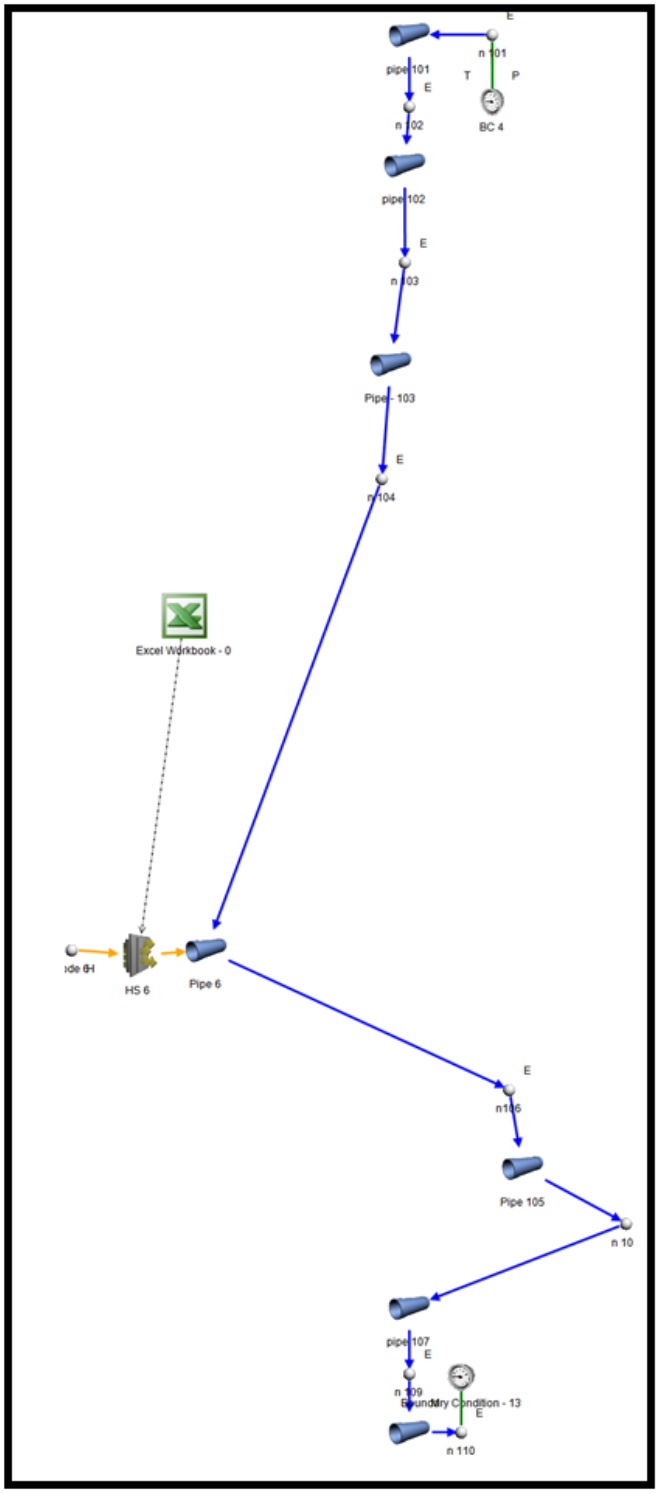

Figure 4.1 - A hot channel MTR Flownex model.

- **Sensitivity study of component and system parameters**

The input parameters of the component and system parameters that were investigated are presented in Chapter 3. These parameters were varied independently from each other using a parametric function in Flownex as already mentioned.

Amongst the component parameters, the heat transfer area and coolant flow channel area in the core needed special attention. Unlike other component parameters in Flownex, the heat transfer area and coolant flow channel area cannot be varied directly in the parametric function. This is because these parameters are not independent parameters. The heat transfer area is dependent on the width (w_y) of the fuel plates and the height (h_z) of the fuel plates, and the coolant flow channel area is dependent on the width (w_y) of the fuel plates and the gap (l_x) between the fuel plates. The width, height and length are independent parameters which can be varied directly. As a result, varying these independent parameters in a parametric function in Flownex will automatically vary the heat transfer area and the coolant flow channel area. To perform this variation of the heat transfer area and the coolant flow channel area in Flownex, a script was written to calculate the heat transfer area of each fuel element in the core using the h_z, w_y and l_x values specified in Flownex (Slabbert, 2011). The script written in Flownex and the formulas that were used are presented in Appendix B. Figure 2.4 in Chapter 2 depicts the dimensions of a plate type fuel element used in the Flownex MTR model. The sensitivity results of the component and system parameters are presented in Chapter 5.

4.2.3 Steps 4 and 5: Select frozen code and provide code documentation, developmental assessment model and correlations

The Flownex code was used in this study as already mentioned in Chapter 1. Frozen version Flownex SE 8.1.11 was used. This code was developed by M-Tech Industrial (Pty) Ltd and thus the code development, assessment etc. were done by them. As a result, the in-depth development assessment was also done by M-Tech. Some verification calculations were performed in this study to ensure that certain correlations or parameters are calculated correctly. The verification results are presented in Chapter 5.

4.2.4 Step 6: Determine code applicability

The applicability of the code to the specified scenario was partially done by Slabbert (2011) and it is thus recommended in this study for further work in future.

4.2.5 Steps 7 and 8: Establish assessment matrix and experiment/code results comparison

These steps were not performed in this study as had been discussed in Section 4.1.

4.2.6 Step 9: Determine code and experiment accuracy

4.2.6.1 Investigation of tolerance (uncertainty) limits and distributions of uncertain input parameters

The input parameters (uncertain parameters) that showed the largest effect on the selected output parameters were identified and selected in Section 4.2.2 (step 3 and 12) using the sensitivity results. These results showed that the uncertain input parameters in terms of the selected output parameters are:

- The width or gap of the coolant flow channel in the hot channel.
- Local power in the hot channel.
- Global mass flow of the coolant.
- Specific heat capacity of the coolant.
- Viscosity of the coolant.
- The width of the fuel plates in the hot channel.
- Conductivity of the coolant.
- Global temperature of the coolant.
- The width of the fuel plates in the cold channel
- Coolant flow channel width in the cold channel.
- Density of the coolant.

As already mentioned in Chapter 3, the uncertainty analysis in Flownex is performed by using a Monte Carlo function. The fluid properties of the coolant were not propagated in the Monte Carlo

function due to the limitation explained in Section 4.2.2.1. In Monte Carlo function, the following should be specified before performing the uncertainty analysis:

- Boundary limits and base values of uncertain input parameters.
- Distributions of uncertain input parameters.
- The number of Monte Carlo runs required.

A method that was followed to choose the number of Monte Carlo runs is presented in Section 4.2.9. In this section, only the tolerance limits and distributions of uncertain input parameters are addressed. The boundary limits and distributions that were assumed for input parameters in the sensitivity calculations were used as a guide.

In the uncertainty analysis it is of importance to investigate the boundary limits and distributions of the above-mentioned uncertain input parameters. This is done to ensure that the total or combined uncertainty of the input parameters on the selected output parameters is investigated precisely. In Chapter 3 it is mentioned that the sources of uncertainty in input parameters can be in the form of manufacturing tolerances (tolerance limits), error in measuring instruments used in the plant, operational fluctuations etc.

The boundary limits of the dimensions of the fuel plates and coolant flow channels were obtained from the manufacturing tolerances or fabrication tolerance of plate type fuel elements. The manufacturing tolerance limits found are -2% and +2% of the base values for the lower and upper limits respectively (IAEA, 1980; USAEC, 1962). In addition to this, a normal distribution was assumed. Equation 4.4 and 4.5 were used to calculate the boundary limits that should be specified in the Monte Carlo function for the dimensions of the fuel plates and coolant flow channels. These values are shown in Table 4-1.

$$\text{Lower limit} = \text{Base value} - \text{Base value} * 2\% \quad (4.4)$$

$$\text{Upper limit} = \text{Base value} + \text{Base value} * 2\% \quad (4.5)$$

Table 4-1 - Specified values of the dimensions of the fuel and coolant flow channels in Monte Carlo function.

Parameter	Base value	Lower limit value	Upper limit value	Unit
Coolant flow channel width or gap in the hot channel (l_x)	0.00223	0.00221	0.00225	m
Coolant flow channel width in the cold channel (l_x)	0.00223	0.00221	0.00225	m
The width of the fuel plates in the hot channel (w_y)	0.06650	0.06584	0.06717	m
The width of the fuel plates in the cold channel (w_y)	0.06650	0.06584	0.06717	m

The boundary limits and distributions of the global mass flow rate and temperature of the coolant, and local power in the hot channel were obtained from operational data from the Nuclear Energy Corporation of South Africa (NECSA) (Botes, 2013). This data is for the reactor power, global mass flow rate and temperature of the coolant. These parameters are normally referred to as the system or operational parameters. The data for each system parameter was initially tested for a normal distribution as previously assumed in the sensitivity study. In this case, a normal fit test was performed by plotting the observed (operational) data against the calculated (fitted) data obtained from using a normal distribution fit equation. In these plots, the frequency is plotted as a function of the parameter of interest (local power, global mass flow rate etc.). Since these plots are known as histogram curves and they are widely used in the test of normal distribution scenarios (Devore & Farnum, 2004) they were plotted or used in this research study to test the data for a normal distribution. The calculated data was obtained using Equation 4.6 which is derived from Equation 3.13. Equation 4.6 has been normalized from Equation 3.13 so as to obtain values of the calculated frequency data.

$$f(x) = f_0(x) \exp\left(\frac{-1}{2}\left(\frac{x-\mu}{\sigma}\right)^2\right) \qquad 4.6$$

In Equation 4.6, x is the parameter of interest (e.g. local power), μ is the average or mean and σ is the standard deviation of the calculated data. The fitted parameters of the observed data from Equation 4.6 are the frequency of the calculated data $f(x)$ and the maximum frequency of the observed data $f_0(x)$. The numerical values of the fitted mean and standard deviation were used to calculate the boundary limits of the system parameters. A detailed description of how to calculate

the boundary limits for these parameters is given in the upcoming paragraphs. Figure 4.2 shows the comparison between the observed (actual reactor operational data) and calculated (Gaussian curve fit) data of the above-mentioned system parameters. A solver function was used in MS Excel whereby the sum error of squares between the observed and calculated data or SSResid (see Chapter 2) was minimized by changing the average, standard deviation and the maximum frequency of the calculated function. This was done to ensure that the observed data fits the calculated values which were chosen as a normal distribution. After running the solver function, the mean, standard deviation and maximum frequency of the observed data that fits a normal distribution were obtained. These parameters are known as fitted parameters, and the numerical values of the mean and standard deviation were used to determine the boundary limits as mentioned above.

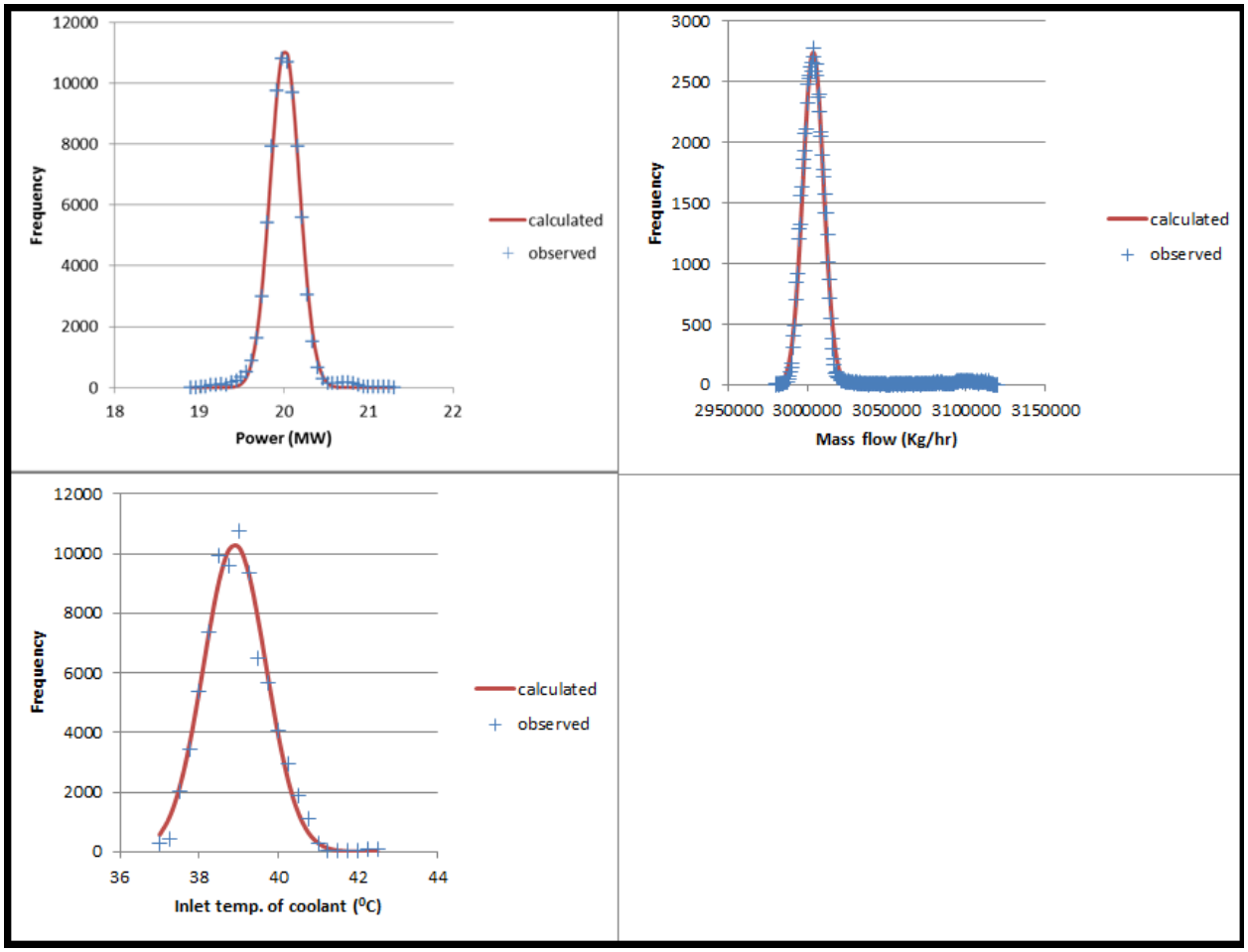

Figure 4.2 - Observed and calculated data comparison for power (top left corner), global mass flow rate of the coolant (top right corner), and global temperature of the coolant (bottom left corner).

Analysis (or characterisation) of Necsa's actual MTR operational data (Source: Botes, 2013).

Using visual inspection, it can be seen that the observed and calculated data for the system parameters follow a normal distribution. In addition to the visual inspection, the r^2 values of these parameters were determined to further prove if they approximate a normal distribution. The procedure of how to determine the r^2 values is presented in Chapter 2. Table 4-2 shows the values of r^2 of the system parameters.

Table 4-2 - r^2 values of system parameter data.

System parameter	r^2 value
Power	0.998
Global mass flow rate of the coolant	0.994
Global temperature of the coolant	0.986

From Table 4-2 it can be seen that the values of r^2 for the system parameters are close to 1. As a result, it can be concluded that they approximate a normal distribution. Thus, a normal distribution for the system parameters was specified in the Monte Carlo function in Flownex. Since the observed data set was fitted for a normal distribution as described above, the fitted parameters (frequency, mean and standard deviation) that will ensure that the observed data of the system parameters best fit a normal distribution were obtained. The numerical values of the fitted parameters obtained for the system parameters are presented in Table 4-3.

Table 4-3 - Fitted parameters of system parameters.

System parameter	Average	Standard deviation	Max. frequency	Unit
1. Reactor power	20	0.2	11115	MW
2. Global mass flow rate of the coolant	$3003*10^3$	$7*10^3$	2743	kg/hr
3. Global temperature of the coolant	38.9	0.8	10309	ºC

Assuming that most of the data points are within a 95.4% confidence interval, Equation 4.5 was used to calculate the operational tolerances for the system parameters. These tolerances give an indication of how the system parameters can vary during plant operation. Equations 4.7 and 4.8 are used in Flownex to calculate the tolerance limits of the data having 95.4% confidence intervals (MTI, 2011). The values of fitted parameters (standard deviation and mean) are used in Equation 4.7 and 4.8 to calculate the tolerance limits of the system parameters.

$$\text{Lower tolerance limit} = \mu - 2\sigma \qquad 4.7$$

$$\text{Upper tolerance limit} = \mu + 2\sigma \qquad 4.8$$

From calculating the tolerance limits of the system parameters, the following variation ranges were obtained:

- The power can vary or deviate by -1.72% and +1.72% from its average or nominal value during plant operation.
- The global mass flow rate of the coolant can vary by -0.44% and +0.44% from its average value during plant operation.
- The global temperature of the coolant can vary by -4.05% and +4.05% from its average value during plant operation.

Using the above variation range, the boundary limits of the system parameters in the Flownex model can be specified. Thus, the boundary limits of the global mass flow rate and temperature of the coolant and local power in the hot channel can be calculated. The boundary limits obtained are presented in Table 4-4. These values are the ones that were specified in the Monte Carlo function in Flownex for the system parameters. In conclusion, operational data was used to determine the variation range (operational fluctuations in terms of percentage variation) of the system parameters. From this variation range, the values of the boundary limits were then calculated using the base values in Flownex of each system parameter. These boundary limits were the ones specified in the Monte Carlo function.

Table 4-4 - Specified values of the system parameters in Monte Carlo function.

Parameter	Nominal value	Lower limit value	Upper limit value	Unit
Local power in the hot channel	189.07	185.82	192.33	kW
Global mass flow rate of the coolant	-69.44	-69.14	-69.75	Kg/s
Global temperature of the coolant	38.00	37.32	40.47	ºC

4.2.7 Step 10: Determine effect of scale

Since a quarter of a full scale core was modelled, step 10 was not investigated. A quarter of a core (which was investigated) still represents the full core and as such cannot be considered a small scale of the reactor core.

4.2.8 Step 11: Determine effect of reactor input parameters and state

This step was not performed as had been discussed in Section 4.1.

4.2.9 Step 13 is actually the propagation of uncertain input parameters

In this step the uncertain input parameters are propagated in the Monte Carlo function in Flownex for uncertainty analysis. This is performed so as to investigate the effect of the combined or total uncertainty of uncertain input parameters on the selected output parameters. As a result, the uncertainty on the selected output parameters is thus quantified and investigated. The combined uncertainty quantification on output parameters is evaluated by producing probability density functions (PDFs) of each selected output parameter. This is one of the main objectives of performing the uncertainty analysis as explained in Chapter 2. After specifying the boundary limits and distributions of uncertain input parameters, the number of Monte Carlo runs must be specified. All the uncertain input parameters follow a normal distribution as determined and investigated or assumed in the above sections. Thus it is expected of all selected output parameters to follow the same distribution as uncertain input parameters i.e. the normal distribution. In determining the optimum number of runs, the following numbers of Monte Carlo runs were performed:

- 5 000.
- 8 000.
- 10 000.
- 15 000.

Due to computational limitations of Flownex, only a maximum of about 15 000 runs were performed. For run numbers more than 15 000, the code gave the error message "Flownex stopped working" and then stopped execution. It was concluded that the convergence of r^2 was already achieved at 10 000 runs, thus resolving this error in the code execution was not further pursued.

From performing these runs, the r^2 values of only the following output parameters were calculated to determine the most efficient computation time:

- Centreline temperature of the fuel in the hot channel.
- Temperature of the coolant in the hot channel.
- Pressure drop in the hot channel.

The r^2 values for the normal distribution fit for each run were calculated to investigate which number of runs provides the highest r^2 values for the above output parameters. This was done so as to test how many runs were required to get a final distribution that approximates a normal distribution. The uncertainty results (data) generated by the Monte Carlo function in Flownex were used to perform this calculation. From these results, the plots of r^2 values versus the number of runs for the above output parameters were produced. Figure 4.3, Figure 4.4 and Figure 4.5 present these plots for each output parameter.

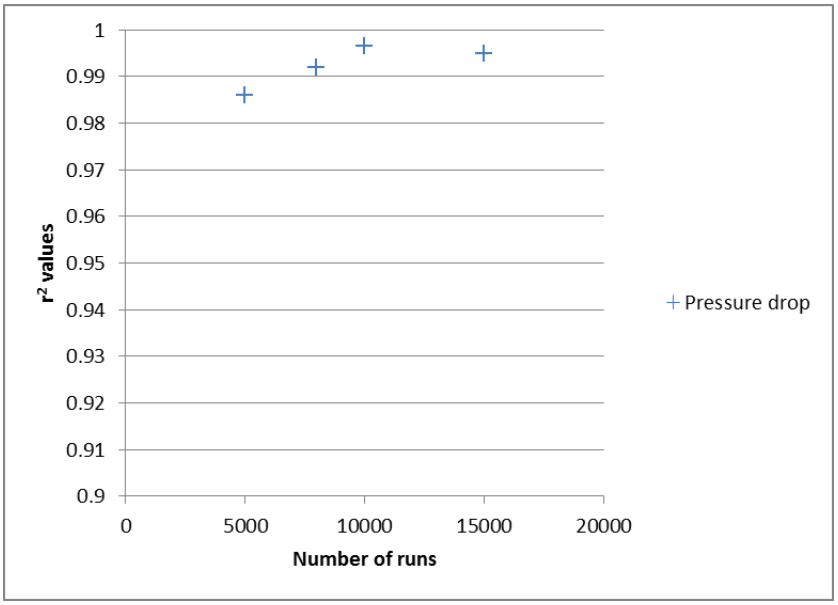

Figure 4.3 - r^2 values vs. number of runs for pressure drop in the hot channel.

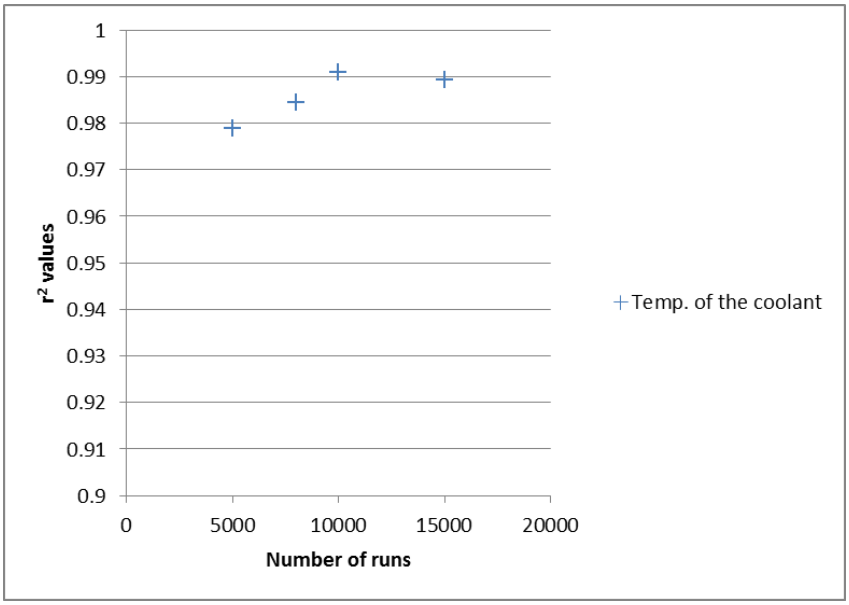

Figure 4.4 - r^2 values vs. number of runs for temperature of the coolant in the hot channel.

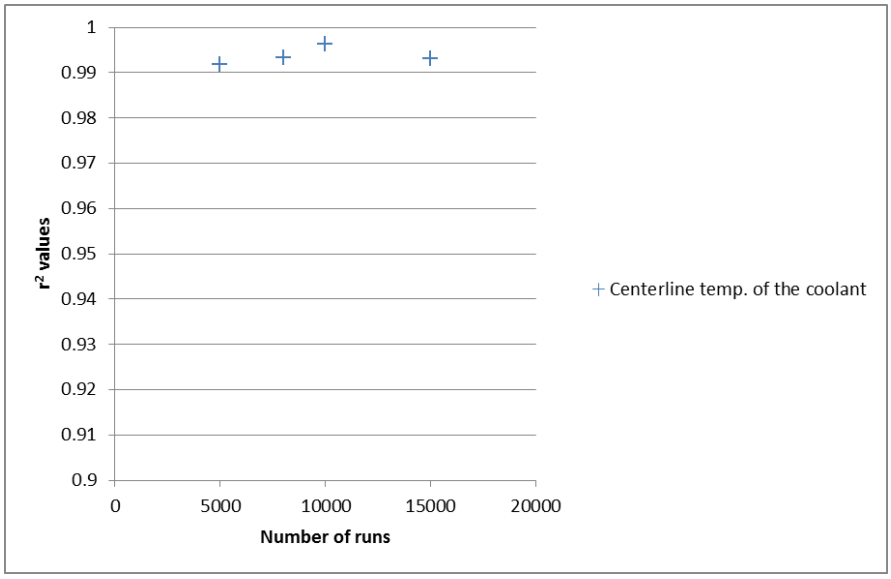

Figure 4.5 - r^2 values vs. number of runs for the centreline temperature of the fuel in the hot channel.

In Figure 4.3, Figure 4.4 and Figure 4.5 it can be seen that the r^2 values increase with an increase in the number of runs from 5 000 to 10 000 runs. This trend is expected as described in the central limit theorem presented in Section 3.6. The highest r^2 value from Figure 4.3, Figure 4.4 and Figure 4.5 is obtained at 10 000 runs. The r^2 value decreases from 10 000 to 15 000 runs as seen in Figure

4.3, Figure 4.4 and Figure 4.5. The percentage decrease of the r^2 value from 10 000 to 15 000 runs for these output parameters is about 0.22%. This percentage decrease is relatively low and thus negligible. As a result, 10 000 Monte Carlo runs were chosen and specified for the uncertainty computations in the Monte Carlo function in Flownex. The results generated by a Monte Carlo function in Flownex were used to construct the probability density functions (PDFs) of the selected output parameters. These results are analysed in step 14.

4.2.10 Step 14: Total uncertainty to calculate specific scenario in a specific NPP

The results (PDFs) and discussion of the uncertainty analysis of the selected output parameters are presented in Chapter 5.

CHAPTER 5 - RESULTS, DISCUSSION AND VERIFICATION

5.1 Introduction

The objective of this chapter is to present the generated results of some of the steps of the code scaling applicability and uncertainty (CSAU) methodology, for steps 3, 5, 12, 13 and 14. Step 3 and 12 are presented in Section 5.2.1, and step 13 and 14 are addressed in Section 5.2.2.

The verification of the Flownex MTR model is presented in Section 5.2.3. This is step 5 of the CSAU methodology. The specifications of the computer used and the time taken to run the simulations are presented in Section 5.3.

5.2 Results and discussion of the CSAU methodology

5.2.1 Step 3 and 12: PIRT and sensitivity analysis results

The sensitivity or parametric results obtained from varying the input parameters independently from each other by ±10% as explained in Chapter 4 are presented in this section. These results present the effect or impact of input parameters on the selected output parameters.

The input parameters that have the largest effect on the centreline temperature of the fuel and cladding surface temperature are presented in Table 5-1, where it can be seen that the local power in the hot channel has the largest effect amongst the uncertain input parameters on the centreline temperature of the fuel and cladding surface temperature. An increase in the local power in the hot channel causes an increase in the fuel and cladding temperature as seen in Table 5-1. The inverse is also observed. Thus the largest contributor to the uncertainty of the fuel and cladding temperatures in the hot channel amongst uncertain input parameters seen in Table 5-1 is the local power in the hot channel.

Table 5-1 – Effect of uncertain input parameters on the centreline temperature of the fuel and cladding surface temperature in the hot channel.

	% Change due to input parameter variation	
Uncertain input parameters	**-10%**	**+10%**
Local power in the hot channel	-5.17	5.51
The width of the fuel plates in the hot channel	5.55	-4.72
Global mass flow of the coolant	4.88	-4.14
Specific heat capacity of the coolant	3.18	-2.74
Coolant flow channel width in the hot channel	2.84	-2.37
Conductivity of the coolant	1.74	-3.31
Viscosity of the coolant	-2.71	2.27
Global temperature of the coolant	-1.90	1.85

Table 5-2 presents the effect of uncertain input parameters on the mass flow rate of the coolant in the hot channel. In Table 5-2 it can be seen that the coolant flow channel width or gap in the hot channel is the main contributor to the uncertainty of the mass flow rate of the coolant in the hot channel. A decrease in coolant flow channel width causes a decrease in the mass flow rate in the hot channel if the velocity remains constant. This is due to the fact that when the coolant flow channel width decreases, the flow area also decreases due to its dependency on the width of the flow channel. This decrease in the flow area causes higher resistance for more coolant to enter the flow channel in the hot channel i.e. allowing limited coolant to enter the coolant flow channel in the hot channel. As a result, the mass flow rate of the coolant in the hot channel decreases due to a decrease in the coolant flow area in the hot channel. This agrees well with the theory presented in Chapter 3. The inverse (increasing a coolant flow channel width) impact is also observed as seen in Table 5-2.

Table 5-2 – Effect of uncertain input parameters on the mass flow rate of the coolant in the hot channel.

	%Change due to input parameter variation	
Uncertain input parameters	**-10%**	**+10%**
Coolant flow channel width in the hot channel	-14.99	15.63
Global mass flow	-10.36	10.35
The width of the fuel plates in the hot channel	-9.70	9.62
Coolant flow channel width in the cold channel	0.83	-0.86
The width of the fuel plates in the cold channel	0.53	-0.53

The effect of uncertain input parameters on the temperature of the coolant in the hot channel is presented in Table 5-3, where it can be seen that the global temperature of the coolant have the largest effect on the temperature of the coolant in the hot channel. Thus the global temperature of the coolant is the main contributor to the uncertainty of the temperature of the coolant in the hot channel amongst uncertain input parameters presented in Table 5-3. An increase in the global temperature of the coolant causes an increase in the temperature of the coolant. This agrees well with the direct effect described in Section 3.3.3.1. The inverse effect is also seen as is evident in Table 5-3.

Table 5-3 – Effect of uncertain input parameters on the temperature of the coolant in the hot channel.

	%Change due to input parameter variation	
Uncertain input parameters	**-10%**	**10%**
Global temperature of the coolant	-6.93	6.94
Specific heat capacity of the coolant	5.16	-4.22
Coolant flow channel width in the hot channel	5.27	-4.04
Global mass flow	3.46	-2.80
The width of the fuel plates in the hot channel	3.21	-2.62
Local power in the hot channel	-2.92	2.91

Table 5-4 presents the effect of uncertain input parameters on the pressure drop in the hot channel. From these results it can be seen that the density of the coolant has the largest effect on the pressure drop in the hot channel. A decrease in the density of the coolant causes a decrease in the pressure drop in the hot channel as seen in Table 5-4. The inverse also applies. From this relationship, it is clear that the pressure drop in the hot channel is directly proportional to the density of the coolant. It should be noted that in this model, the mass flow was fixed as the boundary condition and not the volume flow.

Table 5-4 – Effect of uncertain input parameters on the pressure drop in the hot channel.

	%Change due to input parameter variation	
Uncertain input parameters	**-10%**	**10%**
Density of the coolant	-0.75	0.70
Global mass flow of the coolant	-0.61	0.67

The uncertain input parameters presented in Tables 5.1-5.4 were propagated in the Monte Carlo function in Flownex for uncertainty analysis, except for fluid properties. The fluid properties of the

coolant were not propagated due to the Flownex limitation addressed in Chapter 4. The uncertainty analysis results obtained from propagating the uncertain input parameters of the selected output parameters are presented in Section 5.2.2.

5.2.2 Step 13 and 14: Uncertainty analysis results

As already explained in Chapter 4, the uncertain input parameters (selected in step 3 and 12) were propagated (step 13) in the Monte Carlo function in Flownex to determine their combined uncertainty effect on the selected output parameters. The probability density functions (PDFs) and best estimate plus uncertainty results (step 14) produced from step 13 of the selected output parameters and the discussion thereof are presented in this section. As mentioned in Chapter 4, 10 000 Monte Carlo runs or computations were performed for the steady state uncertainty analysis. In terms of simplifying the PDFs of selected output parameters for better analysis, the results obtained from Monte Carlo computations for these parameters were divided into 21 bins (groups). The range (width or delta) between each bin is the same as will be seen in the PDFs of the selected output parameters. The PDFs of the selected output parameters and discussion thereof will be presented in this section. In this study, a 95.4% confidence interval was chosen for representation of the results, and the limits thereof will be presented for each selected output parameter.

5.2.2.1 Best-estimate plus uncertainty analysis results

- **Cladding surface temperature in the hot channel**

Figure 5.1 shows the PDF of the cladding surface temperature in the hot channel for the calculated (Gaussian curve fit) and observed (Flownex Monte Carlo) data. The calculated data was obtained by using Equation 4.6 as explained in Chapter 4, and the observed data was obtained from Flownex (Monte Carlo results). In Figure 5.1 it can be seen that the cladding surface temperature follows a normal distribution. The r^2 value obtained is 0.998. Equation 4.7 and 4.8 were used to calculate the lower and upper limit of each selected output parameter at a 95.4% confidence interval (95.4% sample population).

The sample mean and standard deviation were obtained from the fitted values (from fitting a normal distribution on the observed data) as explained in Chapter 4. These values were used to calculate the 95.4% confidence interval limits of the cladding surface temperature.

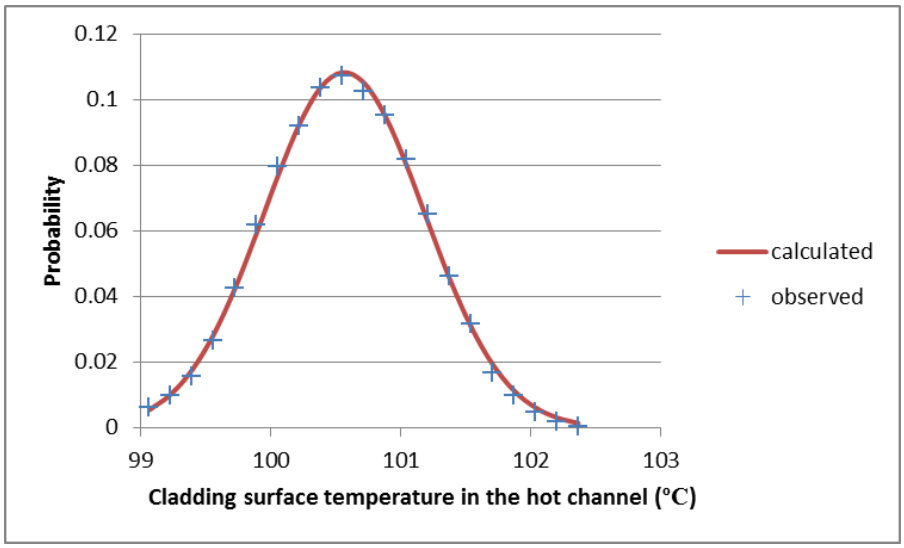

Figure 5.1 - Probability density function of the cladding surface temperature in the hot channel.

The results are listed in Table 5-5. In this table, ΔT represents the difference between the upper limit of the 95.4% confidence interval and the sample mean. The upper limit was used because it is the crucial boundary especially during accidents, thus it is reasonable to do the analysis with respect to the upper limit. It can be seen that ΔT from Table 5-5 is relatively low, and during normal operation the cladding surface temperature in the hot channel can vary by about 1.22%. In addition to this, it can be seen in Figure 5.1 that the probability of the cladding surface of having a value of 101.19ºC (upper limit) is less than 2%. As a result, the chance of the cladding surface temperature to have this value is minimal. From these results it can be concluded that the % deviation in the cladding temperature from the average value is relatively low. As a result, during normal operation, the cladding surface temperature does not exceed the average by a high value.

Table 5-5 - Best estimate plus uncertainty results of the cladding surface temperature in the hot channel.

Parameters of a normal distribution	Value	Unit
1. Sample standard deviation	0.62	
2. Sample mean or average	100.56	ºC
Limits of 95.4% confidence interval		
1. Lower limit	99.33	ºC
2. Upper limit	101.79	ºC
3. ΔT	1.23	ºC
4. %Deviation from the mean	1.22%	

- **Centreline or maximum temperature of the fuel in the hot channel**

The PDF and best estimate plus uncertainty results of the centreline (maximum) temperature of the fuel in the hot channel are presented in Figure 5.2 and Table 5-6 respectively. The r^2 value obtained by comparing the observed (Flownex Monte Carlo) and calculated (Gaussian curve fit) data is 0.996, thus following a normal distribution. The best estimate results from Table 5-6 show that the temperature difference and % deviation from the mean are relatively low. From these results, it can be deduced that the centreline temperature of the fuel is highly controlled i.e. the deviation from the desired (set point) value during normal operation (steady state) is relatively low. Similarly to the cladding surface temperature, the probability of the centreline temperature of the fuel reaching a value at the upper limit is less than 2%, as seen in Figure 5.2.

Regarding the fuel and cladding temperatures, it can be seen that during normal operation the temperature of both parameters are highly maintained close to their desired values (sample mean). From this, it can be deduced that the heat transport in the core during normal operation is effective.

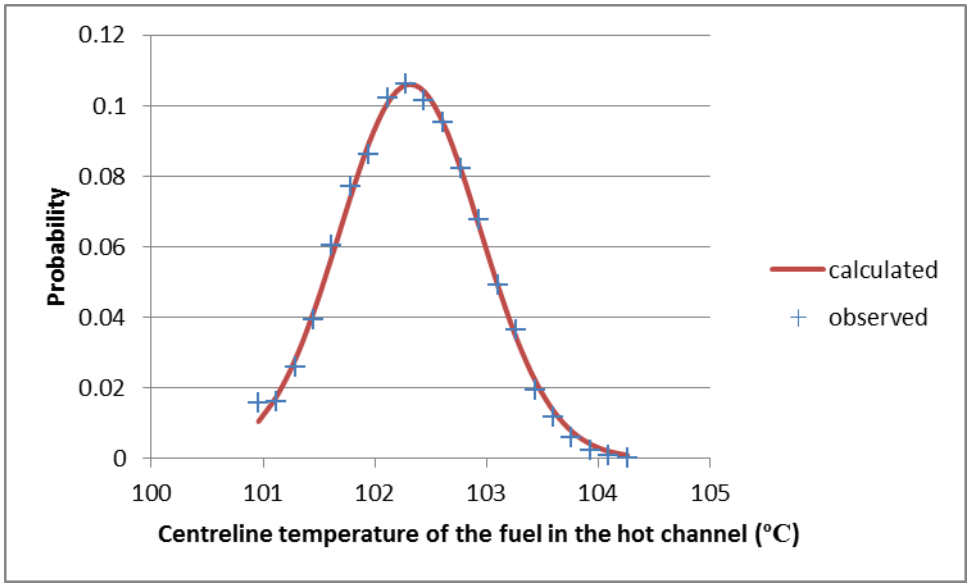

Figure 5.2 - Probability Density Function of the centreline temperature of the fuel in the hot channel.

Table 5-6 - Best estimate plus uncertainty results of the centreline temperature of the fuel in the hot channel.

Parameters of a normal distribution	**Value**	**Unit**
1. Sample standard deviation	0.6	
2. Sample mean or average	102.3	ºC
Limits of 95.4% confidence interval		
1. Lower limit	101.1	ºC
2. Upper limit	103.6	ºC
3. ΔT	1.3	ºC
4. %Deviation from the mean	1.23%	

- **Mass flow rate of the coolant in the hot channel**

Figure 5.3 and Table 5-7 presents the PDF and best estimate results of the mass flow rate of the coolant in the hot channel respectively. The r^2 value obtained by comparing the observed (Flownex Monte Carlo) and calculated (Gaussian curve fit) data is 0.999. Thus follows a normal distribution.

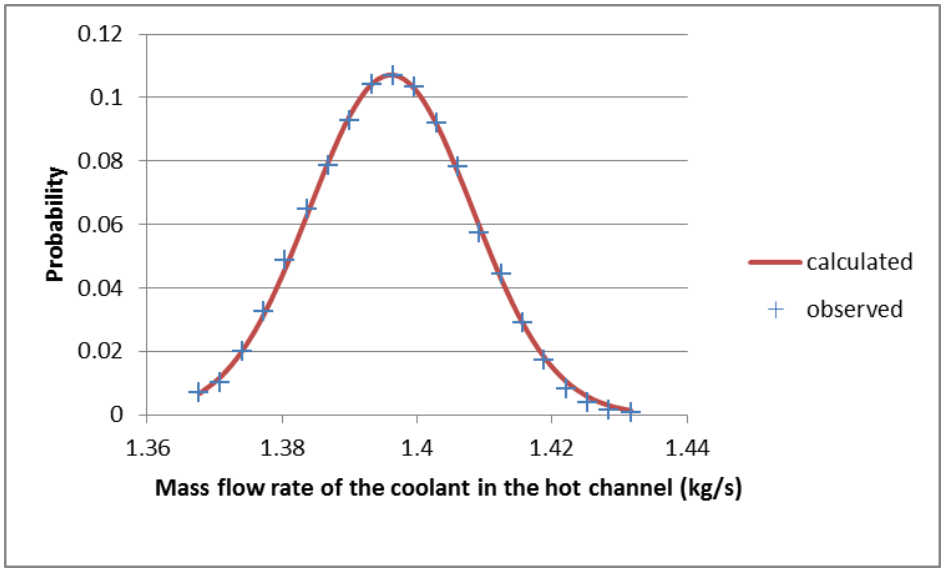

Figure 5.3 - Probability Density Function of the mass flow rate of the coolant in the hot channel.

Table 5-7 - Best estimate plus uncertainty results of the mass flow rate of the coolant in the hot channel.

Parameters of a normal distribution	**Value**	**Unit**
1. Sample standard deviation	0.01	
2. Sample mean or average	1.40	kg/s
Limits of 95.4% confidence interval		
1. Lower limit	1.37	kg/s
2. Upper limit	1.42	kg/s
3. Δm	0.02	kg/s
4. %Deviation from the mean	1.73%	

In Table 5-7 it can be seen that the difference in mass flow rate of the coolant between the average and upper limit is very small. In addition to this, the % deviation from the mean is 2% which is relatively low. From these results, it is observed that during normal operation the set point mass flow rate is achieved. As a result, sufficient heat transport from the hot channel by the coolant is achieved.

- **Temperature of the coolant in the hot channel**

The PDF and best estimate plus uncertainty results of the centreline (maximum) temperature of the fuel in the hot channel are presented in Figure 5.4 and Table 5-8 respectively. The r^2 value obtained by comparing the observed (Flownex Monte Carlo) and calculated (Gaussian curve fit) data is 0.991, thus following a normal distribution.

Table 5-8 - Best estimate plus uncertainty results of the temperature of the coolant in the hot channel.

Parameters of a normal distribution	**Value**	**Unit**
1. Sample standard deviation	0.79	
2. Sample mean or average	55.20	ºC
Limits of 95% confidence interval		
1. Lower limit	53.61	ºC
2. Upper limit	56.79	ºC
3. ΔT	1.59	ºC
4. %Deviation from the mean	2.88%	

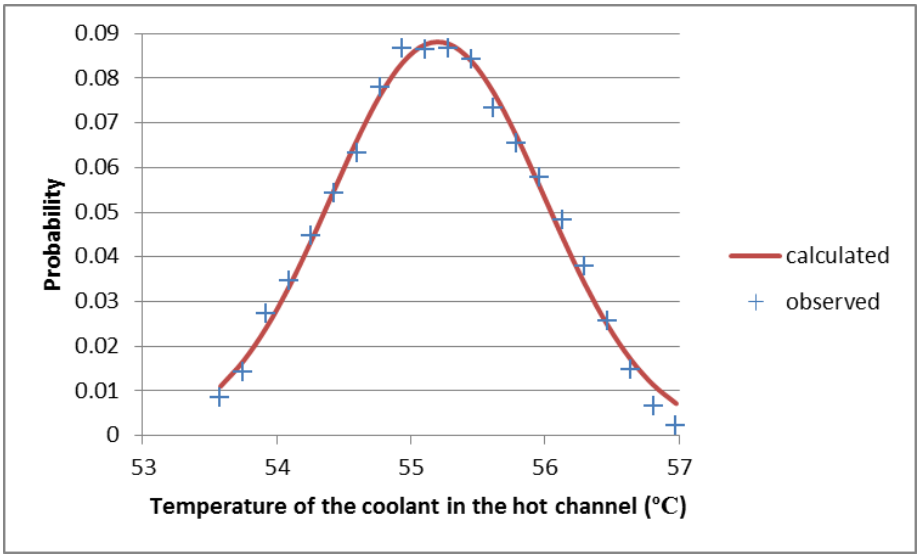

Figure 5.4 - Probability density function of the temperature of the coolant in the hot channel.

From Table 5-8 it can be seen that the upper limit temperature (56.79 ºC) of the coolant in the hot channel is far below its saturation temperature of about 115.17 ºC at 171 kPa (operating pressure),

thus the coolant is in a liquid phase. The upper limit temperature of the cladding is 101.79 ºC. The temperature difference between the mean and the upper limit is about 1.59 ºC which is reasonably low. In addition to this, the % deviation from the mean is also low. This implies that the temperature of the coolant in the hot channel is controlled close to its desired temperature (mean or average value). From this it can be concluded that the coolant does not boil in the hot channel, meaning that there is no two phase flow of the coolant, thus the heat transfer between the fuel and the coolant is effective. The probability of reaching the upper limit temperature value of the coolant is less than 1% as seen in Figure 5.4. In addition to this the temperature of the coolant will in most instances be close and/or at its average value as desired.

- **Pressure drop in the hot channel**

Figure 5.5 and Table 5-9 respectively presents the PDF and best estimate results of the pressure drop in the hot channel. The r^2 value obtained by comparing the observed (Flownex Monte Carlo) and calculated (Gaussian curve fit) data is 0.997. It therefore follows a normal distribution.

In Table 5.9 it can be seen that the difference in the pressure drop between the upper limit and the mean is about 0.05 kPa. This value is very low with respect to the operating pressure of about 171 kPa. Should the operating pressure drop by 0.05 kPa, the % deviation from the optimum operating pressure will be -0.03% which is very low. As a result, the pressure drop in the hot channel is negligible and therefore the coolant does not experience a lot of frictional force in the hot channel. It can be seen from Figure 5.5 that some of the pressure drops are negative i.e. the pressure increased. This arises when the pressure drop due to friction and secondary loss is less than the increase in pressure due to fluid height. For example, in the Monte-Carlo calculations of 10 000 runs, the first entry gives a pressure drop of -0.0200 kPa. A direct substitution of the input parameter for this run yield a pressure drop excluding elevation of 5.7800 kPa. However, the pressure increase due to elevation or height is 5.8066 kPa resulting in a net pressure of -0.0266 kPa.

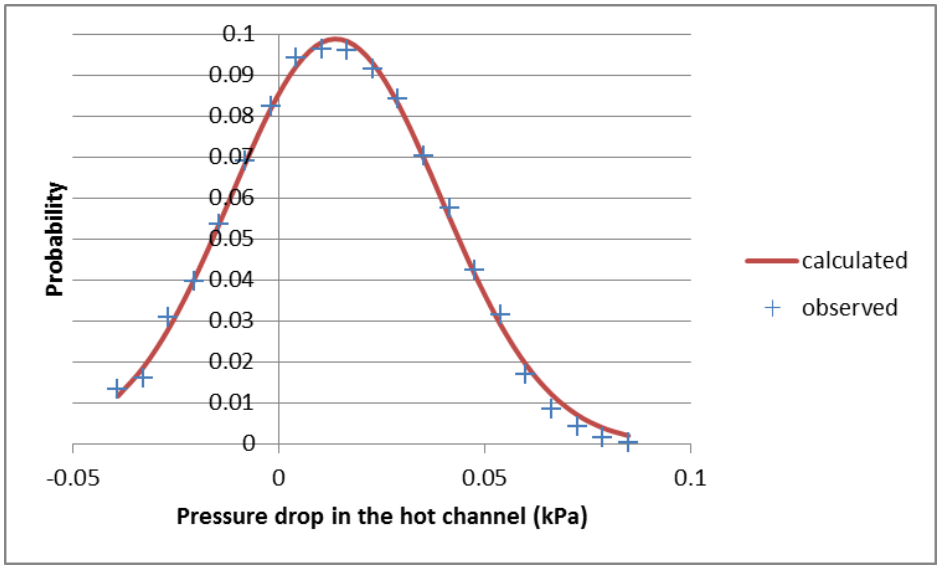

Figure 5.5 - Probability density function of the pressure drop in the hot channel.

Table 5-9 - Best estimate plus uncertainty results of the pressure drop in the hot channel.

Parameters of a normal distribution	**Value**	**Unit**
1. Sample standard deviation	0.03	
2. Sample mean or average	0.01	kPa
Limits of 95% confidence interval		
1. Lower limit	-0.04	kPa
2. Upper limit	0.06	kPa
3. ΔP	0.05	kPa

The conclusion and recommendations of this study are presented in Chapter 6.

- **Normalizing pressure drop**

For interest the normalization of the total pressure drop due to friction and secondary losses against pressure drop due to friction only in the hot channel for 10 Monte-Carlo runs was performed i.e. the investigation of the pressure drop due to friction only with respect to the total pressure drop due to friction and secondary losses. The total pressure drop due to friction and secondary losses in Table 5.10 gives a measure of the pressure drop excluding elevation in the hot channel. In Table 5.10 it can be seen that the ratio between total pressure drop due to friction and secondary losses,

and pressure drop due to friction only is significantly large. As a result, it can be deduced that the pressure drop excluding elevation is governed by the secondary losses.

Table 5-10-Pressure drop normalization

$\Delta P_{\text{friction and secondary losses}}$	$\Delta P_{\text{friction}}$	$\frac{\Delta P_{\text{friction and secondary losses}}}{\Delta P_{\text{friction}}}$
5.778	1.106	5.223
5.827	1.110	5.249
5.853	1.114	5.253
5.794	1.102	5.256
5.841	1.114	5.242
5.833	1.114	5.236
5.795	1.109	5.226
5.775	1.106	5.219
5.783	1.106	5.228
5.789	1.110	5.213

5.2.3 Step 5: Verification

5.2.3.1 Flow area, circumference and heat transfer area of channel 1-8

Mathematical models that were used to verify the calculations of flow area, circumference and heat transfer area in channel 1-8 by the Flownex model are presented in Appendix B. These mathematical models are so called 'back of cigarette box calculations'. Although verifying the flow area in terms of the circumference must seem trivial, it was important to verify that the script written to calculate the heat transfer area was correct. It should be noted that this script was embedded within the Flownex structure.

The comparison of the results is shown in Table 5.11 - 5.13. From these tables it can be seen that Flownex calculated the flow area, circumference and heat transfer area of the channels correctly.

Table 5-11 - Flow area comparison results between a mathematical and Flownex model.

	Flow area (m^2)		
Flow channel NO:	**Mathematical model**	**Flownex model**	**Difference**
1	0.0034	0.0034	0.0000
2	0.0034	0.0034	0.0000
3	0.0034	0.0034	0.0000
4	0.0025	0.0025	0.0000
5	0.0034	0.0034	0.0000
6	0.0009	0.0009	0.0000
7	0.0017	0.0017	0.0000
8	0.0017	0.0017	0.0000
		Ave. %difference	**0**

Table 5-12 - Circumference comparison results between a mathematical and Flownex model.

	Circumference (m)		
Flow channel NO:	**Mathematical model**	**Flownex model**	**Difference**
1	3.16	3.16	0
2	3.16	3.16	0
3	3.16	3.16	0
4	2.34	2.34	0
5	3.16	3.16	0
6	0.82	0.82	0
7	1.58	1.58	0
8	1.58	1.58	0
		Ave. %difference	**0**

Table 5-13 - Heat transfer area comparison results between a mathematical and Flownex model.

	Heat transfer area (m^2)		
Flow channel NO:	**Mathematical model**	**Flownex model**	**Difference**
1	1.90	1.90	0
2	1.90	1.90	0
3	1.90	1.90	0
4	1.40	1.40	0
5	1.90	1.90	0
6	0.49	0.49	0
7	0.95	0.95	0
8	0.95	0.95	0
		Ave. %difference	**0**

5.2.3.2 Outlet temperature of the coolant in flow channel 1-8

Table 5-14 presents the comparison results between a mathematical model used to calculate the outlet temperature in the coolant flow channels 1 to 8 and Flownex. This mathematical model is presented by Equation 3.1. The parameters used to calculate the outlet temperature in different channels are presented in Appendix B.

Table 5-14 - Outlet temperature of the coolant comparison results between a mathematical and Flownex model.

	T_{out} (ºC)		
Flow channel NO:	**Mathematical model**	**Flownex model**	**% Difference**
1	59.24	58.84	0.41
2	58.83	58.43	0.40
3	66.59	66.04	0.56
4	62.11	61.64	0.47
5	58.03	57.64	0.39
6	71.09	70.43	0.66
7	61.53	61.06	0.46
8	56.68	56.32	0.36
		Ave. %difference	**0.46**

As shown in Table 5-14, the average percentage difference is relatively low and the Flownex model calculations of the outlet temperature in the flow channels can therefore be considered

accurate. The exact cause for the noted differences was not investigated. There are a few possibilities, one example being that the velocity calculations could be slightly different for the two methods of calculation.

5.2.3.3 Normal distribution of uncertain input parameters

As already mentioned in Chapter 4 a normal distribution was specified for the uncertain input parameters. This means that a Monte Carlo function in Flownex generates random values of uncertain input parameters from their probability density functions (which are normal PDFs in this case). It is therefore important to verify whether the Monte Carlo function produces a normal distribution for these parameters. This was done by using 10 000 (number of runs) random values generated by a Monte Carlo function to plot the PDFs of each uncertain input parameter. In addition to this, the r^2 method presented in Chapter 2 was used to test for a normal distribution fit. The PDFs of the uncertain input parameters are shown in Figure 5.6 - Figure 5.7. From visual inspection it is evident that they follow a normal distribution. Their r^2 values are presented in Table 5-15, showing that the r^2 values are close to 1. As a result, it can be concluded that Flownex indeed produced a normal distribution for the uncertain input parameters.

Table 5-15 - r^2 values of uncertain input parameter data.

Uncertain input parameter	r^2 value
1. Global mass flow rate of the coolant	0.98
2. Global temperature of the coolant	0.99
3. Local power in the hot channel	0.99
4. Width of the fuel plates in the hot channel	0.99
5. Width or gap of the coolant flow channel in the hot channel	0.99
6. Width of the fuel plates in the cold channel	0.99
7.Width or gap of the coolant flow in the cold channel	0.99

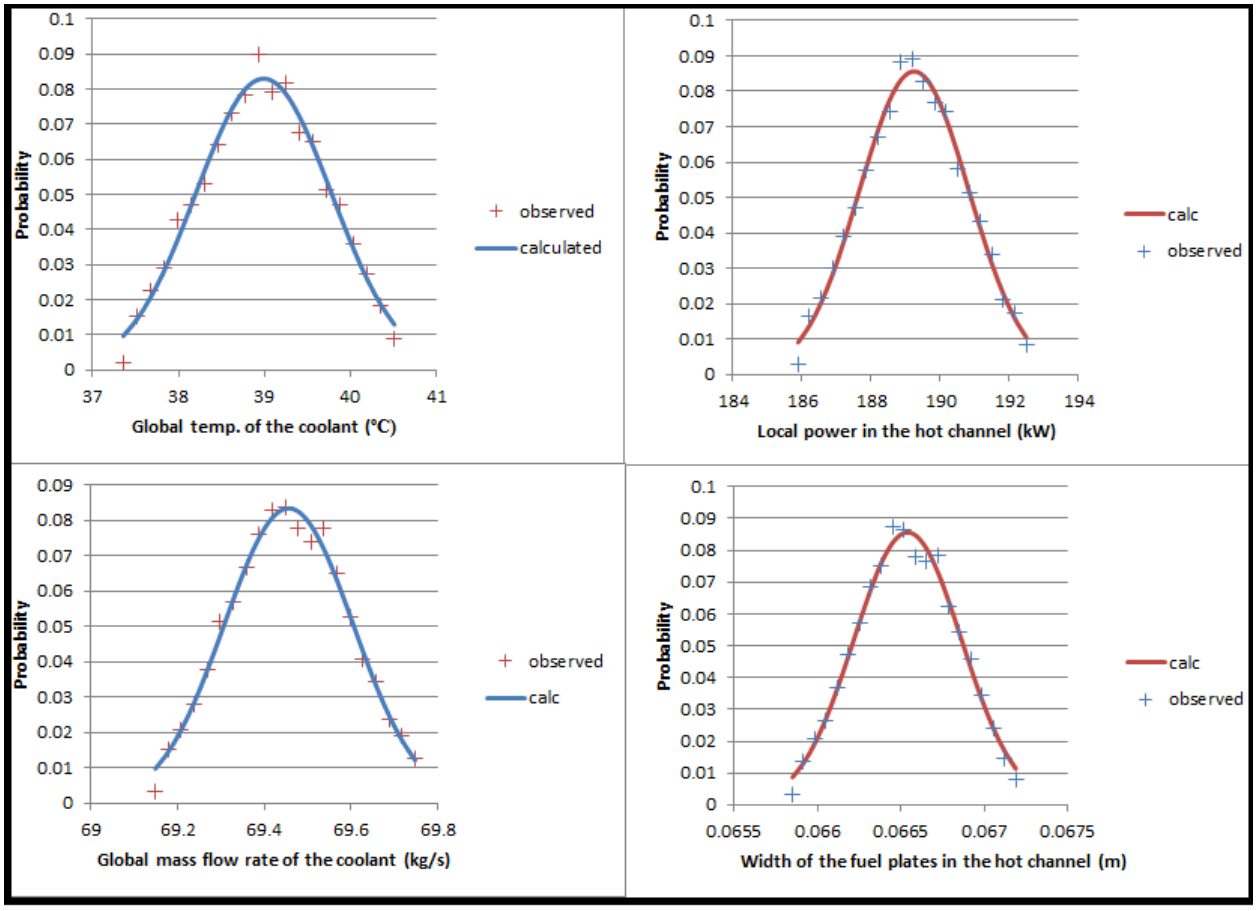

Figure 5.6 - PDF of global temperature of the coolant (top left corner), local power in the hot channel (top right corner), global mass flow rate of the coolant (bottom left corner), and the width of the fuel plates in the hot channel (bottom right corner).

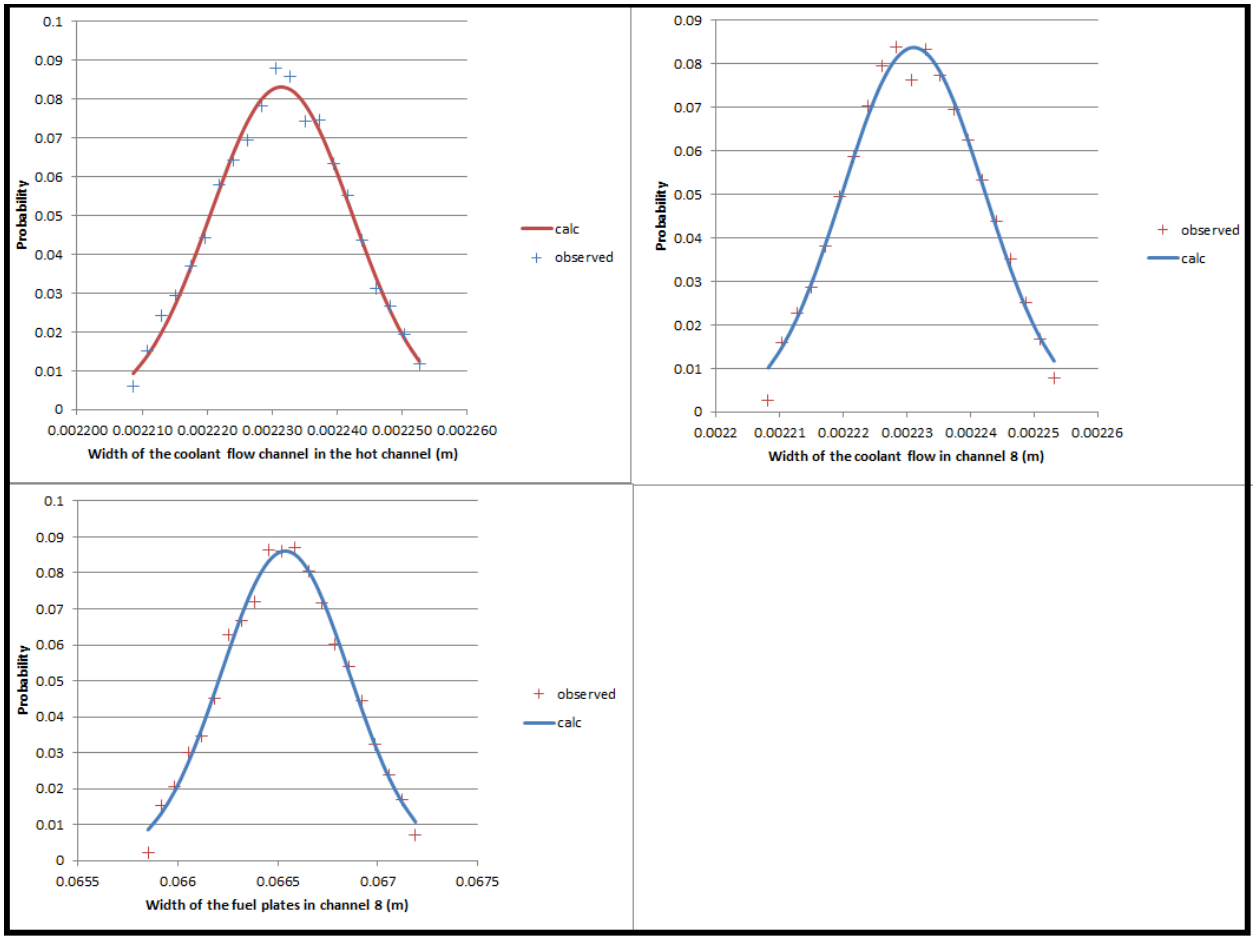

Figure 5.7 - PDF of the width of the coolant flow channel in the hot channel (top right corner), width of the coolant flow in the cold channel (top right corner), and the width of the fuel plates in the cold channel.

5.2.3.4 Monte Carlo results

As already described in Chapter 3, the Monte Carlo function in Flownex varies input parameters simultaneously and randomly within their prescribed range while investigating their effect on output parameters. This variation is done automatically by the Monte Carlo function. To verify that the results of the selected output parameters generated by the Monte Carlo function are correct, the uncertain input parameters were varied manually using the random values generated by Flownex. These random values are the same as the ones used in the Monte Carlo method. The results of the selected output parameters obtained from the Monte Carlo (automatic variation) and manual variation in Flownex were compared. Only 5 runs or variations were performed. The results

obtained showed that there is no difference between automatically and manually varying the uncertain input parameters. The Monte Carlo therefore performs the uncertain input variation accurately to produce the results of the selected output parameters.

5.2.3.5 The Flownex random number generator

The randomness test was used to evaluate whether the Monte Carlo function in Flownex generates the values of uncertain input parameters randomly during Monte Carlo computations. For a parameter with a step profile, this means that each bin (group) of data points of equal width within the range of the parameter will have the same probability of being selected or generated. 10 000 random values of the width of the fuel plate in the hot channel generated by a Monte Carlo random number generator were used. These random (10 000 data points) values were divided into 20 bins or groups having the same interval. The frequency (number of occurrence) of each bin (group) was analysed with respect to the average frequency. It was evaluated whether the frequency in each bin is the same i.e. evaluate whether the data points in each bin have equal chances (equal frequencies) of being generated by the Monte Carlo random number generator. Figure 5.8 depicts the frequency plot of a random number generator, and from this it can be seen that the frequency in each bin is nearly the same. Table 5.16 shows the results of the randomness test. In Table 5.16, the average % deviation from the average frequency is about 4.12% which is considered reasonably low. Thus it can be deduced that the Monte Carlo function in Flownex generates values randomly for input parameters.

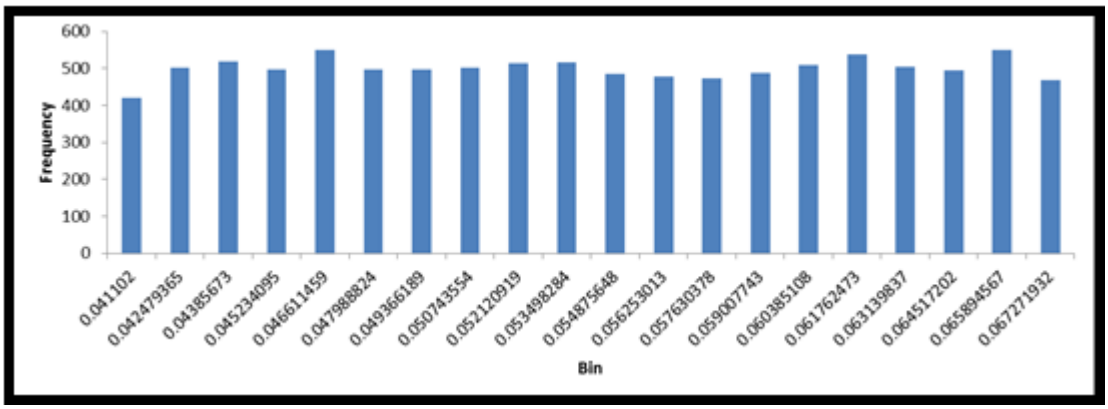

Figure 5.8 - Frequency plot of a Monte Carlo function random number generator.

Table 5-16 - Monte Carlo randomness test.

Number of bins	*Bin*	*Frequency*	*%deviation*	
1	0.041	420	16	
2	0.042	501	0.2	
3	0.044	519	3.8	
4	0.045	497	0.6	
5	0.047	551	10.2	
6	0.048	497	0.6	
7	0.049	496	0.8	
8	0.051	503	0.6	
9	0.052	514	2.8	
10	0.053	517	3.4	
11	0.055	484	3.2	
12	0.056	477	4.6	
13	0.058	472	5.6	
14	0.059	488	2.4	
15	0.060	508	1.6	
16	0.062	537	7.4	
17	0.063	505	1	
18	0.065	495	1	
19	0.066	551	10.2	
20	0.067	468	6.4	
	Average frequency	**500**	***Average %deviation***	**4.12**

5.3 Computer used and the time taken to complete Monte Carlo simulation runs

The specifications of the computer that was used to run the simulations are as follows:

- Processor: Intel (R) Core (TM) i5-3210M CPU @ 2.50GHz.
- RAM: 4.00 GB.
- System type: 64-bit Operating System: windows 7.

The time it took to complete the simulation runs is as follows:

- 5 000 runs took 4.5 hours.
- 10 000 runs took 9 hours.
- 15 000 runs took 12 hours.

CHAPTER 6 - CONCLUSION, PROBLEMS EXPERIENCED AND RECOMMENDATIONS

6.1 Overview of the implementation of the CSAU methodology

The overall objective of this study was to implement some of the steps of the code scaling applicability and uncertainty (CSAU) methodology to perform an uncertainty and sensitivity analysis. The system chosen was the Materials Test Reactor (MTR) model developed by Slabbert (2011). The analysis was done only for steady state computations.

In the CSAU methodology, of all the steps only step 1-6, 9, 12, 13 and 14 were performed. The scenario (step 1) of this study was the uncertainty and sensitivity analysis of the steady state (normal operation), and the system (step 2) used in this study was the IAEA MTR 10 MW benchmark reactor. The phenomena identification and ranking table (PIRT) (step 3) process was used in conjunction with the sensitivity analysis (step 12) results in order to select the uncertain input parameters of the selected output parameters as explained in Chapter 4. The frozen version 8.1.11 (step 4) of the Flownex software code was used. This code was developed by M-Tech Industrial (Pty) Ltd and thus the code development, assessment (step 5) etc. was done by them.

A number of verification calculations were performed in this study to ensure that certain correlations or parameters are calculated correctly. The Flownex MTR model verifications performed were flow area, circumference of the coolant flow channels, outlet temperature in coolant flow channel 1-8, normal distribution of uncertain input parameters, Monte Carlo results and Flownex random number generator. This verification step is important in investigating the correctness of the model in terms of the results it generates. The applicability (step 6) of the code to the specified scenario was partially done by Slabbert (2011), and it is thus recommended in this study for future work to be done. The uncertainty boundaries (step 9) and PDFs of the uncertain input parameters were produced. These uncertain input parameters were propagated (step 13) in the Monte Carlo function in Flownex to investigate their combined uncertainty effect on the selected output parameters.

Uncertainties of the fluid properties of the coolant were not propagated due to a Flownex limitation, as discussed in Chapter 4. As a result, these parameters were not included in the uncertainty analysis. The results generated (in step 13) by the Monte Carlo function of selected output parameters were used to produce the probability density functions (PDFs) (step 14). From these functions, the uncertainty limits of the selected output parameters were determined.

The comparison (step 7 and 8) between the code results against single effect tests (SETs) and integral effect tests (IETs) results was not performed as this is not part of the scope of this study. Step 10 was not performed since a large scale reactor core model was used as presented in Chapter 4. Step 11 was not performed as this study was based on steady state (normal operation) calculations and not transient calculations.

6.2 Conclusions

After performing the sensitivity analysis (step 12), the results thereof were used to rank all input parameters (step 3) with respect to the effect they have on the selected output parameters. The uncertain input parameters in terms of each selected output parameter were therefore selected.

Sensitivity results showed that the uncertain input parameters of both the centreline temperature of the fuel and cladding surface temperature were:

- Local power in the hot channel, global mass flow rate of the coolant, the coolant flow channel width (gap) in the hot channel, specific heat capacity of the coolant, viscosity of the coolant, the width of the fuel plates in the hot channel, conductivity of the coolant, and global temperature of the coolant.

The uncertain input parameters of the mass flow rate of the coolant in the hot channel were:

- Coolant flow channel width in the hot channel, global mass flow rate of the coolant, the width of the fuel plates in the hot channel, the width of the fuel plates in the cold channel, and the coolant flow channel width in the cold channel.

The uncertain input parameters of the temperature of the coolant in the hot channel were:

- Global temperature of the coolant, coolant flow channel width in the hot channel, global mass flow rate of the coolant, the width of the fuel plates in the hot channel and the local power in the hot channel.

Lastly, the uncertain input parameters of the pressure drop in the hot channel were:

- Density of the coolant and global mass flow rate of the coolant.

The uncertainty limits or boundaries of both the coolant flow channel width and the width of the fuel plates were obtained from the manufacturing tolerances as explained in Chapter 4. The uncertainty limits of local power, global mass flow rate and temperature of the coolant as obtained from plant data were found to be ±1.72%, ±0.44% and ±4.05% respectively. These uncertain input parameters follow a normal distribution as presented in Chapter 4. The uncertainty limits and distributions of the above-mentioned uncertain input parameters were used in the Monte Carlo function in Flownex for uncertainty propagation (step 13).

As explained in Chapter 4, it was assumed that 95.4% of the data points lie within 2σ i.e. within a 95.4% confidence interval. The Monte Carlo or uncertainty results (best estimate plus uncertainty results: step 14) showed that the upper limits and % deviation from the mean of the selected output parameters were:

- Centreline temperature of the fuel in the hot channel: Upper limit was found to be 103.6ºC, and the %deviation from the mean value (sample mean) was 1.23%.
- Maximum cladding surface temperature in the hot channel: Upper limit and % deviation from the mean were found to be 101.79ºC and 1.22% respectively.
- Mass flow rate of the coolant in the hot channel: Upper limit was found to be 1.42 kg/s, and % deviation from the mean was 1.73%.
- Temperature of the coolant in the hot channel: Upper limit and % deviation were found to be 56.79ºC and 2.88% respectively.
- Pressure drop in the hot channel: Upper limit was found to be 0.06 kPa, and % deviation from the mean was -0.03%.

From these results, it can be seen that the % deviation from their mean values for the selected output parameters are less than 3%. This value is relatively low. As a result, it can be deduced that during steady state the selected output parameter values should remain close to their mean (average) values. The detailed results and discussion of the best estimate plus uncertainty are presented in Chapter 5. The PDFs are also presented in Chapter 5.

The verification results showed that the difference between the results of the mathematical models and Flownex model was very small or negligible. As a result, it was concluded that the results generated by Flownex are reliable.

6.3 Problems experienced

The input parameters of fluid properties were varied manually (not automatically) for the sensitivity analysis. The results obtained from the sensitivity results (by ranking) showed that some of the fluid properties had a large effect on some selected output parameters. As a result, these fluid properties had to be propagated in the Monte Carlo function for uncertainty analysis. Flownex cannot vary these parameters automatically using the Monte Carlo function, therefore they were not included in the Monte Carlo uncertainty propagation for uncertainty analysis. This is one of the current limitations of Flownex. However, it should be noted that the variation chosen for the fluid properties was ±10%. The uncertainty limits of the fluid properties have not been investigated and therefore this effect could be overestimated.

6.4 Recommendations for future work

The following recommendations for future work can be made following the current study:

- This study was only done on the MTR core. As a result, the balance of the primary loop was not included. Further study with inclusion of the primary loop is recommended.
- The pressure drop due to minor losses (K_{losses}) was not investigated as this was out of the scope of investigation. It is of importance to investigate this parameter as it contributes to the pressure drop in the fuel assemblies.

- This study was based on thermal hydraulic analysis only. The neutronic analysis of the MTR model must also be undertaken as these two analyses are dependent on each other.
- In this study, only the steady state analysis was performed and no transient accident analysis was performed. It is thus recommended to investigate the uncertainty and sensitivity analysis on the MTR model for various transient accidents like Loss Of Flow Accident (LOFA), reactivity insertion accidents, Loss Of Coolant Accident (LOCA) etc.
- It is important to investigate the accuracy of the mathematical model that is used to determine the friction factor for pressure losses. This is because the pressure drop in the fuel assemblies or core is highly dependent on the friction factor. Thus the results obtained for this parameter is used to determine the pressure drop. As a result, the quality assurance on this parameter must be investigated to ensure the pressure drop calculations in the core are correct or good.
- It is highly recommended in future that the results obtained from Flownex be compared to those of other thermal hydraulic codes like RELAP5, TRACE etc. This should be done for quality assurance of the results obtained.
- A nodalization study of the MTR core system should also be undertaken.

BIBLIOGRAPHY

Ánchel, F., Barrachina, T., Miró, R., Verdú, G., Juanas, J. & Macián-Juan, R. 2012. Uncertainty and sensitivity analysis in the neutronic parameters generation for BWR and PWR coupled thermal-hydraulic–neutronic simulations. *Nuclear engineering and design*, 246(1):98-106.

Botes, W. 2013. SAFARI-1 operational data for 17 April to 22 May 2013. Pretoria: South African Nuclear Energy Corporation (NECSA).

Cho, Y., Kim, T., Lim, H. & Park, G. 2010. Effect of uncertainties in best-estimate thermal hydraulic analysis on core damage frequency for PSA. *Nuclear engineering and design*, 240(12): 4021-4030.

D'auria, F. & Galassi, G.M. 1998. Code validation and uncertainties in system thermalhydraulics. *Progress in nuclear energy*, 33(1):175-216.

De Crécy, A., Bazin, P., Glaeser, H., Skorek, T., Joucla, J., Probst, P., Fujioka, K., Chung, B.D., Oh, D.Y., Kyncl, M., Pernica, R., Macek, J.,. Meca, R., Macian, R., D'Auria, F., Petruzzi, A., Batet, L., Perez, M. &. Reventos F. 2008. Uncertainty and sensitivity analysis of the LOFT L2-5 test: results of the BEMUSE programme. *Nuclear engineering and design*, 238(12):3561–3578.

Devore, J.L. & Farnum, N.R. 2004. Applied statistics for engineers and scientists. 2nd ed. Belmont: Duxbury Press.

Fourie, L. (2011). Thermal-hydraulics simulation of a benchmark case for a typical Materials Test Reactor using Relap5 MOD4.0: Masters Mini dissertation. Potchefstroom: North-West University.

Hainoun, A., Ghazi, N. & Mansour Abdul-Moaiz, B. 2010. Safety analysis of the reference research reactor MTR during reactivity insertion accident using the code MERSAT. *Annals of nuclear energy*, 37(6):853–860.

Hamidouche, T., Bousbia-Salah, A., Si-Ahmed, E., Mokeddem, M.Y. & D'Auria, F. 2009. Application of coupled code technique to a safety analysis of a standard MTR research reactor. *Nuclear engineering and design*, 239(10):2104-2118.

Hernandez-Solis, A., Ekberg, C., Demaziere, C., Jensen, A.O. & Bredolt, U. 2011. Uncertainty and sensitivity analyses as a validation tool for BWR bundle thermal–hydraulic predictions. *Nuclear engineering and design*, 241(9):3697-3706.

Hochreiter, L. 2004. Elements of nuclear reactor design: lecture notes. Pennsylvania State University.

Incropera, F., DeWitt, D., Bergman, T. & Lavine, A. 2006. Fundamentals of heat and mass transfer. 6th ed. John Wiley & Sons Inc.

IAEA (International Atomic Energy Agency). 1980. Research reactor core conversion from the use of highly enriched uranium to the use of low enriched uranium fuels guidebook- IAEA TECDOC-233. Technical document. Austria: Vienna.

IAEA (International Atomic Energy Agency). 1992. *Research reactor core conversion guidebook - IAEA TECDOC-643.* Austria: Vienna.

IAEA (International Atomic Energy Agency). 2003. Research reactor utilization, safety, decommissioning, fuel and waste management. (In proceedings of an international conference on research reactor utilization, safety, decommissioning, fuel and waste management. Chile: IAEA)

Isukapalli, S.S., Roy, A. & Georgopoulos, P.G. 1998. Stochastic response surface methods (SRSMs) for uncertainty propagation: application to environmental and biological systems. *Risk analysis*, 18(3):351-363.

Koretsky, M. 2004. Engineering and chemical thermodynamics. John Wiley & Sons Inc.

Kristof, M., Kliment, T., Petruzzi, A. & Lipka, J. 2009. RELAP5 simulation of surge line break accident using combined and best estimate plus uncertainty approaches. *Nuclear engineering and design*, 239(11):2500–2513.

Larson, T.K., Moody, F.J., Wilson, G.E., Brown, W.L., Frepoli, C., Hartz, J., Woods, B.G. & Oriani, L. 2007. IRIS small break loca phenomena identification and ranking table (PIRT). *Nuclear engineering and design*, 237(6):618–626.

Martin, R.P. & O'Dell, L.D. 2005. AREVA's realistic large break LOCA analysis methodology. *Nuclear engineering and design*, 235(16):1713-1725.

Mesado, C., Soler, A., Barrachina, T., Miro, R., Garcia-Diaz, J.C., Masian-Juan, R., Verdu, G. 2012. Uncertainty and Sensitivity of Neutron Kinetic Parameters in the Dynamic Response of a PWRRod Ejection Accident Coupled Simulation. Science and Technology of Nuclear Installations, 10 pages.

Montgomery, D.C. & Runger, G.C. 2002. Applied statistics and probability for engineers. 3rd ed. John Wiley & Sons Inc.

Munson, B.R., Young, D.F. & Okiishi, T.H. 2005. Fundamentals of fluid mechanics. 5th ed. John Wiley & Sons Inc.

MTI (M-Tech Industrial (Pty) Ltd. 2011. Flownex SE User Manual. Potchefstroom: M-Tech Industrial.

Reventos, F. & Perez, M. 2012. Uncertainty analysis methodologies (conference proceedings). Innovative Systems Software, pp. 1-23.

Rousseau, P.G. & Van Eldik, M. 2011. Thermal-fluid systems modelling 1: lecture notes. Potchefstroom: North-West University.

Sage, M. 2006. A Flownex uncertainty analysis of a depressurised loss of forced cooling event for the PBMR. Potchefstroom: NWU (Dissertation - M.Eng).

Salama, A. & El-Morshedy, S. 2012. CFD analysis of flow blockage in MTR coolant channel under loss-of-flow transient: hot channel scenario. *Progress in nuclear energy*, 55:78-92.

Slabbert, R. 2011. Thermal-hydraulics simulation of a benchmark case for a typical Materials Test Reactor using Flownex. Potchefstroom: NWU. (Dissertation - M.Eng).

Srivastava, A., Lele, H.G., Ghosh, A.K., & Kushwaha, H.S. 2008. Uncertainty analysis of LBLOCA for advanced heavy water reactor. *Annals of nuclear energy*, 35(2):323-334.

Todreas, N.E. & Kazimi, M.S. 1990. Nuclear systems I: thermal-hydraulic fundamentals. Taylor & Francis.

USAEC (United States Atomic Energy Commission). 1962. Research reactor fuel element conference: book 1. (In Conference proceedings of the Research Reactor Fuel Element Conference, 17-19 September 1962, Gatlinburg, Tennessee).

USNRC (United States Nuclear Regulatory Commission). 2005. Regulatory Guide. USNRC Regulatory Guide 1.203. United States of America.

Van der Linde, H. 2005. Uncertainty analysis of the PBMR turbo machines. Potchefstroom: NWU. (Dissertation - M.Eng).

Wallis, G.B. 2007. Uncertainties and probabilities in nuclear reactor regulation. *Nuclear engineering and design*, 237(15-17):1586-1592.

Walpole, R., Myers, R., Myers, S. & Ye, K. 2011. Probability and statistics for engineers and scientists. Prentice Hall.

Wilks, S.S. 1944. Mathematical statistics. Princeton, NJ: Princeton University Press.

Wilks, S.S. 1962. Mathematical statistics. 2nd ed. New York: Wiley - a Wiley publication in mathematical statistics.

Wilson, G.E. & Boyack, B.E. 1998. The role of the PIRT process in experiments, code development and code applications associated with reactor safety analysis. *Nuclear engineering and design*, 186:23-37.

WNA (World Nuclear Association) . 2007. Global energy contribution by fuel.

Wilson, G.E. 2013. Historical insights in the development of Best Estimate Plus Uncertainty safety analysis. Nuclear engineering and design, 52: 2-9.

Young, M.Y., Bajorek, S.M., Nissley, M.E. & Hochreiter, L.E. 1998. Application of code scaling applicability and uncertainty methodology to the large break loss of coolant. *Nuclear engineering and design*, 186(1-2):39–52.

APPENDIX A

A. Ranking tables of selected output parameters

Table A-1: Phenomena Identification and Ranking Table of the centreline temperature of the fuel and cladding surface temperature in the hot channel

Input Parameters	Base values of input parameters	%Change of centreline temp. due to -10% input par. Variation	%Change of centreline temp. due to +10% input par. Variation
Pipe6-wy (m)	0.0665	5.55	-4.72
Node 6-Heat input (KW)	189.071	-5.17	5.51
Global Mass flow (Kg/s)	-69.4444	4.88	-4.14
Cp (kJ/kg*K) @ 41 ˚C	4.1	3.18	-2.74
Viscosity(kg/m*s) @ 41 ˚C	0.0006409	-2.71	0.64
Pipe6-lx (m)	0.00223	2.84	-2.37
Conductivity (W/m*K) @ 41 ˚C	0.63202	1.74	-3.31
Global Temperature (˚C)	38	-1.90	1.85
Node 1-Heat input (KW)	459.79	0.25	0.28
Node 2-Heat input (KW)	450.612	0.25	0.28
Node 3-Heat input (KW)	623.9	0.25	0.28
Node 4-Heat input (KW)	387.011	0.26	0.27
Node 5-Heat input (KW)	432.778	0.25	0.28
Node 7-Heat input (KW)	255.334	0.26	0.27
Node 8-Heat input (KW)	201.5004	0.26	0.27
Pipe4-lx (m)	0.00223	0.00	0.00
Pipe7-lx (m)	0.00223	0.00	0.00
Pipe7-wy (m)	0.0665	0.00	0.00
Pipe8-wy (m)	0.0665	-0.36	0.38
Pipe8-lx (m)	2.23E-03	-0.36	0.38
Pipe101-Diameter (m)	0.209845	0.27	0.27
Pipe101-Roughness (µm)	1.5	0.27	0.27
Pipe102-Diameter (m)	0.209845	0.27	0.27
Pipe102-Roughness (µm)	1.5	0.27	0.27
Pipe103-Diameter (m)	0.1597	0.27	0.27
Pipe103-Roughness (µm)	1.5	0.27	0.27
Pipe104-Diameter (m)	0.13612	0.27	0.27
Pipe104-Roughness (µm)	1.5	0.27	0.27

Pipe105-Diameter (m)	0.1597	0.27	0.27
Pipe105-Roughness (µm)	1.5	0.27	0.27
Pipe106-Diameter (m)	0.13612	0.27	0.27
Pipe106-Roughness (µm)	1.5	0.27	0.27
Pipe107-Diameter (m)	0.20985	0.27	0.27
Pipe107-Roughness (µm)	1.5	0.27	0.27
Pipe108-Diameter (m)	0.20985	0.27	0.27
Pipe108-Roughness (µm)	1.5	0.27	0.27
Pipe201-Diameter (m)	0.20985	0.27	0.27
Pipe201-Roughness (µm)	1.5	0.27	0.27
Pipe202-Diameter (m)	6	0.27	0.27
Pipe202-Roughness (µm)	1.5	0.27	0.27
Pipe9-Diameter (m)	0.02483	0.27	0.27
Pipe9-Roughness (µm)	1.5	0.27	0.27
Pipe10-Diameter (m)	0.26199	0.27	0.27
Pipe10-Roughness (µm)	1.5	0.27	0.27
Pipe11-Diameter (m)	0.09963	0.27	0.27
Pipe11-Roughness (µm)	1.5	0.27	0.27
Pipe12-Diameter (m)	0.09963	0.27	0.27
Heat transfer element 1-Thickness (m)	0.000255	0.27	0.27
Heat transfer element 2-Thickness (m)	0.000255	0.27	0.27
Heat transfer element 3-Thickness (m)	0.000255	0.27	0.27
Heat transfer element 4-Thickness (m)	0.000255	0.27	0.27
Heat transfer element 5-Thickness (m)	0.000255	0.27	0.27
Heat transfer element 7-Thickness (m)	0.000255	0.27	0.27
Heat transfer element 8-Thickness (m)	0.000255	0.27	0.27
Pipe12-Roughness (µm)	1.5	0.27	0.27
Heat transfer element 6-Thickness (m)	0.000255	0.13	0.40
Pipe 1-Roughness (µm)	1.5	0.00	0.00
Pipe 2-Roughness (µm)	1.5	0.00	0.00
Pipe 3-Roughness (µm)	1.5	0.00	0.00
Pipe 4-Roughness (µm)	1.5	0.00	0.00
Pipe 5-Roughness (µm)	1.5	0.00	0.00
Pipe3-wy (m)	0.0665	0.00	0.00
Pipe1-wy (m)	0.0665	0.00	0.00
Pipe2-wy (m)	0.0665	0.00	0.00
Pipe5-wy (m)	0.0665	0.00	0.00
Pipe4-wy (m)	0.0665	0.00	0.00
Pipe1-lx (m)	0.00223	0.00	0.00
Pipe2-lx (m)	0.00223	0.00	0.00

Pipe3-lx (m)	0.00223	0.00	0.00
Pipe 6-Roughness (μm)	1.5	-0.05	0.05
Density @ 41 ˚C	991.83	0.00	0.00
Global Pressure (kPa)	170	0.45	-0.46
Bulk modulus @ 41 ˚C	2200000	0.00	0.00
Pipe5-lx (m)	0.00223	0.00	0.00

Table A-2: Phenomena Identification and Ranking Table of the mass flow rate of the coolant in the hot channel

Input Parameters	Base values of input par.	%Change of mass flow rate. due to -10% input par. Variation	%Change of mass flow rate. due to +10% input par. Variation
Pipe6-lx (m)	0.00223	-14.99	15.63
Global Mass flow (Kg/s)	-69.4444	-10.36	10.35
Pipe6-wy (m)	0.0665	-9.70	9.62
Pipe8-lx (m)	0.00223	0.83	-0.86
Pipe8-wy (m)	0.0665	0.53	-0.53
Global Temperature (˚C)	38	0.24	0.20
Global Pressure (kPa)	170	0.02	0.02
Pipe4-lx (m)	0.0665	0.00	-100.00
Pipe7-lx (m)	0.0665	0.00	0.00
Pipe3-wy (m)	0.00223	0.00	0.00
Pipe1-wy (m)	0.00223	0.00	0.00
Pipe2-wy (m)	0.00223	0.00	0.00
Pipe5-wy (m)	0.00223	0.00	0.00
Pipe4-wy (m)	0.00223	0.00	0.00
Pipe3-lx (m)	0.0665	0.00	0.00
Pipe1-lx (m)	0.0665	0.00	0.00
Pipe2-lx (m)	0.0665	0.00	0.00
Pipe5-lx (m)	0.0665	0.00	0.00
Pipe7-wy (m)	0.00223	0.00	0.00
Node 1-Heat input (KW)	459.79	-0.03	-0.03
Node 2-Heat input (KW)	450.612	-0.03	-0.03
Node 3-Heat input (KW)	623.9	-0.03	-0.03
Node 4-Heat input (KW)	387.011	-0.02	-0.02
Node 5-Heat input (KW)	432.778	-0.03	-0.03
Node 6-Heat input (KW)	189.071	0.26	0.24
Node 7-Heat input (KW)	255.334	-0.02	-0.01
Node 8-Heat input (KW)	201.5004	-0.01	-0.01
Heat transfer element 1-Thickness (m)	0.000255	0.00	0.00
Heat transfer element 2-Thickness (m)	0.000255	0.00	0.00
Heat transfer element 3-Thickness (m)	0.000255	0.00	0.00
Heat transfer element 4-Thickness (m)	0.000255	0.00	0.00
Heat transfer element 5-Thickness (m)	0.000255	0.00	0.00
Heat transfer element 6-Thickness (m)	0.000255	0.00	0.00
Heat transfer element 7-Thickness (m)	0.000255	0.00	0.00
Heat transfer element 8-Thickness (m)	0.000255	0.00	0.00

Pipe101-Diameter (m)	0.209845	0.00	0.00
Pipe101-Roughness (µm)	1.5	0.00	0.00
Pipe102-Diameter (m)	0.209845	0.00	0.00
Pipe102-Roughness (µm)	1.5	0.00	0.00
Pipe103-Diameter (m)	0.1597	0.00	0.00
Pipe103-Roughness (µm)	1.5	0.00	0.00
Pipe104-Diameter (m)	0.13612	0.00	0.00
Pipe104-Roughness (µm)	1.5	0.00	0.00
Pipe105-Diameter (m)	0.1597	0.00	0.00
Pipe105-Roughness (µm)	1.5	0.00	0.00
Pipe106-Diameter (m)	0.13612	0.00	0.00
Pipe106-Roughness (µm)	1.5	0.00	0.00
Pipe107-Diameter (m)	0.20985	0.00	0.00
Pipe107-Roughness (µm)	1.5	0.00	0.00
Pipe108-Diameter (m)	0.20985	0.00	0.00
Pipe108-Roughness (µm)	1.5	0.00	0.00
Pipe201-Diameter (m)	0.20985	0.00	0.00
Pipe201-Roughness (µm)	1.5	0.00	0.00
Pipe202-Diameter (m)	6	0.00	0.00
Pipe202-Roughness (µm)	1.5	0.00	0.00
Pipe9-Diameter (m)	0.02483	0.00	0.00
Pipe9-Roughness (µm)	1.5	0.00	0.00
Pipe10-Diameter (m)	0.26199	0.00	0.00
Pipe10-Roughness (µm)	1.5	0.00	0.00
Pipe11-Diameter (m)	0.09963	0.00	0.00
Pipe11-Roughness (µm)	1.5	0.00	0.00
Pipe12-Diameter (m)	0.09963	0.00	0.00
Pipe12-Roughness (µm)	1.5	0.00	0.00
Pipe 1-Roughness (µm)	1.5	0.01	0.01
Pipe 2-Roughness (µm)	1.5	0.01	0.01
Pipe 3-Roughness (µm)	1.5	0.01	0.01
Pipe 4-Roughness (µm)	1.5	0.01	0.01
Pipe 5-Roughness (µm)	1.5	0.01	0.01
Pipe 6-Roughness (µm)	1.5	-0.10	-0.10

Table A-3: Phenomena Identification and Ranking Table of the temperature of the coolant in the hot channel

Input Parameters	Base values of input par.	%Change of the coolant temp. due to -10% input par. Variation	%Change of the coolant temp. due to input par. Variation
Global Temperature (˚C)	38	-6.93	6.94
Pipe6-lx (m)	0.00223	5.27	-4.04
Cp (kJ/kg*K) @ 41 ˚C	4.1	5.16	-4.22
Global Mass flow (Kg/s)	-69.4444	3.46	-2.80
Pipe6-wy (m)	0.0665	3.21	-2.62
Node 6-Heat input (KW)	189.071	-2.92	2.91
Global Pressure (kPa)	170	0.01	-0.01
Node 1-Heat input (KW)	459.79	-0.01	0.01
Node 2-Heat input (KW)	450.612	-0.01	0.01
Node 3-Heat input (KW)	623.9	-0.01	0.01
Node 4-Heat input (KW)	387.011	-0.01	0.01
Node 5-Heat input (KW)	432.778	-0.01	0.01
Node 7-Heat input (KW)	255.334	0.00	0.00
Node 8-Heat input (KW)	201.5004	0.00	0.00
Heat transfer element 1-Thickness (m)	0.000255	0.00	0.00
Heat transfer element 2-Thickness (m)	0.000255	0.00	0.00
Heat transfer element 3-Thickness (m)	0.000255	0.00	0.00
Heat transfer element 4-Thickness (m)	0.000255	0.00	0.00
Heat transfer element 5-Thickness (m)	0.000255	0.00	0.00
Heat transfer element 6-Thickness (m)	0.000255	0.00	0.00
Heat transfer element 7-Thickness (m)	0.000255	0.00	0.00
Heat transfer element 8-Thickness (m)	0.000255	0.00	0.00
Pipe1-lx (m)	0.00223	0.00	0.00
Pipe2-lx (m)	0.00223	0.00	0.00
Pipe1-wy (m)	0.0665	0.00	0.00
Pipe2-wy (m)	0.0665	0.00	0.00
Pipe3-wy (m)	0.0665	0.00	0.00
Pipe5-wy (m)	0.0665	0.00	0.00
Pipe3-lx (m)	0.00223	0.00	0.00
Pipe4-lx (m)	0.00223	0.00	0.00
Pipe4-wy (m)	0.0665	0.00	0.00
Pipe5-lx (m)	0.00223	0.00	0.00
Pipe7-lx (m)	0.00223	0.00	0.00
Pipe7-wy (m)	0.0665	0.00	0.00
Pipe8-wy (m)	0.0665	-0.16	0.16

Pipe8-lx (m)	0.00223	-0.25	0.26
Pipe101-Diameter (m)	0.209845	0.00	0.00
Pipe101-Roughness (µm)	1.5	0.00	0.00
Pipe102-Diameter (m)	0.209845	0.00	0.00
Pipe102-Roughness (µm)	1.5	0.00	0.00
Pipe103-Diameter (m)	0.1597	0.00	0.00
Pipe103-Roughness (µm)	1.5	0.00	0.00
Pipe104-Diameter (m)	0.13612	0.00	0.00
Pipe104-Roughness (µm)	1.5	0.00	0.00
Pipe105-Diameter (m)	0.1597	0.00	0.00
Pipe105-Roughness (µm)	1.5	0.00	0.00
Pipe106-Diameter (m)	0.13612	0.00	0.00
Pipe106-Roughness (µm)	1.5	0.00	0.00
Pipe107-Diameter (m)	0.20985	0.00	0.00
Pipe107-Roughness (µm)	1.5	0.00	0.00
Pipe108-Diameter (m)	0.20985	0.00	0.00
Pipe108-Roughness (µm)	1.5	0.00	0.00
Pipe201-Diameter (m)	0.20985	0.00	0.00
Pipe201-Roughness (µm)	1.5	0.00	0.00
Pipe202-Diameter (m)	6	0.00	0.00
Pipe202-Roughness (µm)	1.5	0.00	0.00
Pipe9-Diameter (m)	0.02483	0.00	0.00
Pipe9-Roughness (µm)	1.5	0.00	0.00
Pipe10-Diameter (m)	0.26199	0.00	0.00
Pipe10-Roughness (µm)	1.5	0.00	0.00
Pipe11-Diameter (m)	0.09963	0.00	0.00
Pipe11-Roughness (µm)	1.5	0.00	0.00
Pipe12-Diameter (m)	0.09963	0.00	0.00
Pipe12-Roughness (µm)	1.5	0.00	0.00
Pipe 1-Roughness (µm)	1.5	0.00	0.00
Pipe 2-Roughness (µm)	1.5	0.00	0.00
Pipe 3-Roughness (µm)	1.5	0.00	0.00
Pipe 4-Roughness (µm)	1.5	0.00	0.00
Pipe 5-Roughness (µm)	1.5	0.00	0.00
Pipe 6-Roughness (µm)	1.5	-0.03	0.03
Density (kg/m^3) @ 41 ˚C	991.83	0.00	0.00
Viscosity (N.s/m^2)@ 41 ˚C	0.0006409	0.00	0.00
Density (kg/m^3) @ 41 ˚C	991.83	0.00	0.00
Conductivity (W/m*K) @ 41 ˚C	0.63202	0.00	0.00
Bulk modulus (kPa) @ 41 ˚C	2200000	0.00	0.00

Table A-4: Phenomena Identification and Ranking Table of the pressure drop in the hot channel

Input Parameters	Base values of input par.	%Change of Pres. due to -10% input par. Variation	%Change of Pres. due to +10% input par. Variation
Density (kg/m^3) @ 41 ˚C	991.83	-0.75	0.59
Global Mass flow (Kg/s)	-69.4444	-0.61	0.67
Global Temperature (˚C)	38	0.03	0.03
Global Pressure (kPa)	170	0.02	0.02
Node 1-Heat input (KW)	459.79	0.00	0.00
Node 2-Heat input (KW)	450.612	0.00	0.00
Node 3-Heat input (KW)	623.9	0.00	0.00
Node 4-Heat input (KW)	387.011	0.00	0.00
Node 5-Heat input (KW)	432.778	0.00	0.00
Node 6-Heat input (KW)	189.071	0.00	0.00
Node 7-Heat input (KW)	255.334	0.00	0.00
Node 8-Heat input (KW)	201.5004	0.00	0.00
Heat transfer element 1-Thickness (m)	0.000255	0.00	0.00
Heat transfer element 2-Thickness (m)	0.000255	0.00	0.00
Heat transfer element 3-Thickness (m)	0.000255	0.00	0.00
Heat transfer element 4-Thickness (m)	0.000255	0.00	0.00
Heat transfer element 5-Thickness (m)	0.000255	0.00	0.00
Heat transfer element 6-Thickness (m)	0.000255	0.00	0.00
Heat transfer element 7-Thickness (m)	0.000255	0.00	0.00
Heat transfer element 8-Thickness (m)	0.000255	0.00	0.00
Pipe1-lx (m)	0.00223	0.00	0.00
Pipe1-wy (m)	0.0665	0.00	0.00
Pipe2-lx (m)	0.00223	0.00	0.00
Pipe2-wy (m)	0.0665	0.00	0.00
Pipe3-lx (m)	0.00223	0.00	0.00
Pipe3-wy (m)	0.0665	0.00	0.00
Pipe4-lx (m)	0.00223	0.00	0.00
Pipe4-wy (m)	0.0665	0.00	0.00
Pipe5-lx (m)	0.00223	0.00	0.00
Pipe5-wy (m)	0.0665	0.00	0.00
Pipe6-lx (m)	0.00223	0.05	0.05
Pipe6-wy (m)	0.0665	0.02	0.02
Pipe7-lx (m)	0.00223	0.00	0.00
Pipe7-wy (m)	0.0665	0.00	0.00
Pipe8-wy (m)	0.0665	0.03	0.03

Pipe8-lx (m)	0.00223	0.05	0.05
Pipe101-Diameter (m)	0.209845	0.00	0.00
Pipe101-Roughness (µm)	1.5	0.00	0.00
Pipe102-Diameter (m)	0.209845	0.00	0.00
Pipe102-Roughness (µm)	1.5	0.00	0.00
Pipe103-Diameter (m)	0.1597	0.00	0.00
Pipe103-Roughness (µm)	1.5	0.00	0.00
Pipe104-Diameter (m)	0.13612	0.00	0.00
Pipe104-Roughness (µm)	1.5	0.00	0.00
Pipe105-Diameter (m)	0.1597	0.00	0.00
Pipe105-Roughness (µm)	1.5	0.00	0.00
Pipe106-Diameter (m)	0.13612	0.00	0.00
Pipe106-Roughness (µm)	1.5	0.00	0.00
Pipe107-Diameter (m)	0.20985	0.00	0.00
Pipe107-Roughness (µm)	1.5	0.00	0.00
Pipe108-Diameter (m)	0.20985	0.00	0.00
Pipe108-Roughness (µm)	1.5	0.00	0.00
Pipe201-Diameter (m)	0.20985	0.00	0.00
Pipe201-Roughness (µm)	1.5	0.00	0.00
Pipe202-Diameter (m)	6	0.00	0.00
Pipe202-Roughness (µm)	1.5	0.00	0.00
Pipe9-Diameter (m)	0.02483	0.00	0.00
Pipe9-Roughness (µm)	1.5	0.00	0.00
Pipe10-Diameter (m)	0.26199	0.00	0.00
Pipe10-Roughness (µm)	1.5	0.00	0.00
Pipe11-Diameter (m)	0.09963	0.00	0.00
Pipe11-Roughness (µm)	1.5	0.00	0.00
Pipe12-Diameter (m)	0.09963	0.00	0.00
Pipe12-Roughness (µm)	1.5	0.00	0.00
Pipe 1-Roughness (µm)	1.5	0.00	0.00
Pipe 2-Roughness (µm)	1.5	0.00	0.00
Pipe 3-Roughness (µm)	1.5	0.00	0.00
Pipe 4-Roughness (µm)	1.5	0.00	0.00
Pipe 5-Roughness (µm)	1.5	0.00	0.00
Pipe 6-Roughness (µm)	1.5	0.00	0.00
Viscosity (kg/m*s) @ 41 ˚C	0.0006409	0.08	-0.07
Conductivity (W/m*K) @ 41 ˚C	0.63202	0.00	0.00
Cp (kJ/kg*K) 41 ˚C	4.1	0.03	-0.01
Bulk modulus (kPa) @ 41 ˚C	2200000	0.00	0.00

APPENDIX B

B. Flownex® script

This script was used to calculate the heat transfer area, flow coolant channel area, and the circumference of the coolant flow channel using the width (w_y) of the fuel plates, the gap (l_x) between fuel plates and the height (h_z) of the fuel plates within the Flownex platform. The values of the width (w_y) of the fuel plates, the gap (l_x) between fuel plates and the height (h_z) of the fuel plates in all the coolant channels are equal. Their values are as follows:

- w_y= 0.0665 m
- l_x= 0.00223 m
- h_z= 0.6 m

The script is listed below:

```
//script using directives
//css_ref IPS.Core.dll;
//css_ref IPS.PluginInterface.dll;
//css_ref IPS.Units.dll;
using System;
using IPS.Properties;
using IPS.Scripting;

//script must be derived from IComponentScript
public class Script:IPS.Scripting.IComponentScript
{

double [ ] N_watergaps;
// next set of parameters
IPS.Properties.Double _Output1;
IPS.Properties.Double _Output2;
```

```
IPS.Properties.Double _Output3;

//Declare Components
IPS.Plugin.ComponentBase [ ] N_wy;
IPS.Plugin.ComponentBase [ ] N_lx;
IPS.Plugin.ComponentBase [ ] P_hz;
IPS.Plugin.ComponentBase [ ] Pipe;
IPS.Plugin.ComponentBase [ ] HeatTE;

//Declare Variables for length, width and height of water gap
IPS.Properties.Double [  ]  wy;
IPS.Properties.Double [  ]  lx;
IPS.Properties.Double [  ]  hz;
IPS.Properties.Double [  ]  area;
IPS.Properties.Double [  ]  circ;
IPS.Properties.Double [ , ]  htArea;

//constructer initialises parameters
public Script()
{
_Output1= new IPS.Properties.Double();
_Output2 = new IPS.Properties.Double();
_Output3 = new IPS.Properties.Double();

N_wy  = new IPS.Plugin.ComponentBase [13] ;
N_lx  = new IPS.Plugin.ComponentBase [13] ;
P_hz  = new IPS.Plugin.ComponentBase [13] ;
Pipe  = new IPS.Plugin.ComponentBase [13] ;
HeatTE  = new IPS.Plugin.ComponentBase [13] ;
```

```
wy  = new  IPS.Properties.Double [13];
lx  = new  IPS.Properties.Double [13];
hz  = new  IPS.Properties.Double [13];
area  = new  IPS.Properties.Double [13];
circ  = new  IPS.Properties.Double [13];
htArea  = new  IPS.Properties.Double [13,4];

N_watergaps = new double[13];

//N_watergaps[1] = ];
//N_watergaps[2] = ];
//N_watergaps[3] = ];
//N_watergaps[4] = ];
//N_watergaps[5] = ];
//N_watergaps[6] = ];
//N_watergaps[7] = ];
//N_watergaps[8] = ];


//set initial values
_Output1.Value = 0;
_Output2.Value = 0;
_Output3.Value = 0;

//time1 = new double[100];
//mdot1   = new double[100];

//-------------------------------------------------------------------------------------------------------------
----------
//set mdot tables using RELAP5 data
//-------------------------------------------------------------------------------------------------------------
```

```
----------


    }

    //do pre simulation initialisation here
    public override void Initialise()
{

//Establish link with component: width y of water gap of FE
N_wy[6] =   (IPS.Plugin.ComponentBase)this.Project.GetComponent("Node_6_wy");
N_wy[8] =   (IPS.Plugin.ComponentBase)this.Project.GetComponent("Node_8_wy");
N_wy[1] =   (IPS.Plugin.ComponentBase)this.Project.GetComponent("Node_1_wy");
N_wy[2] =   (IPS.Plugin.ComponentBase)this.Project.GetComponent("Node_2_wy");
N_wy[3] =   (IPS.Plugin.ComponentBase)this.Project.GetComponent("Node_3_wy");
N_wy[4] =   (IPS.Plugin.ComponentBase)this.Project.GetComponent("Node_4_wy");
N_wy[5] =   (IPS.Plugin.ComponentBase)this.Project.GetComponent("Node_5_wy");
N_wy[7] =   (IPS.Plugin.ComponentBase)this.Project.GetComponent("Node_7_wy");
//Establish    link    with    component:    length    x    of    water    gap    of    FE
N_lx[6] =   (IPS.Plugin.ComponentBase)this.Project.GetComponent("Node_6_lx");
N_lx[8] =   (IPS.Plugin.ComponentBase)this.Project.GetComponent("Node_8_lx");
N_lx[1] =   (IPS.Plugin.ComponentBase)this.Project.GetComponent("Node_1_lx");
N_lx[2] =   (IPS.Plugin.ComponentBase)this.Project.GetComponent("Node_2_lx");
N_lx[3] =   (IPS.Plugin.ComponentBase)this.Project.GetComponent("Node_3_lx");
N_lx[4] =   (IPS.Plugin.ComponentBase)this.Project.GetComponent("Node_4_lx");
N_lx[5] =   (IPS.Plugin.ComponentBase)this.Project.GetComponent("Node_5_lx");
N_lx[7] =   (IPS.Plugin.ComponentBase)this.Project.GetComponent("Node_7_lx");
//Establish link with component:height z of water gap of FE
P_hz[6] =   (IPS.Plugin.ComponentBase)this.Project.GetComponent("Pipe 6");
P_hz[8] =   (IPS.Plugin.ComponentBase)this.Project.GetComponent("Pipe 8");
P_hz[1] =   (IPS.Plugin.ComponentBase)this.Project.GetComponent("Pipe 1");
```

```
P_hz[2] =   (IPS.Plugin.ComponentBase)this.Project.GetComponent("Pipe 2");
P_hz[3] =   (IPS.Plugin.ComponentBase)this.Project.GetComponent("Pipe 3");
P_hz[4] =   (IPS.Plugin.ComponentBase)this.Project.GetComponent("Pipe 4");
P_hz[5] =   (IPS.Plugin.ComponentBase)this.Project.GetComponent("Pipe 5");
P_hz[7] =   (IPS.Plugin.ComponentBase)this.Project.GetComponent("Pipe 7");
//Establish link with component pipe  element
Pipe[6] =   (IPS.Plugin.ComponentBase)this.Project.GetComponent("Pipe 6");
Pipe[8] =   (IPS.Plugin.ComponentBase)this.Project.GetComponent("Pipe 8");
Pipe[1] =   (IPS.Plugin.ComponentBase)this.Project.GetComponent("Pipe 1");
Pipe[2] =   (IPS.Plugin.ComponentBase)this.Project.GetComponent("Pipe 2");
Pipe[3] =   (IPS.Plugin.ComponentBase)this.Project.GetComponent("Pipe 3");
Pipe[4] =   (IPS.Plugin.ComponentBase)this.Project.GetComponent("Pipe 4");
Pipe[5] =   (IPS.Plugin.ComponentBase)this.Project.GetComponent("Pipe 5");
Pipe[7] =   (IPS.Plugin.ComponentBase)this.Project.GetComponent("Pipe 7");

//Establish link with component:heat transfer element
HeatTE[6] =   (IPS.Plugin.ComponentBase)this.Project.GetComponent("HS 6");
HeatTE[8] =   (IPS.Plugin.ComponentBase)this.Project.GetComponent("HS 8");
HeatTE[1] =   (IPS.Plugin.ComponentBase)this.Project.GetComponent("HS 1");
HeatTE[2] =   (IPS.Plugin.ComponentBase)this.Project.GetComponent("HS 2");
HeatTE[3] =   (IPS.Plugin.ComponentBase)this.Project.GetComponent("HS 3");
HeatTE[4] =   (IPS.Plugin.ComponentBase)this.Project.GetComponent("HS 4");
HeatTE[5] =   (IPS.Plugin.ComponentBase)this.Project.GetComponent("HS 5");
HeatTE[7] =   (IPS.Plugin.ComponentBase)this.Project.GetComponent("HS 7");

//Establish link with variables for width y of water gap
wy[6] = (IPS.Properties.Double)N_wy[6].GetPropertyFromFullDisplayName("{Heat
Transfer}Heat input");
wy[8] = (IPS.Properties.Double)N_wy[8].GetPropertyFromFullDisplayName("{Heat Transfer}
Heat input");
wy[1] = (IPS.Properties.Double)N_wy[1].GetPropertyFromFullDisplayName("{Heat Transfer}
```

```
Heat input");
wy[2] = (IPS.Properties.Double)N_wy[2].GetPropertyFromFullDisplayName("{Heat
Transfer}Heat input");
wy[3] = (IPS.Properties.Double)N_wy[3].GetPropertyFromFullDisplayName("{Heat
Transfer}Heat input");
wy[4] = (IPS.Properties.Double)N_wy[4].GetPropertyFromFullDisplayName("{Heat
Transfer}Heat input");
wy[5] = (IPS.Properties.Double)N_wy[5].GetPropertyFromFullDisplayName("{Heat
Transfer}Heat input");
wy[7] = (IPS.Properties.Double)N_wy[7].GetPropertyFromFullDisplayName("{Heat
Transfer}Heat input");

//Establish link with variables for length x of water gap
lx[6] = (IPS.Properties.Double)N_lx[6].GetPropertyFromFullDisplayName("{Heat
Transfer}Heat input");
lx[8] = (IPS.Properties.Double)N_lx[8].GetPropertyFromFullDisplayName("{Heat
Transfer}Heat input");
lx[1] = (IPS.Properties.Double)N_lx[1].GetPropertyFromFullDisplayName("{Heat
Transfer}Heat input");
lx[2] = (IPS.Properties.Double)N_lx[2].GetPropertyFromFullDisplayName("{Heat
Transfer}Heat input");
lx[3] = (IPS.Properties.Double)N_lx[3].GetPropertyFromFullDisplayName("{Heat
Transfer}Heat input");
lx[4] = (IPS.Properties.Double)N_lx[4].GetPropertyFromFullDisplayName("{Heat
Transfer}Heat input");
lx[5] = (IPS.Properties.Double)N_lx[5].GetPropertyFromFullDisplayName("{Heat
Transfer}Heat input");
lx[7] = (IPS.Properties.Double)N_lx[7].GetPropertyFromFullDisplayName("{Heat
Transfer}Heat input");
```

```
//Establish link with variables for height h of water gap
hz[6] = (IPS.Properties.Double)P_hz[6].GetPropertyFromFullDisplayName("{Geometry}Length");
hz[8] = (IPS.Properties.Double)P_hz[8].GetPropertyFromFullDisplayName("{Geometry}Length");
hz[1] = (IPS.Properties.Double)P_hz[1].GetPropertyFromFullDisplayName("{Geometry}Length");
hz[2] = (IPS.Properties.Double)P_hz[2].GetPropertyFromFullDisplayName("{Geometry}Length");
hz[3] = (IPS.Properties.Double)P_hz[3].GetPropertyFromFullDisplayName("{Geometry}Length");
hz[4] = (IPS.Properties.Double)P_hz[4].GetPropertyFromFullDisplayName("{Geometry}Length");
hz[5] = (IPS.Properties.Double)P_hz[5].GetPropertyFromFullDisplayName("{Geometry}Length");
hz[7] = (IPS.Properties.Double)P_hz[7].GetPropertyFromFullDisplayName("{Geometry}Length");

//Establish link with variables for pipe area
area[6] = (IPS.Properties.Double)Pipe[6].GetPropertyFromFullDisplayName("{Geometry,Inlet}Area");
area[8] = (IPS.Properties.Double)Pipe[8].GetPropertyFromFullDisplayName("{Geometry,Inlet}Area");
area[1] = (IPS.Properties.Double)Pipe[1].GetPropertyFromFullDisplayName("{Geometry,Inlet}Area");
area[2] = (IPS.Properties.Double)Pipe[2].GetPropertyFromFullDisplayName("{Geometry,Inlet}Area");
area[3] = (IPS.Properties.Double)Pipe[3].GetPropertyFromFullDisplayName("{Geometry,Inlet}Area");
area[4] = (IPS.Properties.Double)Pipe[4].GetPropertyFromFullDisplayName("{Geometry,Inlet}Area");
```

```
area[5] = (IPS.Properties.Double)Pipe[5].GetPropertyFromFullDisplayName("{Geometry,Inlet}
Area");
area[7] = (IPS.Properties.Double)Pipe[7].GetPropertyFromFullDisplayName("{Geometry,Inlet}
Area");

//Establish link with variables for pipe circ
circ[6] = (IPS.Properties.Double)Pipe[6].GetPropertyFromFullDisplayName("{Geometry,Inlet}
Circumference");
circ[8] = (IPS.Properties.Double)Pipe[8].GetPropertyFromFullDisplayName("{Geometry,Inlet}
Circumference");
circ[1]= (IPS.Properties.Double)Pipe[1].GetPropertyFromFullDisplayName("{Geometry,Inlet}
Circumference");
circ[2]= (IPS.Properties.Double)Pipe[2].GetPropertyFromFullDisplayName("{Geometry,Inlet}
Circumference");
circ[3]= (IPS.Properties.Double)Pipe[3].GetPropertyFromFullDisplayName("{Geometry,Inlet}
Circumference");
circ[4]= (IPS.Properties.Double)Pipe[4].GetPropertyFromFullDisplayName("{Geometry,Inlet}
Circumference");
circ[5]= (IPS.Properties.Double)Pipe[5].GetPropertyFromFullDisplayName("{Geometry,Inlet}
Circumference");
circ[7]= (IPS.Properties.Double)Pipe[7].GetPropertyFromFullDisplayName("{Geometry,Inlet}
Circumference");


//Establish link with variables for heat transfer element area
htArea[6,1] = (IPS.Properties.Double)HeatTE[6].GetPropertyFromFullDisplayName("{Conduct
ion}Area upstream surface");
htArea[6,2] = (IPS.Properties.Double)HeatTE[6].GetPropertyFromFullDisplayName("{Conduct
ion}Layers[0].{Geometry}Area downstream surface");
htArea[6,3] = (IPS.Properties.Double)HeatTE[6].GetPropertyFromFullDisplayName("{Conduct
ion}Layers[1].{Geometry}Area downstream surface");
```

```
htArea[8,1] = (IPS.Properties.Double)HeatTE[8].GetPropertyFromFullDisplayName("{Conduct
ion}Area upstream surface");
htArea[8,2] = (IPS.Properties.Double)HeatTE[8].GetPropertyFromFullDisplayName("{Conduct
ion}Layers[0].{Geometry}Area downstream surface");
htArea[8,3] = (IPS.Properties.Double)HeatTE[8].GetPropertyFromFullDisplayName("{Conduct
ion}Layers[1].{Geometry}Area downstream surface");

htArea[1,1] = (IPS.Properties.Double)HeatTE[1].GetPropertyFromFullDisplayName("{Conduct
ion}Area upstream surface");
htArea[1,2] = (IPS.Properties.Double)HeatTE[1].GetPropertyFromFullDisplayName("{Conduct
ion}Layers[0].{Geometry}Area downstream surface");
htArea[1,3] = (IPS.Properties.Double)HeatTE[1].GetPropertyFromFullDisplayName("{Conduct
ion}Layers[1].{Geometry}Area downstream surface");

htArea[2,1] = (IPS.Properties.Double)HeatTE[2].GetPropertyFromFullDisplayName("{Conduct
ion}Area upstream surface");
htArea[2,2] = (IPS.Properties.Double)HeatTE[2].GetPropertyFromFullDisplayName("{Conduct
ion}Layers[0].{Geometry}Area downstream surface");
htArea[2,3] = (IPS.Properties.Double)HeatTE[2].GetPropertyFromFullDisplayName("{Conduct
ion}Layers[1].{Geometry}Area downstream surface");

htArea[3,1] = (IPS.Properties.Double)HeatTE[3].GetPropertyFromFullDisplayName("{Conduct
ion}Area upstream surface");
htArea[3,2] = (IPS.Properties.Double)HeatTE[3].GetPropertyFromFullDisplayName("{Conduct
ion}Layers[0].{Geometry}Area downstream surface");
htArea[3,3] = (IPS.Properties.Double)HeatTE[3].GetPropertyFromFullDisplayName("{Conduct
ion}Layers[1].{Geometry}Area downstream surface");

htArea[4,1] = (IPS.Properties.Double)HeatTE[4].GetPropertyFromFullDisplayName("{Conduct
ion}Area upstream surface");
```

```
htArea[4,2] = (IPS.Properties.Double)HeatTE[4].GetPropertyFromFullDisplayName("{Conduct
ion}Layers[0].{Geometry}Area downstream surface");
htArea[4,3] = (IPS.Properties.Double)HeatTE[4].GetPropertyFromFullDisplayName("{Conduct
ion}Layers[1].{Geometry}Area downstream surface");

htArea[5,1] = (IPS.Properties.Double)HeatTE[5].GetPropertyFromFullDisplayName("{Conduct
ion}Area upstream surface");
htArea[5,2] = (IPS.Properties.Double)HeatTE[5].GetPropertyFromFullDisplayName("{Conduct
ion}Layers[0].{Geometry}Area downstream surface");
htArea[5,3] = (IPS.Properties.Double)HeatTE[5].GetPropertyFromFullDisplayName("{Conduct
ion}Layers[1].{Geometry}Area downstream surface");

htArea[7,1] = (IPS.Properties.Double)HeatTE[7].GetPropertyFromFullDisplayName("{Conduct
ion}Area upstream surface");
htArea[7,2] = (IPS.Properties.Double)HeatTE[7].GetPropertyFromFullDisplayName("{Conduct
ion}Layers[0].{Geometry}Area downstream surface");
htArea[7,3] = (IPS.Properties.Double)HeatTE[7].GetPropertyFromFullDisplayName("{Conduct
ion}Layers[1].{Geometry}Area downstream surface");

}

//do post simulation cleanup here
public override void Cleanup()
   {
  }

//script main execution function - called every cycle
   public override void Execute(double Time)
   {
// ----------------------------------------------------------------------------------------------------------
----------
```

```
// calculations for power
area[6].Value = 12.0 * wy[6].Value * lx[6].Value * 0.5;
area[8].Value = 23.0 * wy[8].Value * lx[8].Value * 0.5;
area[1].Value = 23.0 * wy[1].Value * lx[1].Value;
area[2].Value = 23.0 * wy[2].Value * lx[2].Value;
area[3].Value = 23.0 * wy[3].Value * lx[3].Value;
area[4].Value = 17.0 * wy[4].Value * lx[4].Value;
area[5].Value = 23.0 * wy[5].Value * lx[5].Value;
area[7].Value = 23.0 * wy[7].Value * lx[7].Value * 0.5;

circ[6].Value = 12.0 * (wy[6].Value  + lx[6].Value);
circ[8].Value = 23.0 * (wy[8].Value  + lx[8].Value);
circ[1].Value = 23.0 *2* (wy[1].Value  + lx[1].Value);
circ[2].Value = 23.0 *2* (wy[2].Value  + lx[2].Value);
circ[3].Value = 23.0 *2* (wy[3].Value  + lx[3].Value);
circ[4].Value = 17.0 *2* (wy[4].Value  + lx[4].Value);
circ[5].Value = 23.0 *2* (wy[5].Value  + lx[5].Value);
circ[7].Value = 23.0 * (wy[7].Value  + lx[7].Value);


htArea[6,1].Value = circ[6].Value * hz[6].Value;
htArea[6,2].Value = htArea[6,1].Value;
htArea[6,3].Value = htArea[6,1].Value;

htArea[8,1].Value = circ[8].Value * hz[8].Value;
htArea[8,2].Value = htArea[8,1].Value;
htArea[8,3].Value = htArea[8,1].Value;

htArea[1,1].Value = circ[1].Value * hz[1].Value;
htArea[1,2].Value = htArea[1,1].Value;
htArea[1,3].Value = htArea[1,1].Value;
```

```
htArea[2,1].Value = circ[2].Value * hz[2].Value;
htArea[2,2].Value = htArea[2,1].Value;
htArea[2,3].Value = htArea[2,1].Value;

htArea[3,1].Value = circ[3].Value * hz[3].Value;
htArea[3,2].Value = htArea[3,1].Value;
htArea[3,3].Value = htArea[3,1].Value;

htArea[4,1].Value = circ[4].Value * hz[4].Value;
htArea[4,2].Value = htArea[4,1].Value;
htArea[4,3].Value = htArea[4,1].Value;

htArea[5,1].Value = circ[5].Value * hz[5].Value;
htArea[5,2].Value = htArea[5,1].Value;
htArea[5,3].Value = htArea[5,1].Value;

htArea[7,1].Value = circ[7].Value * hz[7].Value;
htArea[7,2].Value = htArea[7,1].Value;
htArea[7,3].Value = htArea[7,1].Value;

Output1.Value = circ[1].Value;
Output2.Value = htArea[1,3].Value;



// ------------------------------------------------------------------------------------------------------------
----------
}

  //any processing you want to do before steady state
```

```
    public override void ExecuteBeforeSteadyState()
    {
    Execute(0.0);

    }
   //any processing you want to do while solving steady state
    public override void ExecuteSteadyState()
    {
    Execute(0.0);
    }

  //any processing you want to do after steady state
    public override void ExecuteAfterSteadyState()
    {
    Execute(0.0);
    }

[PropertyUsage(UseProperty.DYNAMIC)]
        public IPS.Properties.Double Output1
        { get { return _Output1;   }  }

          [PropertyUsage(UseProperty.DYNAMIC)]
        public IPS.Properties.Double Output2
        { get { return _Output2;   }  }

}
```

APPENDIX C

C. PDFs of system parameters and their r^2 values

The PDFs of the system parameters are shown in Figure C.1-C.3.

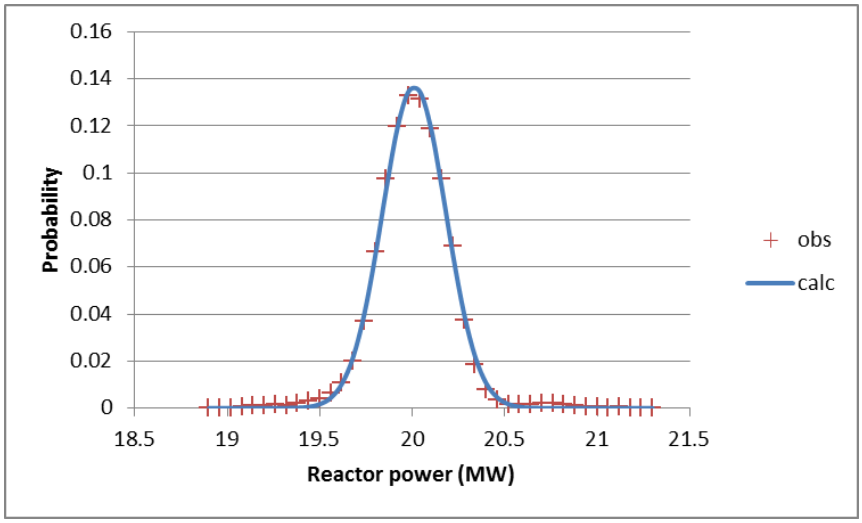

Figure C.1: PDF of the reactor power

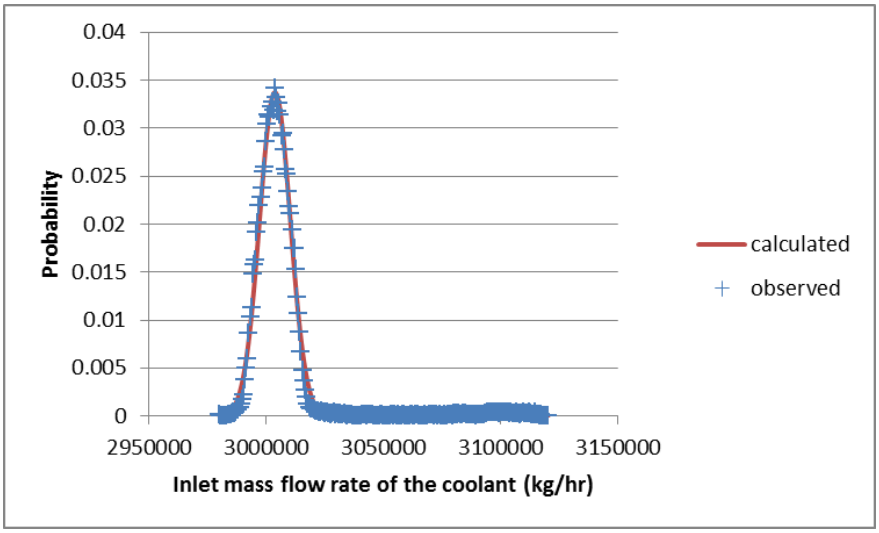

Figure C.2: PDF of the inlet mass flow rate of the coolant

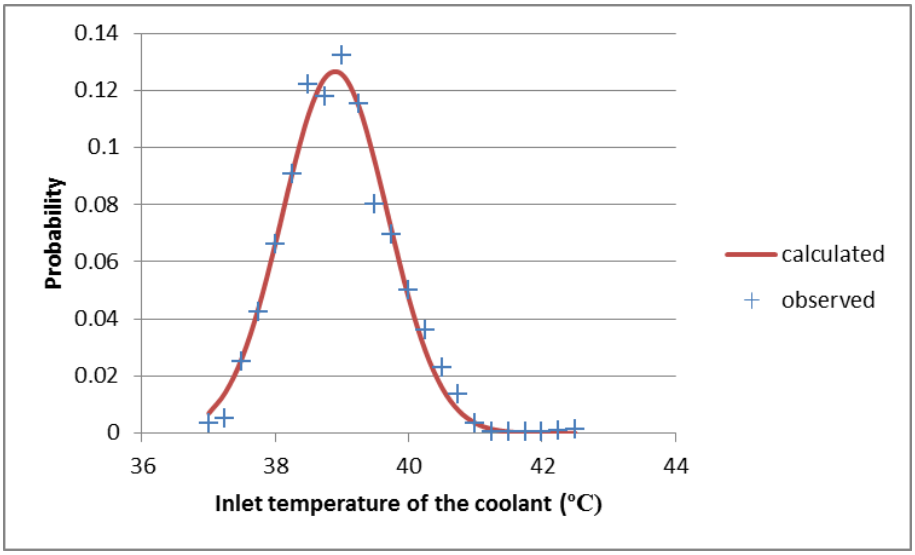

Figure C.3: PDF of the inlet temperature of the coolant

The r^2 values determined from the PDF of each system parameter are shown in Table C.1.

Table C-1: r^2 values of the system parameters

System parameter	r^2 value
Power	0.998
Global mass flow rate of the coolant	0.994
Global temperature of the coolant	0.986

APPENDIX D

D. Steps for performing sensitivity and uncertainty analysis in the Flownex® code

D.1 Sensitivity analysis

The following are the steps that are followed when performing a sensitivity analysis in the Flownex® code (Flownex® manual, 2011):

- Open the existing Flownex® project,
- In Flownex® menu bar click configuration, and double click sensitivity analysis setup,
- Right click in the sensitivity analysis configuration pane and select add,
- You can rename the sensitivity analysis configuration to the name you prefer e.g. Sensitivity study of global parameters,
- Right click in the input variables pane and select add single input. This allows you to add input variables or parameters that you want to investigate,
- Click the browse icon so as to select the input variables,
- On the component pane, select the component e.g. Pipe 6. From here, select the property of the component selected on the property pane e.g. Length of Pipe 6. Then press ok. Follow the same procedure to add other input variables,
- Enter the low and high value. Specify the distribution that the input variable follows. If the input variable follows a normal distribution the nominal value can be ignored. Thus it is not necessary to enter a nominal value of the input variables,
- In the sensitivity analysis configuration pane, set the Monte-Carlo option to false and the parametric option to true. This is because in this case only the sensitivity (parametric) analysis is performed not Monte-Carlo,
- Enter the number of runs of your choice. If you want to focus only on the lower and upper values specify 2 runs,

- Right click in the results pane and select add. This is done so as to add the output variables or parameters of interest,
- Select the browse icon,
- Select a component and its property as already explained.
- After adding all output parameters of interest, right click on the sensitivity analysis you added on the sensitivity analysis configuration pane and select set as active. This basically activates the sensitivity analysis added,
- On the input variables pane, set enable Monte-Carlo to false and enable parametric study to true. This again deactivates the Monte-Carlo function and activates the parametric function in Flownex®,
- Close the sensitivity analysis configuration window,
- Set the solver to sensitivity analysis. The solver tab can be found under libraries on the right pane on the Flownex® canvas,
- On the menu bar, click home and from here click run sensitivity analysis. Press save after the simulation run is complete,
- Browse to a location where you saved this Flownex® project or file, on this location there will be a folder with the same name as a Flownex® project or file saved,
- Open this folder, and open a tasks folder, and open a 'SensitivityAnalysis.sao' file,
- Open this file with a text editor e.g. notepad. In this file the independent (input parameters) and dependent (output parameters) variables are outlined. The results of the output parameters for each input variable run are well indicated. In addition to this, the standard deviation and mean of output parameters are shown.

D.2 Uncertainty analysis: Monte-Carlo

The following are the steps that are followed when performing an uncertainty analysis in the Flownex® code (Flownex® manual, 2011):

- Open the existing Flownex® project,
- In Flownex® menu bar click configuration, and double click sensitivity analysis setup,

- Right click in the sensitivity analysis configuration pane and select add and set to active,
- You can rename the sensitivity analysis configuration to the name you prefer e.g. Uncertainty analysis,
- Set enable Monte-Carlo to true, and set enable parametric study to false,
- Enter the number of Monte-Carlo runs to be performed,
- Right click on the input variable pane to add input parameters of interest as already explained with its low, nominal and high values. The distribution of the input variable is also specified
- Right click on the results pane to add output parameters of interest,
- Close the sensitivity analysis configuration window and run the sensitivity analysis as explained above. The same procedure as in the parametric (sensitivity) analysis is followed to retrieve the Monte-Carlo results in the project folder.